PREDICTION OF PARAMETRIC ROLL OF SHIPS IN REGULAR AND IRREGULAR SEA

A Thesis

by

HISHAM MOIDEEN

Submitted to the Office of Graduate Studies of
Texas A&M University
in partial fulfillment of the requirements for the degree of

MASTER OF SCIENCE

December 2010

Major Subject: Ocean Engineering

Prediction of Parametric Roll of Ships in Regular and Irregular Sea

PREDICTION OF PARAMETRIC ROLL OF SHIPS IN REGULAR AND IRREGULAR SEA

A Thesis

by

HISHAM MOIDEEN

Submitted to the Office of Graduate Studies of
Texas A&M University
in partial fulfillment of the requirements for the degree of

MASTER OF SCIENCE

Approved by:

Chair of Committee,	Jeffrey M. Falzarano
Committee Members,	Moo Hyun Kim
	Tamàs Kalmàr-Nagy
Head of Department,	John Niedzwecki

December 2010

Major Subject: Ocean Engineering

ABSTRACT

Prediction of Parametric Roll of Ships in Regular and Irregular Sea.

(December 2010)

Hisham Moideen, B.Tech, Cochin University of Science and Technology, India

Chair of Advisory Committee: Dr. Jeffrey M. Falzarano

This research was done to develop tools to predict parametric roll motion of ships in regular and irregular sea and provide guidelines to avoid parametric roll during initial design stage. A post Panamax hull form (modified C11 Hull form, Courtesy of MARIN) was used to study parametric roll in ships.

The approach of the study has been to simplify the roll equation of motion to a single degree of freedom equation so as to utilize the tools available to analyze the system retaining the non-linear character of the system. The Hill' equation is used to develop highly accurate stability boundaries in the Ince-Strutt Diagram. The effect of non-linear damping has also been incorporated into the chart for the first time providing a simple method to predict the bounded roll motion amplitude. Floquet theory is also extended to predict parametric roll motion amplitude. Forward speed of the vessel has been treated as a bifurcation parameter and its effects studied both in head and following sea condition.

In the second half of the research, parametric roll of the vessel in irregular sea is investigated using the Volterra Quadratic model. GM variation in irregular sea was

obtained using transfer functions of the Volterra model. Heave and pitch coupling to roll motion was also studied using this approach. Sensitivity studies of spectral peak period and significant wave height on roll motion amplitude were also carried out. Forward speed effects were also evaluated using the Volterra approach.

Based on the study, the Hill's equation approach was found to give more accurate prediction of parametric roll in regular sea. The boundaries in the stability chart were more accurately defined by the Hill's equation. The inclusion of non-linear damping in the stability chart gave reasonably accurate bounded motion amplitude prediction. The Volterra approach was found to be a good analytical prediction tool for parametric roll motion in irregular sea. Using the Volterra model, it was found that there is a high probability of parametric roll when the spectral modal period is close to twice the natural period of roll.

To my parents and friends

ACKNOWLEDGEMENTS

I would like to thank my advisor and committee chair Dr. Jeffrey M. Falzarano for his active guidance and support during the course of my research. He has been a source of inspiration and motivation for me to excel. I would also like to thank my committee Dr. Moo Hyun Kim and Dr. Tamàs Kalmàr-Nagy for sharing their knowledge and willingness to serve on my committee. I am very grateful to Dr. Frans van Walree of MARIN for providing us the hull model and valuable model test data report. I would also like to thank Dr. Cheung H. Kim , Dr. Richard Mercier and Dr. Alan Palazzolo for helping me learn the basics of hydrodynamics and non-linear dynamics which greatly helped me achieve my research objectives.

I am grateful to my research mates Mr. Ziyong Su and Mr. Chandan Lakhotia for sharing their knowledge and Ms. Erin A. Rooney for helping me edit my thesis. I would also like to thank my friend Mr. Zaki Reza for making available to me softwares, which were crucial to my research. I am indebted to my parents and my brother for their love and support without which I would not have been able to complete my research.

NOMENCLATURE

GM	- Metacentric height	$\underline{B}(t)$	- Periodic Matrix
GZ	- Righting Arm	$T_{\min}$	- Minimum Period
DOF	- Degree of Freedom	α	- Stability Parameter (frequency ratio square)
[M]	- Mass Matrix	Φ	- Fundamental Matrix
[A]	- Added Mass/Inertia Matrix	$\underline{H}$	- Monodromy Matrix
[X]	- Displacement Matrix	$x^n{}_k(t)$	- Normal Solution
[B]	- Damping Matrix	ψ_{Mk}	- K^{th} eigenvector of Monodromy Matrix
[C]	- Stiffness Matrix	λ_{MK}	- K^{th} eigenvalue of Monodromy Matrix
[F]	- Forcing Matrix	ρ_{Mk}	- Characteristic component of eigenvalues of Monodromy matrix
ω	- Forcing Frequency	$p_k(t)$	- Fundamental Matrix
ϕ	- Roll Amplitude	τ	- Non-Dimensional Time
ω_n	- Natural Frequency	g	- Acceleration due to gravity
ω_D	- Damped Frequency	β	- Heading Angle
ζ	- Damping Ratio	ω_e	- Encounter Frequency
$\delta GM(t)$	- Time Varying GM	k	- Wave Number

A_n, B_n	- Hill Coefficients of GM Variation	μ_1	- Linear Damping Coefficient
C_n, S_n	- Fourier Coefficients of GM Variation	μ_2	- Quadratic Damping Coefficient
B_e	- Eddy Damping Component	λ	- Wave Length
B_w	- Wave Damping Component	KB	- Distance to Centre of Buoyancy from Keel
B_f	- Friction Damping Component	BM	- Metacentric Radius
B_{BKN}	- Bilge Keel Normal Damping Component	KG	- Distance to Centre of Gravity from Keel
B_{BKH}	- Bilge Keel Horizontal Damping Component	δGM_1	- 1st Order GM Variation
B_{BKw}	- Bilge Keel Wave Damping Component	δGM_2	- 2nd Order GM Variation
B_1	- Linear Damping Component	η	- Wave Elevation
B_2	- Quadratic Damping Component	η_3	- Heave RAO
B_3	- Cubic Damping Component	η_5	- Pitch RAO
B_{eq}	- Equivalent Damping	$r(x,t)$	- Relative Wave Profile
$v(x)$	- Transfer Function of Relative Wave Profile	$f(\omega)$	- Transfer Function of 1st order GM Variation
$u_1(\omega_m, \omega_n)$	- 2nd Order Transfer Function of GM Variation	$v_1(\omega_m, \omega_n)$	- 2nd Order Transfer Function of GM Variation

TABLE OF CONTENTS

CHAPTER Page

LIST OF FIGURES

Page

Page

Page

Page

Page

Page

Page

LIST OF TABLES

CHAPTER I

INTRODUCTION

1.1 Problem Statement

Ship stability has always been a topic of research in the field of Naval Architecture and Marine Engineering. Roll stability has been of particular interest and has been studied extensively over the last few centuries. Major emphasis is laid on the static roll stability of the vessel during the design stage, but over the past few decades the issue of dynamic stability has earned widespread attention . Parametric roll is one of the modes of vessel capsize due to loss of dynamic stability in waves. Parametric rolling is a form of parametric vibration due to the time varying stiffness in the case of ships in waves. Several studies have been carried out to predict parametric roll in regular waves using Mathieu equation as a basis. This research attempts to utilize more accurate methods to predict the occurrence of parametric roll in regular and irregular waves and provide design guidelines to avoid parametric roll. In the first part of the thesis parametric roll in regular sea is studied. The roll motion equation is modeled as a Hill's equation to capture non-harmonic variation of roll restoring moment. A comparison between the Mathieu's equation and the Hill's equation is also carried out. Damped systems behave differently since a threshold value is to be achieved for unstable motion. Linear damping tends to increase the threshold value of the stiffness variation required to instigate roll motion at resonant frequencies.

This thesis follows the style of Journal of Ocean Engineering.

The influence of non-linear damping on the stability boundaries have not been investigated in the past. The effects of non-linear damping which controls the bounded roll motion amplitude is studied and incorporated into the stability charts as part of the research.

In the second part of the research parametric roll characteristics of the vessel in a random seaway is investigated. The time varying metacentric height GM (which is an important parameter for occurrence of parametric roll) is represented as a Volterra series. 1^{st} and 2^{nd} order transfer functions are utilized to obtain the GM variation in irregular seaway. The stochastic parametric roll response is obtained by solving the parametric roll equations in time domain using the irregular GM obtained using the Volterra method. This system can be treated as a random dynamical system. The statistical properties of the response are estimated from different realizations. The effects of different parameters of the wave spectrum on the roll response are also evaluated.

An uncoupled single degree of freedom (DOF) motion model is used in the analysis since there are more analytical tools to tackle the problem in 1-DOF . The linear coupling effects of surge and sway on the roll motion are investigated to assess the effect coupling. Non-linear coupling effects of heave and pitch on roll motion are also incorporated.

Modern container ships have large variation in sectional hull shape along the depth making them susceptible to parametric roll. The container damage incident of APL China (1998) leading to loss of containers due to excessive roll in head sea is a clear

indication that parametric roll does occur and can be dangerous. Also an ITTC benchmark for parametric roll is being developed for parametric roll. As a result there is a need to develop accurate methods to predict parametric rolling of ships in longitudinal seaway and provide guidelines, which can be utilized in the design stage to avoid occurrence of the phenomenon in sea going vessels.

1.2 Background

Parametric systems are a class of time varying systems. Parametric vibrations are vibrations that result from the time variation of coefficients (mass, damping, stiffness) in the equation of motion. The coefficients are sometimes called parameters, and hence the name parametric vibration. It is interesting to note that parametric vibrations can occur in the absence of direct excitation, i.e. if the variation in the parameter (which may be due to an indirect excitation) is high enough, then the system may vibrate. Such vibrations are called parametrically excited vibrations. Depending on the amount of damping in the system the resulting amplitudes of vibrations can be much larger in comparison to the vibrations that arise from a direct excitation. This can be critical if the system is designed to direct excitation criteria. Large amplitude motions are generally associated with resonance. The same applies to parametric systems. Apart from the primary resonance when excitation frequency tunes up with the natural frequency of the system, sub and super-harmonic resonances can occur in parametrically exited systems. This makes the design process much more difficult because of the possibilities of multiple resonant zones. In order to analyze the parametric dynamical systems, the dynamic equilibrium equations in state space (1^{st} order) form is considered. Such a class

of system can be analyzed using a mathematical tool called *Floquet Theory* (Floquet, 1883). The idea is to capture time varying parameters in a periodic matrix. This matrix is further used to obtain the fundamental matrix, which in turn produces the monodromy and matrizant matrices. The eigenvalues of the matrizant matrix is used to study the local stability of the dynamical system. Details of Floquet theory will be discussed in Chapter II. The same theory can also be extended for systems with multiple degrees of freedom. This tool is very useful when dealing with parametric or non-linear system stability analysis. One of the major drawbacks of the theory is that it can only be applied to systems with periodic variation in the parameter. For other non-linear systems a harmonic solution is assumed and local stability of perturbations about the solution are studied using Floquet theory.

A certain class of parametric systems which have harmonic variation of stiffness can be described by the Mathieu's equation (Mathieu, 1868). These equations are applicable only for single degree of freedom system and a certain restricted class of systems with multi-degrees of freedom. The Mathieu's equation evolved from the Floquet Theory but does not require solving for the matrizant matrix. For non-harmonic but periodically varying stiffness there is a different class of differential equations called the Hill's equation (Hill, 1886). The Hill's equation utilizes the method of Fourier fit to represent the non-harmonic variation of stiffness. If a Mathieu's equation is used for representing a non-harmonic variation of stiffness then we are essentially considering only the first harmonic and neglecting higher order harmonics of the Fourier expansion. Stability charts called *Ince-Strutt* diagram (van der Pol and Strutt, 1928) can be developed for

each of these equations which define the stable and unstable region in the parameter space. These charts are very accurate and can serve as a tool in determining the stability of the system. They also provide details on the type of parametric resonance causing the instability. This information is very critical and can be used to stabilize the system. This is known as parametric stabilization. It is a very common to see that a system susceptible to parametric vibration tends to exhibit the phenomenon when the excitation frequency (frequency of variation of the parameter) is twice the natural frequency of the system. This is called the primary resonance in the parametric system. Other modes of resonance may also occur depending on the range of excitation frequency. Thus it is important to study the parametric stability of the system using stability charts.

Parametric roll is not a new phenomenon to researchers. (Grim, 1952; Kerwin, 1955) were the first to investigate ship rolling in longitudinal waves. Kerwin considered two harmonics in his solution to obtain the criteria for stability of both damped and undamped roll equation of motion. Apart from ships, parametric roll is also found to occur in spars (Koo et al., 2004). Roll motion in beam sea has been a topic of immense research over a century (Froude, 1863; Odabashi, 1977). Roll motion is particularly interesting near the resonant frequency. Large amplitude motion due to resonance makes the roll motion highly non-linear. This is due to the presence of viscous damping in roll. Apart from the non-linear damping, the restoring moment also becomes non-linear as the roll angle increases. Due to the port-starboard symmetry in the upright condition the restoring arm (GZ) is often modeled as a polynomial of odd power. This leads to multiple solutions and complicated dynamics. The complicated dynamics of roll motion

in beam sea leading to capsize has been extensively studied by (Falzarano, 1990; Falzarano et al., 1992; Kan, 1992; Nayfeh, 1986; Thompson and Souza, 1996). Parametric roll motion is attributed to the variation of the GZ in waves leading to varying restoring moment in roll. Often the linear part of the righting arm, the metacentric height (GM) is used as an approximation to GZ if the roll amplitude is small. Two approaches have been used to obtain the variation in GM. One method is to estimate it from the Froude-Krylov force (Dunwoody, 1989a; Munif and Umeda, 2006; Umeda et al., 1995) while the other method is to estimate the GM from the varying geometry of the underwater hull with wave position(ABS, 2004; Belenky et al., 2003; Bulian et al., 2004; Hua et al., 2001; Spyrou et al., 2008). In this study large angle stability analysis is carried out in regular waves and GM is obtained from the slope at origin of the righting arm curve.

Roll motion in astern sea was studied by (Dunwoody, 1989a), where the roll moment was obtained by integrating the Froude-Krylov forces over the submerged part of the vessel due to the wave profile. A quasi-static equilibrium is considered and the roll moment is equated to the still water restoring moment to obtain the GM in wave. Model test studies of roll motion leading to capsize in astern seas was carried out by (Hamamoto et al., 1996; Umeda et al., 1995). Head sea parametric roll which is a relatively new phenomenon was studied by (Munif and Umeda, 2006). They studied the parametric roll characteristics of Icelantic trawler. Single Degree Of Freedom (DOF) and 6 DOF models were used to predict parametric roll. The varying restoring moment was derived from the Froude-Krylov forces acting on the vessel. The vessel did not have any

significant variation in restoring moment due to the wave elevation effects. Their studies have found that 1 DOF equation fails to capture parametric rolling in the absence of forward speed whereas the 6 DOF model successfully identifies parametric roll with zero forward speed. Many of the analyses in regular waves use the Mathieu's equation and the corresponding Ince-Strutt diagram to predict the occurrence of parametric roll.

(Bulian et al., 2004) studied the parametric roll characteristics of a Ro-Ro passenger ship in regular waves in head sea condition. The time varying righting arm was obtained by carrying out large angle stability analysis for different wave crest position along the length of the vessel. In their analytical model the righting arm GZ was divided into two parts:- a harmonically varying term which included a linear term that captured the GM variation and a quadratic term which captured the non-linear aspect of the right arm. The 2^{nd} term consisted of a cubic term of roll angle. The coefficients in the harmonic terms were depended on the wave height, wave length and relation between heave, pitch and wave. Calculation of these coefficients for each wave position is a tedious task. Mathieu's equation was used as the basis to predict occurrence of parametric roll in the linearized model. Many of the previous studies on parametric roll have been to predict the occurrence of parametric roll and not to predict the roll amplitude. An attempt to estimate the roll motion amplitude in longitudinal sea was made by (Bulian, 2003). He developed a time domain model of roll motion where GZ is reproduced as a combination of polynomial fits and Fourier fits. The time domain model was then converted into a frequency domain by assuming a harmonic form for the response. The analysis was carried out to predict the roll response in the 1^{st} parametric instability zone. Using the

averaging technique he was able to obtain an equation of polynomials in amplitude and phase which when solved would give possible amplitudes and corresponding phase for the system. Such an analysis is a good procedure to study the various domains of attraction and region of capsize for a ship. Considering the large amount of calculations to be carried out, it is not a suitable procedure during the initial design stage.

A general practice is to approximate a non-harmonic variation of GM by a harmonic one so as to use the Mathieu's equation for prediction. Sea going ships in general are not symmetric about the design water line, as a result the variation in GM in waves is asymmetric. Studies have shown that modeling the actual variation in GM as a harmonic variation is a crude approximation (ABS, 2004; Spyrou et al., 2008). The current study proposes to utilize a much more simplified model with reasonable approximation that can handle non-harmonic variation of stiffness and also give a good estimate of the roll motion amplitude without much detailed calculations that can aid preliminary design to avoid parametric rolling in ships. In the regular wave analysis GZ is estimated using large angle stability for both fixed trim and free trim conditions. In both these conditions a quasi-static equilibrium or hydrostatic balance is maintained at each position of the wave crest. The volume displacement of the vessel thus remains the same throughout the analysis. It is seen that the maximum variation in GM occurs when the wave length is close to the ship length, as a result analysis will be carried out for the critical case of wave length equal to the ship length . The effects of forward speed of the vessel on roll motion are also investigated.

So far we have discussed the response in idealized regular waves. The only physical phenomenon close to this would be the case of swells. Swells are not very common in an irregular sea but they do occur, which supports the study in regular waves. Real seaway is irregular/random and far from regular. Studying parametric roll motion in an irregular seaway would be more accurate. However, much less research has been done in this direction. The study of parametric roll in an irregular seaway necessitates the estimation of GZ or GM (if a linearized model is used) in irregular waves. (Paulling, 1961) was among the first to estimate time varying GM and GZ in regular waves. He estimated the Bonjean curves for different angles of heel and hydrostatically balanced the vessel to obtain the righting moment from the Bonjean curves. The volume of the vessel remained constant during the calculation. (Dunwoody, 1989b) came up with a procedure to develop the metacentric height spectra. He used the potential theory to estimate the fluid pressure of incident waves. The roll moment was obtained by integrating the fluid pressure around the vessel assuming quasi-static equilibrium. He expressed the variation in GM as a linear function of wave elevation and wave acceleration. Thus he developed a metacentric height spectrum from a wave spectrum. Using this method he studied the roll motion in astern seas (Dunwoody, 1989a). A similar approach was used by (Palmquist, 1994). He developed a transfer function for 1^{st} order GM variation using the Froude-Krylov forces and quasi-static equilibrium. He was the first to study the 2^{nd} order variation in GM which he called slowly varying GM. He expressed the *slowly varying* GM as a polynomial fit of the envelope of the 1^{st} order GM variation. Thus the total GM

variation was expressed as sum of linear (1^{st} order) + slowly varying (2^{nd} order) variations.

Another approach to study ship motions in irregular waves is to replace the irregular wave train by an equivalent wave (Grim, 1961). The idea is to reduce the number of random variables to two by substituting the irregular wave with a single wave (with wave length equal to ship length) using the method of least square convergence. The amplitude and mean value of the wave are modeled as stochastic processes. The Grim effective wave concept was further developed by (Bulian, 2008). He added a harmonic term introducing an additional stochastic amplitude or effectively adding a stochastic phase term to the original Grim effective wave equation. This approach was used to obtain the restoring arm in an irregular seaway which was converted into an analytical model using bi-variate polynomial fitting in roll angle and effective wave amplitude. The linearized model of GZ was subjected to statistical linearization and the resulting model was used to study the parametric roll stability.

Fully non-linear simulation codes have also been used by some of the researchers to study the parametric roll behavior of ships. (Belenky et al., 2003) used LAMP to study the parametric roll behavior of the C11 Hull form. Another non-linear code FREDYN was also used to study the roll characteristics of the C11 Hull form (France et al., 2001). They also carried out model tests to study the parametric stability of the vessel in regular waves (head sea condition). The influence of vessel forward speed and heading angle on

the roll motion was also investigated. The use of highly non-linear codes demands a lot of computing memory and time. Such methods are not apt in the early stages of design.

In this study the approach developed by (Hua et al., 1994) to represent the GM variation in an irregular seaway using the Volterra series is utilized. Two major reason for adapting the method are:

1. The approach uses a transfer function to estimate the GM variation which is a classical way of estimating the response in a stochastic seaway. It also avoids the need to calculate GZ for individual waves or the use of statistical linearization.

2. The model can capture the dynamic effects of heave and pitch on GM variation in comparison to the quasi-static assumption used in many of the previous studies which fail to handle large heave and pitch motions.

The method attempts to express the stability parameters (breadth, sectional moment about keel and sectional area) as a Taylor series expansion of the draft about the mean waterline. The method was further used to estimate the transfer functions of the Volterra series. This method helps us estimate GM directly from the Volterra model instead of using a polynomial approximation to estimate the 2^{nd} order GM (Palmquist, 1994). The model can also be extended to higher orders to give more accurate results. The resulting GM variation is used in a simulation model to study parametric roll in an irregular seaway. Thus the influence of the spectrum parameters such as peak period (T_P) and significant wave height (H_S) on the roll variance can be studied.

1.3 Objectives

The main objectives of the research are summarized below

1. To model the parametric roll equation of motion as a Hill's equation so that the non-harmonic variation of the metacentric height (GM) in regular waves can be studied. Compare the accuracy of the Hill's equation to the Mathieu's equation modeling.

2. Study the effects of non-linear damping on the stability regions of the Ince-Strutt diagram and develop a surface separating the stable and unstable region using the method of equivalent linear damping.

3. Assess the importance of dynamic GM variations considering the effects of Heave and Pitch motion in comparison to the fixed or free trim condition.

4. To estimate the GM variation in an irregular seaway using Transfer functions. The Hull geometry characteristics are captured in Transfer Functions (1^{st} and 2^{nd} Order) using the Volterra Method (Hua 2001). The stochastic GM variation is used to estimate the roll response in an irregular seaway.

5. Study the significance of the spectral properties such as significant wave height (H_S) and peak period (T_P) on roll response statistics, and develop guidelines to avoid parametric roll.

CHAPTER II

MATHEMATICAL FORMULATION AND SHIP PARAMETERS

2.1 Equation of Motion

Ship motion can be treated as a dynamical system with six degrees of freedom with three linear and three angular displacements. The various ship motions and their sign conventions are shown in Figure 1. The origin of the body fixed coordinates of the ship is fixed at amidships.

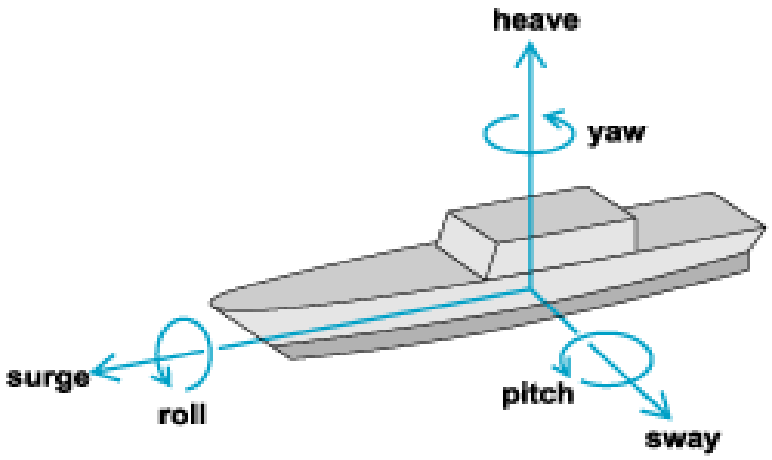

Figure 1. Different ship motions and their sign convention

The equation of motion for the 6 degrees of freedom with external excitation can written in the matrix form as below,

$$[M + A(\omega)]\left[\ddot{X}\right] + \left[B(\omega)\right]\left[\dot{X}\right] + [C][X] = [F] \tag{2-1}$$

where, M is the mass matrix, A is the added mass/ added inertia matrix, B is the radiated wave damping matrix and C is the hydrostatic stiffness matrix. All the above matrices are of order 6x6. The elements of the matrices can be represented as

$M_{ij}, A_{ij}, B_{ij}, C_{ij}$, with i=1..6,j=1..6. The indices stand for surge, sway, heave, roll, pitch and yaw respectively. X is the displacement matrix and F denotes the external excitation matrix. Both these matrices are of order 6x1. The dots above the X's denote time derivatives. ω is the forcing frequency.

For the head sea condition considering linear hydrostatics, the vertical plane motions (heave, pitch, surge) can be de-coupled from the horizontal plane motions (sway, roll, yaw). Appendix A discusses the effect of sway and roll coupling on roll motion. The roll motion is coupled to sway and yaw through added mass/added inertia terms and radiated damping terms. For the zero speed case, by selecting a different ship fixed coordinate system as the origin we can eliminate the added inertia coupling effects. If the coupling terms in the damping matrix are negligible the roll equation of motion completely decouples from the sway and yaw motion. For the head sea condition there is no direct external forcing in the roll direction, and the equation of motion can be represented as

$$\left(I_{44} + A_{44}\left(\omega_D\right)\right)\ddot{\phi} + \left(B_{44}\left(\omega_D\right)\right)\dot{\phi} + C\phi = 0 \tag{2-2}$$

Here, ϕ denotes the roll amplitude (rad) and $\omega_D = \omega_n\sqrt{(1-\zeta^2)}$ is the damped roll natural frequency (rad/sec), where ω_n - natural frequency of roll and ζ - damping ratio.

It is well known that the ship stability in waves is quite different from that of the calm water condition. This is due to the fact that the wave profile tends to change the underwater hull shape and the shape of water plane which in turn affects the restoring arm and the restoring moment. Figure 2 shows the comparison of restoring arm in wave

condition to that of still water. The righting arm with the wave crest position at amidships tends to be smaller than the still water condition and that due to wave trough at amidships tends to be larger than the still water level. With the wave crest amidships, there is a loss of water plane area at the bow and aft sections resulting in a reduction in the water plane inertia. Due to the wall sided shape of the midship sections there is no significant loss of water plane area amidships. In the case of wave trough amidships, there is an increase in the water plane area at the bow and stern due to the flare above the water line. This increases the water plane inertia and the righting arm. Such variations in GZ are seen for hulls that have a significant transition in the hull shape along the depth of the vessel.

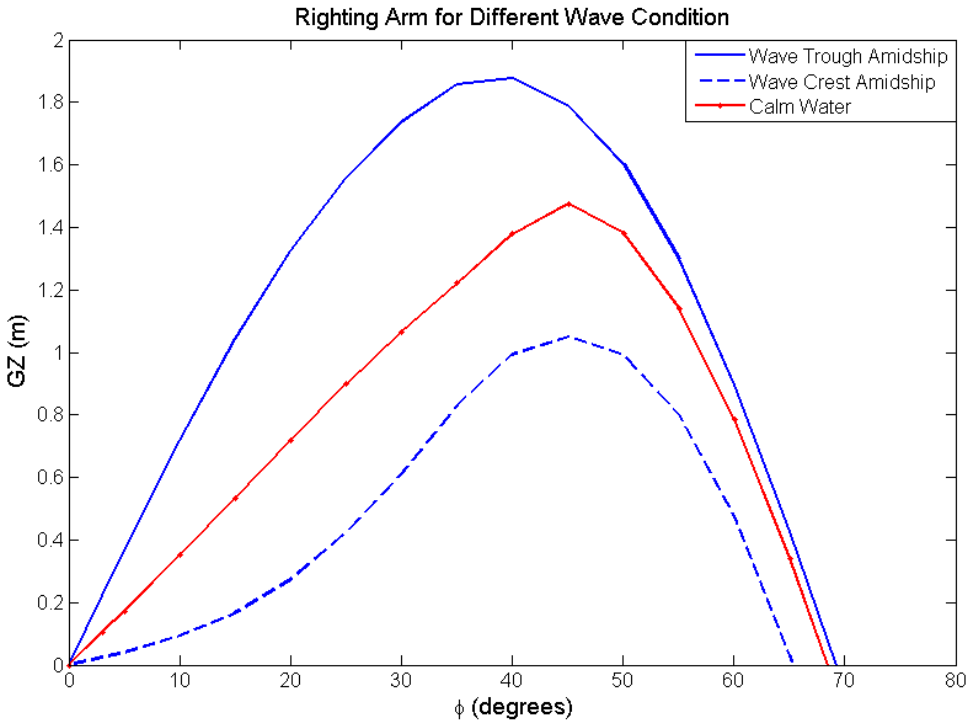

Figure 2. Righting arm for different wave conditions (H=L/40, λ=L)

For roll motion $C = \nabla gGZ$ in Eq. (2-2). Due to the symmetric shape of the hull about the ship centre line, the righting arm is often represented as an odd polynomial of roll angle. The righting arm for the ship can be represented as

$$GZ = C_1\phi + C_3\phi^3 + C_5\phi^5 + \ldots \tag{2-3}$$

Here C_1 = GM is the slope of the righting arm at the origin.

Since the higher powers in Eq. (2-3) are only important for large amplitudes of motion, we can neglect them. Using the linearized the righting arm, Eq. (2-2) becomes

$$\left(I_{44} + A_{44}\left(\omega_D\right)\right)\ddot{\phi} + \left(B_{44}\left(\omega_D\right)\right)\dot{\phi} + \nabla gGM\phi = 0 \tag{2-4}$$

If the waves are periodic, the righting arm and the metacentric height vary periodically. The time varying GM may be expressed as a variation from the still water GM as

$$GM(t) = GM_0 + \delta GM\left(t\right) \tag{2-5}$$

Here GM_0 is the still water metacentric height and $\delta GM\left(t\right)$ is the time varying GM in waves.

The general equation of motion in roll considering the time varying linearized righting arm may be represented as

$$\left(I_{44} + A_{44}\left(\omega_D\right)\right)\ddot{\phi} + \left(B_{44}\left(\omega_D\right)\right)\dot{\phi} + \nabla g\left(GM_0 + \delta GM\left(t\right)\right)\phi = 0 \tag{2-6}$$

Using the transformations in Eq. (2-7), Eq. (2-6) can be converted into a non-dimensional form given by Eq. (2-8)

$$\tau = \omega t, \quad \omega_D = \sqrt{\frac{g\Delta GM_0}{(I + A_{44}(\omega_D))}}, \qquad \alpha = \left(\frac{\omega_D}{\omega}\right)^2, \quad \mu = \frac{B_{44}(\omega_D)}{(I + A_{44}(\omega_D))\omega} \tag{2-7}$$

$$\frac{d^2}{d\tau^2}\phi + \mu\frac{d}{d\tau}\phi + \left(\alpha + \frac{\delta GM(t)}{GM_0}\alpha\right)\phi = 0 \tag{2-8}$$

Eq. (2-8) is the basic equation used to analyze ship parametric roll in regular waves. Different approaches used in the regular wave analysis differ in the method of representation of $\delta GM(t)$. The variation in GM can be represented as a harmonic term with constant amplitude (δGM) i.e.

$$\delta GM(t) = \delta GM \cos\tau \tag{2-9}$$

In this case, Eq. (2-8) has the form of a damped Mathieu's equation. The general form of the damped Mathieu's equation is given by Eq. (2-10)

$$\frac{d^2}{d\tau^2}\phi + \mu\frac{d}{d\tau}\phi + (\alpha + \gamma\cos\tau)\phi = 0 \tag{2-10}$$

For the roll equation $\gamma = \dfrac{\delta GM}{GM_0}\alpha$

Alternatively, if the time varying stiffness term is represented as a Fourier series i.e.

$$\delta GM(t) = \sum_{n=0}^{\infty}(C_n\cos(n\tau) + S_n\sin(n\tau)) \tag{2-11}$$

Then Eq. (2-8) has the form of a damped Hill's Equation. The general form of the damped Hill's equation is given by Eq. (2-12)

$$\frac{d^2}{d\tau^2}\phi + \mu\frac{d}{d\tau}\phi + \left(\alpha + \gamma\sum_{n=1}^{\infty}\left(A_n\cos(n\tau) + B_n\sin(n\tau)\right)\right)\phi = 0 \tag{2-12}$$

Comparing with Eq. (2-8) we see that $\alpha = \gamma$

The Fourier coefficients A_n and B_n are derived from C_n and D_n .

Further details of how these coefficients are derived will be discussed in Chapter III.

2.2 Non-linear Damping

As discussed earlier, large amplitude rolling motion is complicated due to the presence of non-linear damping and non-linear restoring moment. These terms are particularly important because they control the resulting bounded roll motion amplitude. Various components of roll damping maybe classified as shown in Eq. (2-13) (Chakrabarti, 2001)

$$B_{eq} = B_f + B_e + B_W + B_L + B_{BK} \tag{2-13}$$

Here, B_{eq} is the equivalent or total damping, B_f is the hull skin friction damping, B_E is the hull eddy shedding damping, B_W is the free surface radiated wave damping, B_L is the lift force damping and B_{BK} is the bilge keel damping.

The bilge keel damping is composed of different components as shown in Eq. (2-14)

$$B_{BK} = B_{BKH} + B_{BKN} + B_{BKW} \tag{2-14}$$

Here B_{BKN} is the normal force damping due to the normal force on the bilge keel and

B_{BKN} is hull pressure damping due to the pressure changes caused by the bilge themselves. B_{BKW} is the wave damping of the bilge keel.

Estimating non-linear damping is a complicated task since some of these components are coupled to each other. Empirical formulas based on experimental studies are developed to evaluate each of these components. A detailed list of various methods available for evaluating each of the components is given by (Himeno, 1981). It is general practice to present the non-linear damping $B\left(\dot{\phi}\right)$ as shown in Eq. (2-15)

$$B\left(\dot{\phi}\right) = B_1\dot{\phi} + B_2\dot{\phi}\left|\dot{\phi}\right| + B_3\dot{\phi}^3 \tag{2-15}$$

The coefficients of linear damping (B_1), quadratic drag (B_2) and cubic damping (B_3) are obtained from the various components of the roll damping. The non-linear models used in the current study neglects the cubic damping part. In general, B_1 includes the non-viscous damping components (B_L, B_{KW}, B_W) where as B_1 is composed of the viscous damping components ($B_f, B_e, B_{BKH}, B_{BKN}$). Details of calculation of (B_1) and (B_2) can be found in (Himeno, 1981).

The equation of motion for parametric rolling with non-linear damping and linear time varying stiffness is given by Eq. (2-16)

$$\left(I_{44} + A_{44}\left(\omega_D\right)\right)\ddot{\phi} + \left(B_1\left(\omega_D\right)\right)\dot{\phi} + B_2\left(\omega_D\right)\left|\dot{\phi}\right|\dot{\phi} + \nabla g\left(GM_0 + \delta GM\left(t\right)\right)\phi = 0 \tag{2-16}$$

The form of the quadratic damping makes it difficult to analyze analytical models. An equivalent linear form of the non-linear damping is used to develop analytical models.

The following form of non-linear damping model (amplitude depended) is utilized where energy balance in damping is used (Chakrabarti, 2001)

$$B\left(\dot{\phi}\right) = B_{eq}\dot{\phi} \tag{2-17}$$

where,

$$B_{eq} = B_1 + \frac{8}{3\pi} B_2\left(\omega R_0\right) \tag{2-18}$$

Here R_0 is the roll amplitude. As seen from Eq. (2-18), the equivalent damping is dependent on the roll motion amplitude that is not known ahead of time. This makes the use of equivalent damping a little tricky.

Substituting Eq. (2-18) into Eq. (2-16) and non-dimensionalizing we get,

$$\frac{d^2}{d\tau^2}\phi + \left(\mu_1 + \mu_2\left(R_0\right)\right)\frac{d}{d\tau}\phi + \left(\alpha + \frac{\delta GM\left(t\right)}{GM_0}\alpha\right)\phi = 0 \tag{2-19}$$

Here, $\mu_1 = \dfrac{B_1(\omega_D)}{(I + A_{44}(\omega_D))\omega}$ and $\mu_2 = \dfrac{8}{3\pi}\dfrac{B_2(\omega_D)\omega_D}{(I + A_{44}(\omega_D))\omega}$ are the linear and quadratic damping coefficients.

Depending on the method of representation of time varying GM ($\delta GM\left(t\right)$) we get Mathieu's equation (Eq. (2-20)) and Hill's equation (Eq. (2-21)) with non-linear damping. The main motive towards using the method of equivalent damping is to develop a method to incorporate the effects of non-linear damping into the stability boundaries and predict the amplitude of parametric rolling motion. At this point in time,

no studies have been done using the above proposed method to predict the roll motion amplitude.

$$\frac{d^2}{d\tau^2}\phi + \left(\mu_1 + \mu_2\left(R_0\right)\right)\frac{d}{d\tau}\phi + \left(\alpha + \gamma\cos\tau\right)\phi = 0 \tag{2-20}$$

$$\frac{d^2}{d\tau^2}\phi + \left(\mu_1 + \mu_2\left(R_0\right)\right)\frac{d}{d\tau}\phi + \left(\alpha + \gamma\sum_{n=1}^{\infty}\left(C_n\cos(n\tau) + S_n\sin(n\tau)\right)\right)\phi = 0 \tag{2-21}$$

2.3 Ship Parameters

In order to develop tools to analyze parametric rolling it is essential to select a ship that is known to exhibit parametric rolling. For the current study a modified C11 Hull form is used (Courtesy of MARIN). The model called *Pram* aft body is a typical post-Panamax container hull form with a fuller aft section. Extensive model test studies of this model have been done (MARIN Report No 17701-2-SMB, 2005). The results of the model tests confirm that the hull form is susceptible to parametric rolling motion. Here the modified C11 hull form is used as the basis to study parametric rolling in ships. Throughout the current work, all the results shown are for the Pram aft body hull form. In addition to above mentioned studies, several researchers (Belenky et al., 2003; France et al., 2001) have also used the hull form for their studies on parametric rolling motion in ships. The main particulars of the modified C11 hull form are given in Table 1. Important parameters to be noted are the still water GM and the roll natural period. The critical wave period is taken equal to the length between perpendiculars. It is interesting to note that the critical wave period is close to half the natural roll period which essentially makes the hull form susceptible to parametric instability.

Table 1
Main Particulars of C11 hull form (pram aft body)

L_{PP} (m)	262.00
B (m)	40.00
D (m)	24.45
Mean Draught (m)	11.50
Displacement (tones)	69128.00
KG (m)	18.37
GM_t (m)	1.96
Natural Roll Period ,T_Φ (sec)	25.14

The body plan of the hull form is shown in Figure 3. The sharp variation in the hull form along the depth of the vessel can be seen from the body plan. The aft and forward section of the vessel has a large variation in the section shape along the depth. These are typical for container ships in order to reduce the resistance and achieve higher transit speed. The variation of the sectional shape and wide flared decks are clearly evident from the 3D wire mesh model shown in Figure 4.

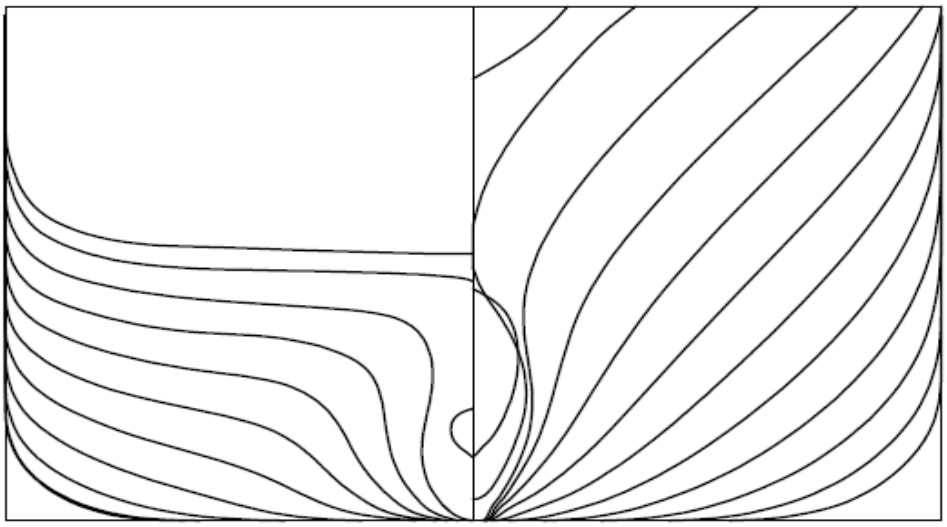

Figure 3. Body plan of modified C11 hull form (not to scale)

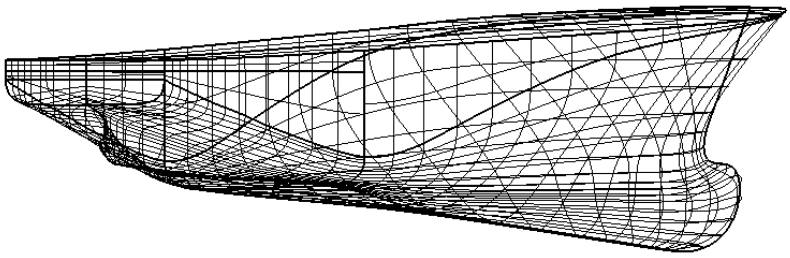

Figure 4. 3D wire-mesh model of C11 hull form

Figure 5 shows the fish eye view of the underwater hull of C11 hull form in waves. Two extreme cases of vessel with wave crest amidships and wave trough amidships are shown to indicate the change in underwater hull shape. This change can lead to change in water plane area resulting in different metacentric height which is the main cause for parametric roll motion in ships.

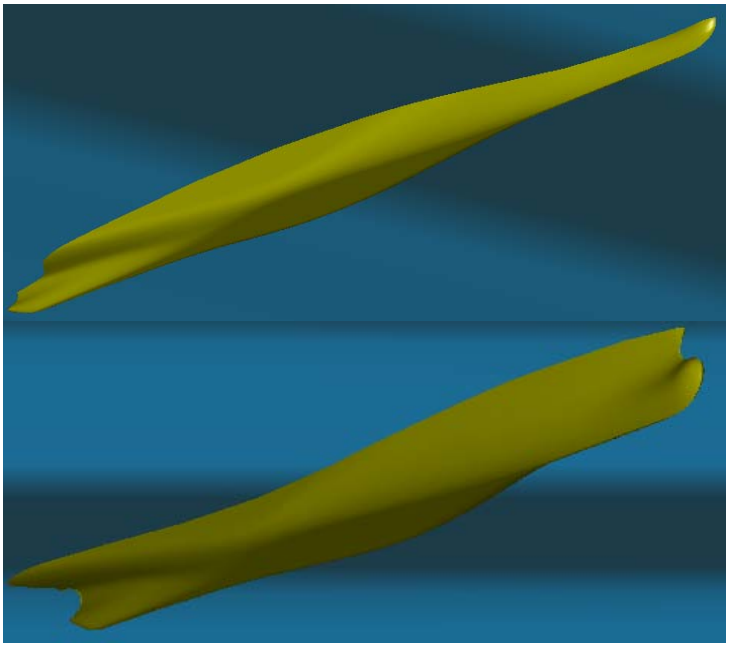

Figure 5. Change in underwater hull form in waves of modified C11 hull form. Top -Wave crest amidships, Bottom -Wave trough amidships. Wave length=Ship L_{PP}

CHAPTER III

REGULAR WAVE ANALYSIS

3.1 Floquet Theory

As discussed in Chapter I, Floquet theory is a mathematical tool for studying the local stability of linear differential equations with time varying periodic coefficients. Floquet theory provides the means to assess the local stability of equilibrium solutions or limit cycles. The equation of motion is represented in the state space (1st order) form as given by Eq. (3-1)

$$\frac{d}{dt}(\underline{X}) = \underline{B}(t)\,\underline{X} \tag{3-1}$$

where $\underline{X}$ is the state space matrix of order (Nx1) and $\_B(t)$ is the periodic time varying coefficient matrix with period $T_{\min}$ such that $B(t+T_{\min}) = B(t)$ of order (NxN). Here N is the number of states in the system and $T_{\min}$ is the minimum period of the system.

Now if χ is a solution to Eq. (3-1) then

$$x(t+T_{\min}) = \alpha x(t) \tag{3-2}$$

$$x(t+lT_{\min}) = \alpha^{l} x(t) \tag{3-3}$$

If α is the l^{th} root of 1 then

$$x(t+lT_{\min}) = x(t) \tag{3-4}$$

If Φ is the fundamental matrix such that

$$\frac{d}{dt}\underline{\Phi} = \underline{B}(t)\underline{\Phi} \tag{3-5}$$

Then

$$\underline{\Phi}\left(t + T_{\min}\right) = \underline{\Phi}\left(t\right)\underline{H} \tag{3-6}$$

where

$$\det\left(\underline{H}\right) = e^{\int_0^{T_{\min}} trace\left(\underline{B}(s)\right)ds} \tag{3-7}$$

From linear algebra,

$$\det\left(\underline{H}\right) = \bigcup_{i=1}^{n} \lambda_i \tag{3-8}$$

where λ_i are the eigenvalues of the matrix *Monodromy* matrix $\underline{H}$

If $\underline{\Phi}_M\left(t\right)$ is a solution to Eq. (3-5) such that

$$\underline{\Phi}_M\left(t_0\right) = I_N \tag{3-9}$$

Then $\underline{\Phi}_M\left(t_0\right)$ is called the *Matrizant* matrix. Here I_N is the identity matrix of order (NxN)

If $\underline{x}_k^{\,n}\left(t\right)$ is a normal solution of Eq. (3-5) which is defined as

$$\underline{x}_k^{\,n}\left(t\right) = \sum_{j=1}^{N}\left(\underline{\psi}_{Mk}\right)_j \underline{\Phi}_{Mj}\left(t\right) = \underline{\Phi}_M\left(t\right)\underline{\psi}_{Mk} \tag{3-10}$$

where, $\underline{\psi}_{MK}$ is the k[th] eigenvector of $\underline{H}$ such that

$$\underline{H}_M \underline{\psi}_{Mk} = \underline{\lambda}_{Mk} \underline{\psi}_{Mk} \tag{3-11}$$

Using Eq. (3-10), (3-11) and (3-6) we get

$$\underline{x}_k^{\,n}\left(t + T_{\min}\right) = \lambda_{Mk} \underline{x}_k^{\,n}\left(t\right) \tag{3-12}$$

If ρ_{Mk} is the characteristic exponent defined as

$$\rho_{Mk} = \frac{1}{T_{\min}} \ln\left(\lambda_{Mk}\right) \tag{3-13}$$

The total solution to Eq. (3-1) is given by

$$\underline{x}\left(t\right) = \sum_{k=1}^{N} \alpha_k \underline{x}_k^{\,n}\left(t\right) \tag{3-14}$$

where α_k are constants. Substituting Eq. (3-13) and (3-12) into (3-14) we get

$$\underline{x}\left(t\right) = \sum_{k=1}^{N} \alpha_k e^{\rho_{MkR} t} \left(\cos\left(\rho_{MkI}\right) + i \sin\left(\rho_{MkI}\right)\right) \underline{p}_k\left(t\right) \tag{3-15}$$

Here ρ_{MkR} & ρ_{MkI} are the real and imaginary parts of the characteristic exponent and $\underline{p}_k\left(t\right)$ is the auxiliary function defined as $\underline{p}_k\left(t\right) = e^{-\rho_{Mk} t} \underline{x}_k^{\,n}\left(t\right)$

From Eq. (3-15) it is clear that with ρ_{MkR} >0 the solution will increase over time, i.e the periodic solution or equilibrium point under consideration is unstable. In terms of the eigenvalues of the Monodromy matrix, if $\left|\lambda_{Mk}\right| > 1$ then the solution is unstable.

From the above discussion it is clearly evident that the Floquet theory can be effectively used to study the stability of parametric rolling motion in regular waves. Since the periodic time varying coefficient is the only requirement for applying Floquet theory the method can also be extended to study the parametric rolling motion under the influence of non-linear damping.

3.2 Mathieu's Equation and Stability Criteria

Floquet theory requires the evaluation of the monodromy matrix $\Phi_M\left(T_{\min}\right)$ in order to analyze the stability of the solution. This requires numerical integration of the solution. Mathieu (Mathieu, 1868) used Floquet theory to develop a methodology to determine the stability of a special class of equations that satisfy the Floquet theory conditions (Eq. (3-1)) and the periodicity condition $B\left(t+T_{\min}\right)=B\left(t\right)$. The special class of equation has the general form given by Eq. (3-16)

$$\frac{d^2x}{d\tau^2}+\left(\alpha+\gamma\cos\tau\right)x=0 \tag{3-16}$$

Eq. (3-16) is the most general form of the Mathieu's equation. The damped form of this equation given by Eq. (2-10) will be used to discuss the criteria for stability of the Mathieu's equation. The periodic matrix with $T_{\min}=2\pi$ is given by

$$B\left(t\right)=\begin{bmatrix} 0 & 1 \\ -\left(\alpha+\gamma\cos\tau\right) & -\mu \end{bmatrix} \tag{3-17}$$

From linear algebra the product of eigenvalues of matrix $B\left(t\right)$ is given by

$$\lambda_1 \bullet \lambda_2 = e^{-2\pi\mu} \tag{3-18}$$

From Floquet theory stable solutions imply that $|\lambda_i| \leq 1$, i.e.

Now $\lambda_1 \bullet \lambda_2 < 1$, since $\mu > 1$ (assuming positive damping) (3-19)

For Eq. (3-19) to hold, the eigenvalues of the periodic matrix must be real or they should be complex conjugates of each other. If the eigenvalues are a complex conjugate pairs then

$$\lambda^2 < 1, \Rightarrow |\lambda| < 1 \tag{3-20}$$

If the eigenvalues are real then

$$\lambda_1 < 1 \text{ and } \lambda_2 > 1 \text{ or } \lambda_1 > 1 \text{ and } \lambda_2 < 1 \tag{3-21}$$

This would mean unstable solutions since one of the eigenvalues is greater than 1 and the solution would increase with time. Thus stable solutions exist only when the eigenvalues are complex conjugate pairs. The boundary separating the stable from the unstable solution is given by $|\lambda| = 1$, i.e. $\lambda = 1$ or $\lambda = -1$.

Using Eq. (3-12) we see that

$$x_k{}^n \left(t + lT_{\min}\right) = \lambda_{Mk}{}^l e^{il|\lambda_{Mk}} x_k{}^n \left(t\right) \tag{3-22}$$

For $\lambda = 1$, l=1 satisfies the boundary condition of marginal stability with $T_{\min} = 2\pi$ and for $\lambda = -1$, l=2 with $T_{\min} = 4\pi$. To summarize, the system transitions from the stable to unstable response as one of the eigenvalues of the periodic matrix exits the right

boundary at $\lambda = 1$ (2π periodic solution) and from unstable to stable response as the eigenvalues passes back through the boundary at $\lambda = 1$ (2π periodic solution). The same applies to the boundary at $\lambda = -1$ (4π periodic solution). Also considering the form of the solution we see that the response will be made up of 2π & 4π periodic solutions and their higher harmonics. Figure 6 is a schematic representation of the same.

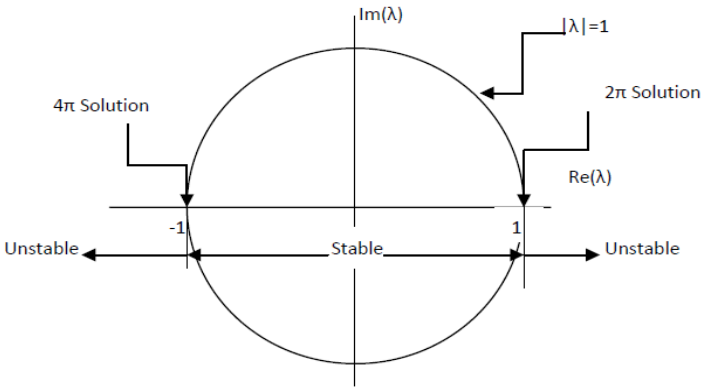

Figure 6. Stability/Instability transition points for normal solutions through 2π and 4π periodic states

3.3 Ince-Strutt Diagram or Stability Charts

The stability of the solution of the Mathieu's equation was investigated by van der Pol and Strutt (van der Pol and Strutt, 1928). They developed a graphical representation of the solution of the Mathieu's equation, which is commonly known as the Ince-Strutt diagram. The diagram is essentially a plot in the parameter (α, γ) domain with curves separating the stable and the unstable region. In many of the literature this diagram is often referred to as stability charts because they provide an easy and convenient method to determine the stability of Mathieu's equation. Both terminologies are used in this

work. Several methods have been developed by researchers to develop the stability boundaries. (Stoker, 1950) used the perturbation method to develop a relationship between the parameters in the Mathieu's equation in the first instability zone. This method has good accuracy close to the α axis and in the first instability zone. The method fails to identify the exact boundary of marginal stability as we move away from the α axis and super harmonic regions. A more robust method, which has good accuracy within the (α,γ) domain for practical purposes, is the Hill's infinite determinant method. We know from the discussion on stability of Mathieu's equation that there are transition values of α and γ for which the Mathieu's equation has solutions that consist of 2π or 4π periodic solutions. Hence it is appropriate to assume a Fourier series representation of the 2π or 4π periodic solution to determine the transition values of α and γ.

For the case of the 2π periodic solution, the response is approximated as

$$x(\tau)=\sum_{j=0}^{\infty}\left(a_j\cos(j\tau)+b_j\sin(j\tau)\right) \tag{3-23}$$

and for the 4π periodic solution as

$$x(\tau)=a_0+\sum_{\substack{j=0\\ j=odd}}^{\infty}\left(a_j\cos\left(\frac{j\tau}{2}\right)+b_j\sin\left(\frac{j\tau}{2}\right)\right) \tag{3-24}$$

Substituting Eq. (3-23) and Eq. (3-24) into the damped Mathieu's equation and setting the secular terms zero we obtain a set of linear homogenous equations in a_j & b_j. We can write the resulting equations in the matrix form as

$$[P][A]=0 \tag{3-25}$$

where, $[P]$ is the parametric matrix consisting of parameters (α,γ) and damping (μ). The determinant of $[P]$ is often referred to as the Hill's determinant. $[A]$ is the matrix containing the Fourier coefficients of response (a_j, b_j). Neglecting the trivial solution ($a_j = b_j = 0$), the determinant of $[P]$ should be equal to zero for Eq. (3-25) to hold. The parametric and coefficient matrices for 2π and 4π periodic solutions are given by

$$\begin{bmatrix} \alpha & \frac{\gamma}{2} & 0 & 0 & 0 & ... & 0 \\ \gamma & \alpha-1 & \mu & \frac{\gamma}{2} & 0 & ... & 0 \\ 0 & \mu & \alpha-1 & 0 & \frac{\gamma}{2} & ... & 0 \\ 0 & \frac{\gamma}{2} & 0 & \alpha-4 & \mu & \frac{\gamma}{2} & 0 \\ .. & & & & & & .. \end{bmatrix} \begin{bmatrix} a_1 \\ b_1 \\ a_2 \\ b_2 \\ a_3 \\ b_3 \\ \\ .. \end{bmatrix} \tag{3-26}$$

$$\begin{bmatrix} \alpha-\frac{1}{4}+\frac{\gamma}{2} & \frac{\mu}{2} & \frac{\gamma}{2} & 0 & 0 & ... & 0 \\ \frac{\mu}{2} & \alpha-\frac{1}{4}-\frac{\gamma}{2} & 0 & \frac{\gamma}{2} & 0 & ... & 0 \\ \frac{\gamma}{2} & 0 & \alpha-\frac{9}{4} & \frac{3\mu}{2} & \frac{\gamma}{2} & ... & 0 \\ 0 & \frac{\gamma}{2} & -\frac{3\mu}{2} & \alpha-\frac{9}{4} & 0 & \frac{\gamma}{2} & 0 \\ .. & & & & & & .. \end{bmatrix} \begin{bmatrix} a_0 \\ b_0 \\ a_1 \\ b_1 \\ a_2 \\ b_2 \\ \\ .. \end{bmatrix} \tag{3-27}$$

By setting the Hill's determinant to zero we obtain the implicit relationship between α, γ and μ. The implicit relation is for the marginal stability condition. The boundary

obtained separates the stable and unstable region. The Ince-Strutt diagram or the stability chart for the undamped and damped Mathieu's equation are obtained by plotting the implicit relationship between the parameters derived from the Hill's determinant. These are is shown in Figure 7 and Figure 8 respectively. In order for the method to produce true boundaries we have to take into account all the terms in the Fourier expansion, this would lead to a Hill's determinant of infinite dimension and thus the name for the method. For practical application we truncate the Fourier series and the number of terms in the Fourier series determine the order of the matrix. Higher orders of the Hill's determinant provide a more accurate stability boundary of the Ince-Strutt diagram. From the stability chart for the undamped Mathieu's equation it is clearly evident that the unstable region reduces in size as we move along the α axis or higher harmonic regions. For parametric roll motion study the first two harmonic regions are of particular interest and the study will be concentrated on these two zones.

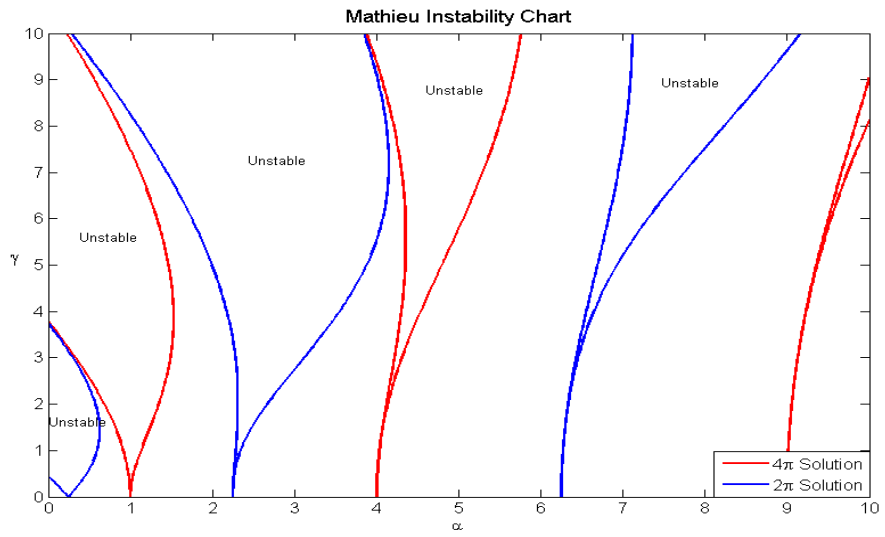

Figure 7. Ince-Strutt diagram for undamped Mathieu's equation (the region between the curves corresponding to 2π and 4π is stable)

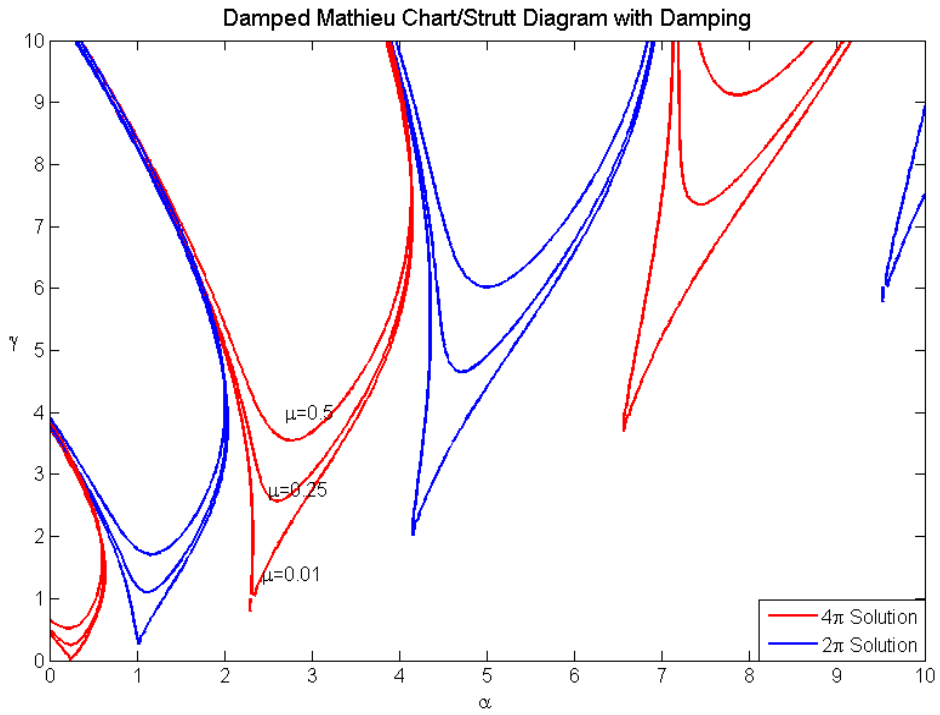

Figure 8. Ince-Stutt diagram for damped Mathieu's equation (the region between the curves corresponding to 2π and 4π is stable)

An interesting point to note from the stability chart for undamped Mathieu's equation is the point where these curves intersect the α axis. The unstable region tends to expand from these points and as result there are more chances of parametric instability when the frequency ratio $\left(\frac{\omega_n}{\omega}\right)$ is close to these points. In order to determine the critical α values, let us consider the undamped Mathieu's equation (Eq. (2-10)) with γ=0. The solution of the resulting equation is given by

$$x(\tau) = A_c \cos\left(\sqrt{\alpha}\tau\right) + A_S \sin\left(\sqrt{\alpha}\tau\right) \tag{3-28}$$

where, A_c and A_S are constants.

The period of the response is given by $T_x = \frac{2\pi}{\sqrt{\alpha}}$. The period of the solution with 2π periodic terms in general is given by $\frac{2\pi}{j}$. Comparing the two periods we get

$$\alpha = j^2, j = 1,2,3 \tag{3-29}$$

Applying the same for solutions with 4π periodic terms with period $\frac{4\pi}{j}$, we get

$$\alpha = \left(\frac{j}{2}\right)^2, j = 1,3,5 \tag{3-30}$$

As a result the first instability zone appears at $\alpha = \frac{1}{4}$ which is a sub-harmonic resonance zone. Other instability zones appear at $\alpha = 1, \frac{9}{4}, 4..$ and so on which are cases of primary resonance and super harmonic resonance. Since the variation in stiffness (γ) required is small in the unstable region near $\alpha = \frac{1}{4}$, there is a high probability of parametric instability when the parametric excitation frequency is close to twice the natural frequency of the system.

3.4 Influence of Linear Damping

For the damped Mathieu's equation, the curves are lifted off from the α axis due to the presence of the damping coefficient. This is clearly evident in Figure 7. Damping in general can be thought to reduce the unstable region of the stability chart. If we examine

the stability chart for the damped Mathieu's equation we see that the curves tend to be wider for higher values of γ. Thus linear damping tend to reduce the unstable region for smaller values of γ and increase the unstable region for higher values of γ. If the stiffness variation of a ship can be represented as a harmonic variation, then the system can be modeled as a damped Mathieu system and the corresponding stability chart can be used to predict the occurrence of parametric roll. For a ship the linear radiated wave damping is a function of response frequency. In the case of parametrically excited roll motion, the ship rolls at its natural frequency due to the absence of direct forcing. For this reason parametric roll motion can be considered as an unforced motion where the motion amplitude is dependent on the magnitude of the variation in stiffness which in turn depends on the indirect forcing. Only the head and following sea cases are studied in this work and the radiated wave damping and the added inertia in roll remain the same for the parametric roll equation of motion.

3.5 Hill's Equation and Stability Charts

So far we have discussed differential equations with the time varying stiffness represented by a single harmonic term. Now we shift our focus to differential equations with non-harmonic stiffness variation. By Fourier theorem we know that any time series can be represented by a Fourier series. For a ship, the hull form is asymmetric about the design water line and also about amidships. As a result the variation in restoring moment will be asymmetric and not harmonic in general. Approximating the variation in stiffness by a Fourier series will be more accurate for ships. The resulting differential equation is called the Hill's equation (Hill, 1886) represented by Eq. (2-12). The Hill's equation can

be thought of as an extension of the Mathieu's equation considering higher order harmonics. Since the variation in stiffness is periodic we can still apply the Floquet theorem to the Hill's equation. In order to develop the curves for marginal stability we follow the same procedure as for Mathieu's equation. Substituting the solution as a Fourier expansion of 2π and 4π periodic terms into Eq. (2-12) and setting the coefficients of secular terms to zero we get the following parametric and coefficient matrices respectively,

$$\begin{bmatrix} \alpha & \frac{\gamma A_1}{2} & \frac{\gamma B_1}{2} & \frac{\gamma A_2}{2} & \frac{\gamma B_2}{2} & \dots & 0 \\ \gamma A_1 & \alpha-1 & \frac{\gamma B_2}{2}+\mu & \frac{\gamma(A_3+A_1)}{2} & \frac{\gamma(B_3+B_1)}{2} & \dots & 0 \\ \gamma B_1 & \frac{\gamma B_2}{2}-\mu & \alpha-1-\frac{\gamma A_2}{2} & \frac{\gamma(B_3-B_1)}{2} & \frac{\gamma(A_3-A_1)}{2} & \dots & 0 \\ \gamma A_2 & \frac{\gamma(A_3+A_1)}{2} & \frac{\gamma(B_3-B_1)}{2} & \alpha-4+\frac{\gamma A_4}{2} & 2\mu+\frac{\gamma B_2}{2} & \dots & 0 \\ .. & & & & & & .. \end{bmatrix} \begin{bmatrix} a_1 \\ b_1 \\ a_2 \\ b_2 \\ a_3 \\ b_3 \\ \\ .. \end{bmatrix} \tag{3-31}$$

$$\begin{bmatrix} \alpha-\frac{1}{4}+\frac{\gamma A_1}{2} & \frac{\gamma B_1}{2}+\frac{\mu}{2} & \frac{\gamma(A_2+A_1)}{2} & \frac{\gamma(B_2+B_1)}{2} & \frac{\gamma(A_2+A_3)}{2} & \dots & 0 \\ \gamma B_1-\frac{\mu}{2} & \alpha-\frac{1}{4}-\frac{\gamma A_1}{2} & \frac{\gamma(B_2-B_1)}{2} & \frac{\gamma(A_2-A_1)}{2} & \frac{\gamma(B_3-B_2)}{2} & \dots & 0 \\ \frac{\gamma(A_2+A_1)}{2} & \frac{\gamma(B_2-B_1)}{2} & \alpha-\frac{9}{4}+\frac{\gamma A_3}{2} & \frac{\gamma B_3}{2}+\frac{3\mu}{2} & \frac{\gamma(A_1+A_4)}{2} & \dots & 0 \\ \frac{\gamma(B_1+B_2)}{2} & \frac{\gamma(A_1-A_2)}{2} & \frac{\gamma B_3}{2}-\frac{3\mu}{2} & \alpha-\frac{9}{4}-\frac{\gamma A_3}{2} & \frac{\gamma(B_4-B_1)}{2} & \dots & 0 \\ .. & & & & & & .. \end{bmatrix} \begin{bmatrix} a_0 \\ b_0 \\ a_1 \\ b_1 \\ a_2 \\ b_2 \\ \\ .. \end{bmatrix} \tag{3-32}$$

Both Eq. (3-31) and Eq. (3-32) when equated to zero yields two solutions. Neglecting the trivial solution we see that the Hill's determinant should be equal to zero for the equations to hold. Thus we obtain the relationship between the parameters and the

damping coefficient, which can be plotted in the parameter domain to obtain the curves of marginal stability for the damped Hill's equation.

Comparing the parametric matrices of Hill's equation (Eq. (3-31) and Eq. (3-32)) to that of Mathieu's equation (Eq. (3-26) and Eq. (3-27)) we see that the coefficients of higher harmonics in the Hill's equation populate the parametric matrices of the Mathieu's equation. In this manner we incorporate the actual variation in the stiffness into the Hill's determinant. Thus the Ince-Strutt diagram developed for Hill's equation will be specific to the system and will change according to the system stiffness. Now we have a much more accurate model which is system specific and the marginal stability boundaries are more realistic and accurate. It is also interesting to note that we can obtain the corresponding Hill's determinant for Mathieu's equation from that for Hill's equation by setting the higher harmonic coefficients ($B_1, A_2, B_2..$) to zero. This confirms the consistency of the method. We will utilize the Hill's equation and the corresponding stability charts to study the parametric roll motion of ships in regular waves.

3.6 Hydrodynamic Analysis

Now that we have developed an accurate model which represents our system, the next step is to evaluate the hydrodynamics coefficients (added inertia, radiated wave damping, non-linear damping) of the vessel (C11 hull form) under study. In order to estimate the hydrodynamic properties we use a linear strip theory program SHIPMO (Beck and Troesch, 1989). The program provides all the coefficient matrices of Eq. (2-1) Only the data for roll motion are extracted from the output for our current study since we

are considering a single degree of freedom equation of motion. The hydrodynamic properties of the vessel are calculated for a frequency range of 0.1 rad/sec to 1.5 rad/sec and forward speeds of 0 m/sec to 10 m/sec. The added inertia in roll is shown in Figure 9. The peak added mass is close to twice the natural frequency $\left(\omega_n = 0.25\right)$ of the vessel in roll. The linear and non-linear damping coefficients for the zero forward speed case are shown in Figure 10. It is clear that the non-linear damping is an order of magnitude greater than linear damping and cannot be neglected for large amplitude motions.

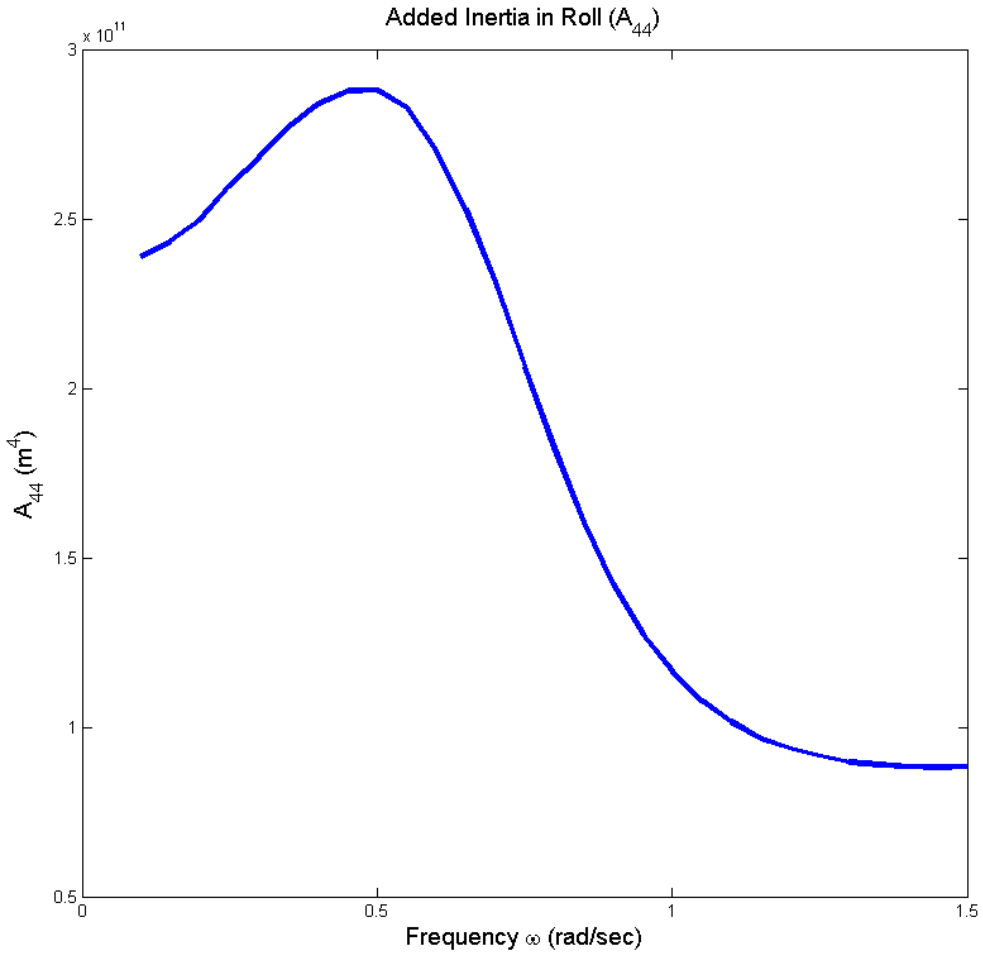

Figure 9. Added inertia in roll as function of frequency for C11 hull form

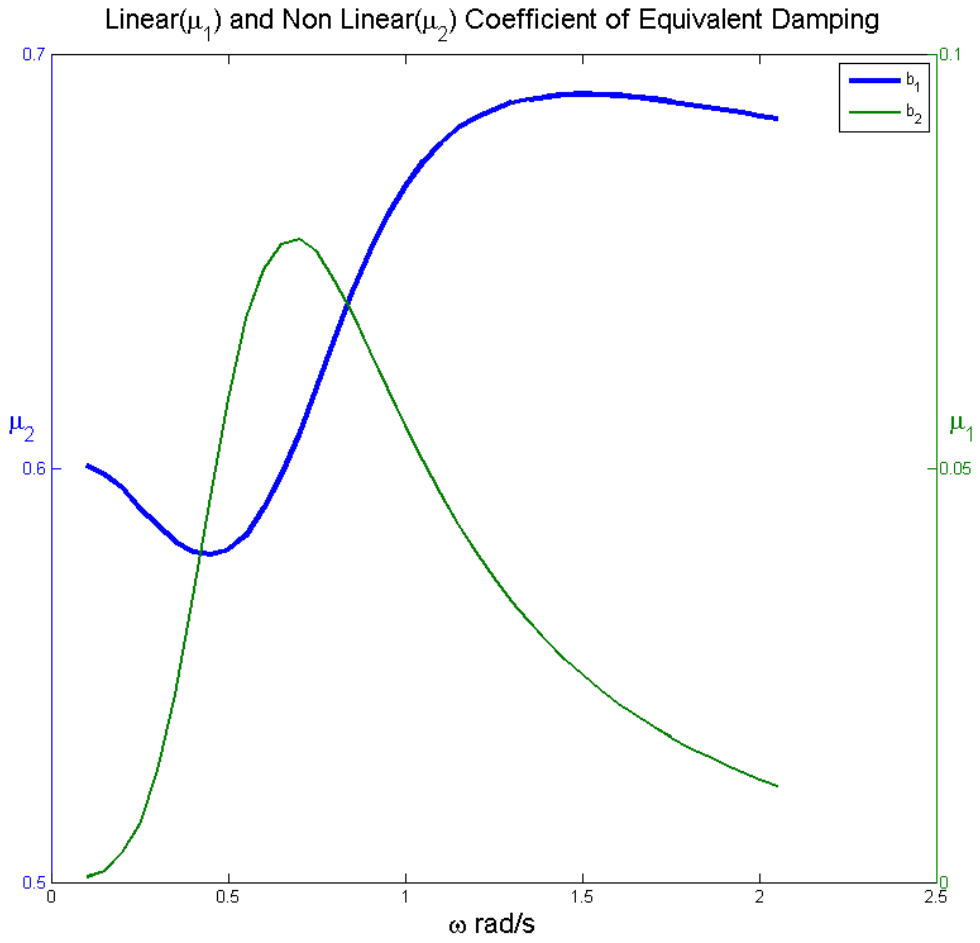

Figure 10. Linear and non-linear damping coefficients as function of frequency for C11 hull form

Also the magnitude of the linear damping coefficient is very small for the vessel, further increasing the chances of parametric roll motion since the linear damping coefficient determines the threshold value of stiffness variation required to invoke parametric roll motion. As discussed only the hydrodynamic properties at or close to the natural frequency of roll are important in the equation of motion since parametric roll is a case of indirectly forced motion. The important hydrodynamic properties of the vessel are summarized in Table 2.

Table 2
Hydrodynamic properties of C11 hull form (pram aft body) estimated using SHIPMO

Displacement-∇(m^3)	6.857×10^7
Roll inertia- I_{44} (m^4)	1.919×10^{10}
Added inertia in roll- $A_{44}(\omega_n)$ (m^4)	2.597×10^{11}
Radiated wave damping in roll- $B_{44}(\omega_n)$ (m^4/sec)	1.736×10^9
Non-linear damping in roll- $B_2(\omega_n)$ (tones)	1.4317×10^{10}
GM_t (m)	1.92
Natural Roll Period ,T_Φ (sec)	27.2

The displacement, GM and the natural period are slightly off the actual ship values, but not significantly and therefore good for qualitative study. Due to software limitations, the entire hull (bulbous bow & transom) are not modeled causing the discrepancy.

3.7 Estimation of GM in Regular Waves

To study the parametric roll characteristics in regular waves we have to estimate the stiffness variation of the vessel in regular waves. A linearized model will be utilized in the analysis and the righting arm is approximated as GM. A standard hydrostatic software (refer MAXSURF© manual) is used to estimate metacentric height in waves. To obtain a time varying GM, the metacentric height for different positions of the wave crest along the length of the ship is estimated. The GM is estimated for the free trim conditions. The following assumptions are made in the estimation of GM in regular waves using the hydrostatic software

1. The displacement of the vessel is assumed to be constant i.e. the vessel is hydrostatically balanced over the wave.

2. The effects of heave and pitch motion on the wave profile is neglected.

3. The wave elevation effects are considered to be the primary cause of GM variation.

In order to determine the critical wave period, the GM in free trim condition is estimated for waves with different wavelength to ship length ratios. From the stability charts we see that the variation in stiffness required for parametric rolling is less near the frequency ratio of ½ in the 1st instability zone. For this reason when the wave frequency is twice or equal to the natural frequency there are more chances of parametric rolling. For C11 hull form the corresponding wave has wavelength very close to the ship length. The case of wavelength equal to ship length appears to be the most critical wavelength for C11 Hull form. The Hill's stability charts for each of the wavelengths can be utilized to determine the critical wavelength or wave period. Deep water wave equations are used in the analysis. The wavelength of the wave is given by

$$\lambda = \frac{2\pi g}{\omega^2} \tag{3-33}$$

Here, ω is the wave frequency in rad/sec and g is the acceleration due to gravity (m/sec^2).

Once the critical period is determined, the threshold wave height that instigates parametric rolling can be estimated using the Hill's stability chart. The GM is estimated for 11 positions of the wave crest along the vessel and we obtain 5 Fourier coefficients to represent the GM variation.

The time varying GM is represented as

$$GM(t) = GM_{mean} + \sum_{j=1}^{4}\left(C_n \cos(\omega t) + S_n \sin(\omega t)\right) \tag{3-34}$$

where GM_{mean} is the sum of still water GM and the zero frequency component of the Fourier expansion.

The Fourier coefficients of the Hill's equation in Eq. (2-12) are obtained from the coefficients in Eq. (3-34) using the following relationship

$$\begin{aligned} A_1 &= \frac{C_1}{GM_{mean}}, B_1 = \frac{S_1}{GM_{mean}}, A_2 = \frac{C_2}{GM_{mean}}, B_2 = \frac{S_2}{GM_{mean}}, \\ A_3 &= \frac{C_3}{GM_{mean}}, B_3 = \frac{S_3}{GM_{mean}}, A_4 = \frac{C_4}{GM_{mean}}, B_4 = \frac{S_4}{GM_{mean}} \end{aligned} \tag{3-35}$$

The linear damping ratio is given by

$$\zeta = \frac{B_{44}(\omega_n)}{\left(I + A_{44}(\omega_n)\right)\omega_n} = 0.003 \tag{3-36}$$

Hence $\omega_D \sim \omega_n$

The procedure of Fourier fitting the time varying GM can also be extended to other terms of the time varying coefficients of the polynomial fit of GZ (Bulian, 2005). The entire time varying righting arm can be reproduced in time domain simulation models in this manner. The effects of the non-linear righting arm are be evaluated using this procedure in section 3.10.7.

3.8 Influence of Forward Speed

Unlike offshore structures ships move in a seaway. This property of ships adds a different dimension to the problem of parametric vibration. The effect of forward speed is similar to that of Doppler effect. Due to the forward speed of the vessel, depending on the direction of wave approach, the vessel tends to encounter waves at different frequencies. There is an apparent shift in the frequency of waves as viewed from the ships perspective due to the velocity of the ship, similar to that of Doppler shift. In terms of parametric instability this effect has mixed consequences. As discussed in previous sections, parametric roll is very sensitive to the frequency ratio. A change in forcing frequency, in this case the encounter frequency, leads to a change in frequency ratio which in turn can instigate parametric roll, increase or decrease the amplitude of parametric roll already present, or even kill the motion depending on the frequency ratio. Thus by merely changing the forward speed, a vessel could jump into large amplitude roll motions without any indication. The scenario becomes critical if the vessel has its parameters (α, γ) for the design speed very close to the boundary between the stable and unstable region of the Ince-Strutt diagram. In this case a small change in the forward speed can lead to parametric rolling of the vessel. This is a very dangerous situation since the speed of the vessel is not constant in waves. Considering these consequences, it is necessary to investigate the influence of forward speed on the parametric roll properties of the vessel and to indentify the safe speed zones.

An added advantage of studying the safe speed zones is that it can be used as a tool for parametric stabilization. Depending on the location of the parameters, the speed of the

vessel can be increased or decreased to stabilize the vessel. Such stability charts can be very useful to captains of vessels known to exhibit parametric roll motions.

The encounter frequency for a vessel moving with a forward speed of U is given by

$$\omega_e = \omega - kU\cos(\beta) \tag{3-37}$$

where, k is the wave number and ω wave frequency

In deep water, the following dispersion relation holds

$$\omega^2 = gk \tag{3-38}$$

Combining Eq. (3-38) and (3-37) we get

$$\omega_e = \omega - \frac{\omega^2}{g}U\cos(\beta) \tag{3-39}$$

Here, g is the acceleration due to gravity and β is the heading angle measured clockwise from the surge direction.

For following sea waves $\beta = 0$ and Eq. (3-39) becomes

$$\omega_e = \omega - \frac{\omega^2}{g}U \tag{3-40}$$

The parametric vibration parameter α in this case is given by $\alpha = \left(\frac{\omega_D}{\omega_e}\right)^2$

Thus for each forward velocity we would obtain different α and the parametric roll stability of the vessel changes with forward speed. Since the waves encountered by the

ship are the same the GM variation will be same as for zero speed, but due to the Doppler effect the frequency of GM variation will be the encounter frequency instead of the wave frequency. For this reason the Hill's coefficients remain the same and so does the corresponding Ince-Strutt diagram.

3.9 Flow Chart of Parametric Roll Analysis in Regular Waves

The process of checking for parametric roll in regular waves for a vessel can be summarized in the following flow chart shown in

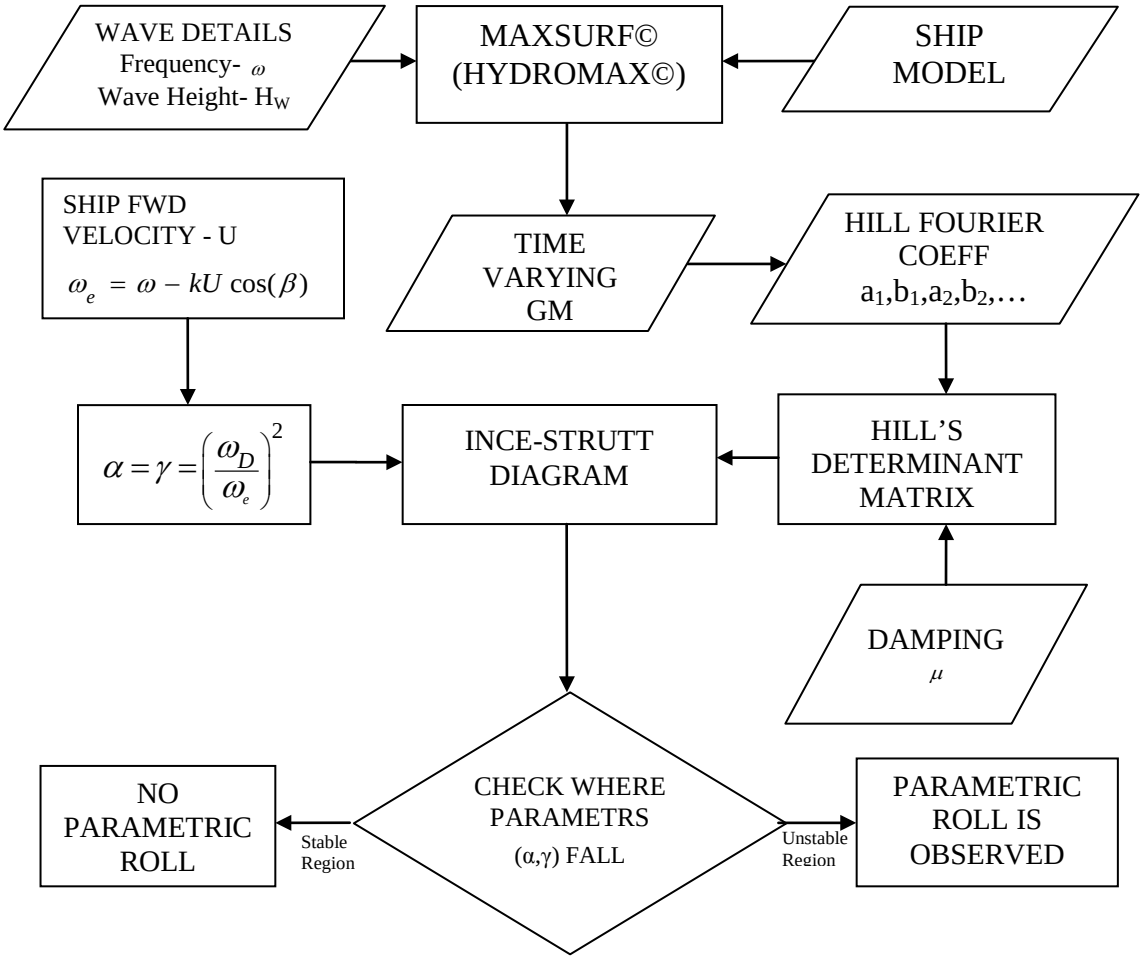

Figure 11. Flow chart for prediction of parametric roll in regular waves

3.10 Results

3.10.1 Varying linear and non-linear damping

As discussed in Chapter II, the damping coefficients in the equation of motion for parametric roll are not constant and vary with the forcing frequency. This is clearly evident from the formulation for linear and non-linear damping coefficients given by

$$\mu_1 = \frac{B_1(\omega_D)}{(I + A_{44}(\omega_D))\omega} \tag{3-41}$$

$$\mu_2 = \frac{8}{3\pi}\frac{B_2(\omega_D)\omega_D}{(I + A_{44}(\omega_D))\omega} \tag{3-42}$$

These damping coefficients can be represented as a function of frequency ratio parameter α so that they can be included in the Hill's determinant matrix and be incorporated into the Ince-Strutt diagram. The linear damping coefficient can be represented as

$$\mu_1 = \frac{B_1(\omega_D)}{(I + A_{44}(\omega_D))}\frac{\sqrt{\alpha}}{\omega_D} \tag{3-43}$$

The nonlinear damping coefficient can be represented as

$$\mu_2 = \frac{8}{3\pi}\frac{B_2(\omega_D)}{(I + A_{44}(\omega_D))}\sqrt{\alpha} \tag{3-44}$$

In many of the previous studies the stability charts show only constant damping curves as shown in Figure 8. Such a representation is not accurate. Figure 12 shows the variation of linear damping coefficient with α.

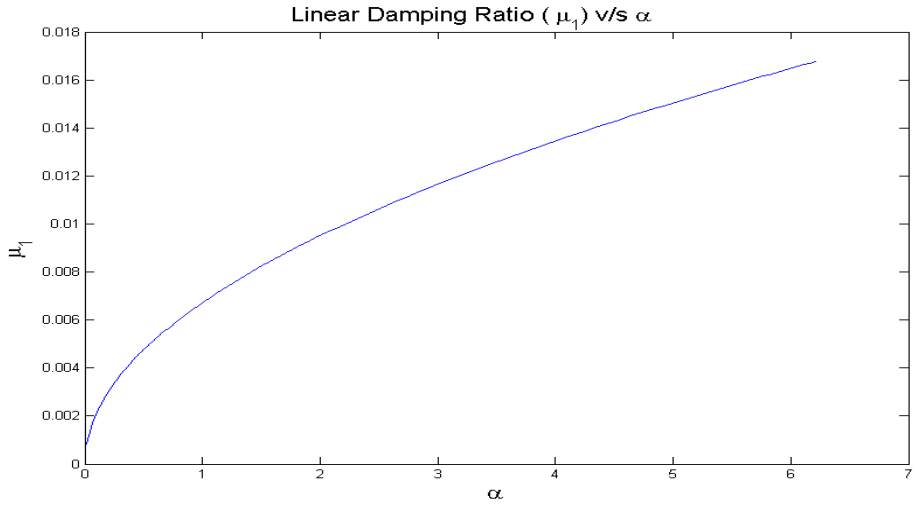

Figure 12. Variation of linear damping ratio with α for C11 hull form

The total equivalent damping coefficient can be represented as

$$\mu = \mu_1 + \mu_2 R_0 \tag{3-45}$$

where R_0 is the resulting roll motion amplitude. Variation of equivalent damping with α and R_0 is shown in Figure 13.

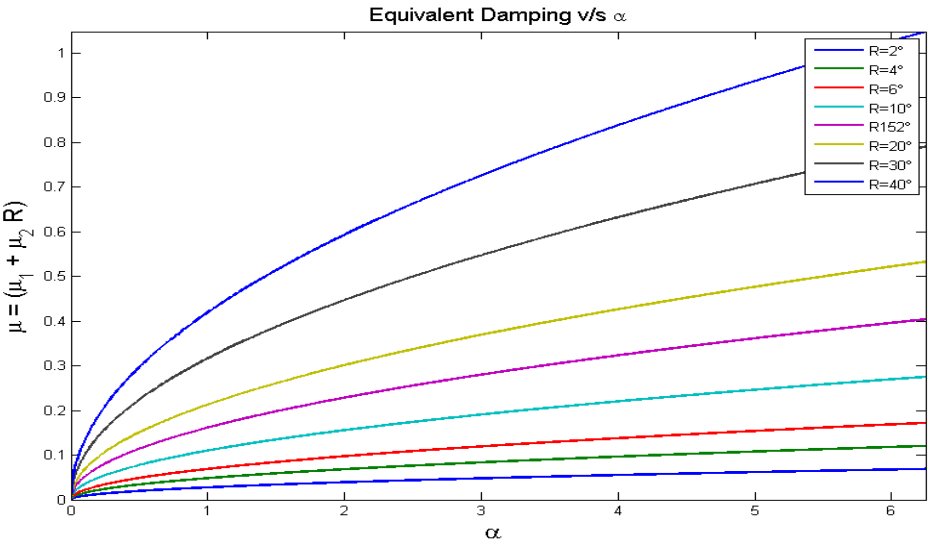

Figure 13. Equivalent damping v/s α

3.10.2 Comparison of Mathieu to Hill's form

In this section we shall evaluate the accuracy of representing the GM variation in the Hill's equation form to that of the Mathieu's equation form. The GM variation in wave is estimated considering a wave of wavelength equal to the ship length and a wave steepness of 1/40. The procedure discussed in Figure 11 is followed. The GM variation in the wave is shown in Figure 14. Zero percent meaning wave crest at bow.

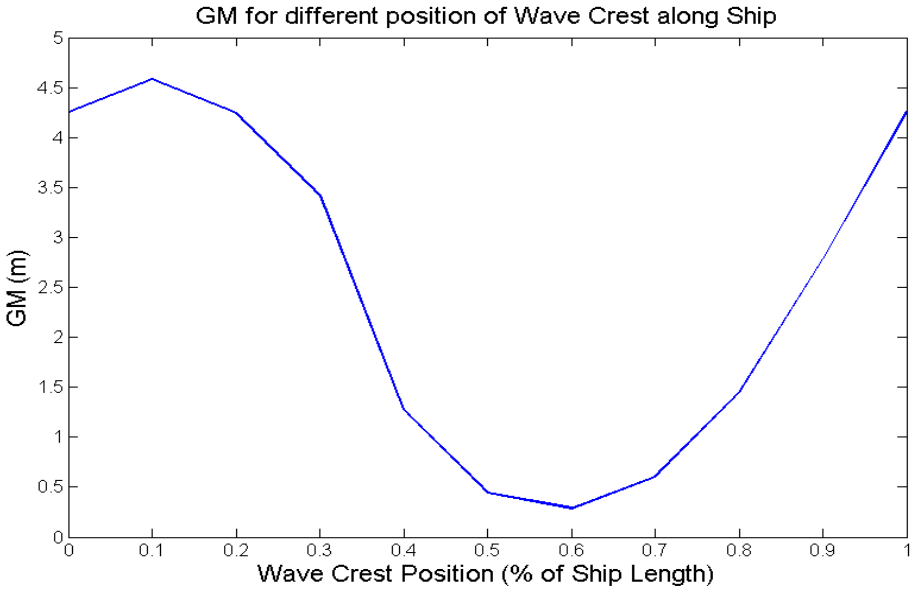

Figure 14. GM for various positions of crest along the length of the ship

The general approach is to approximate this using a harmonic variation so as to represent it using the Mathieu's equation and use the corresponding Ince-Strutt diagram to predict the occurrence of parametric roll. Figure 15 shows the comparison between the cosine fit and the actual GM variation. A phase shifted case is also shown. The phase shift used is $\pi/8$. The poor coherence between the actual and approximation can be clearly seen from the figure.

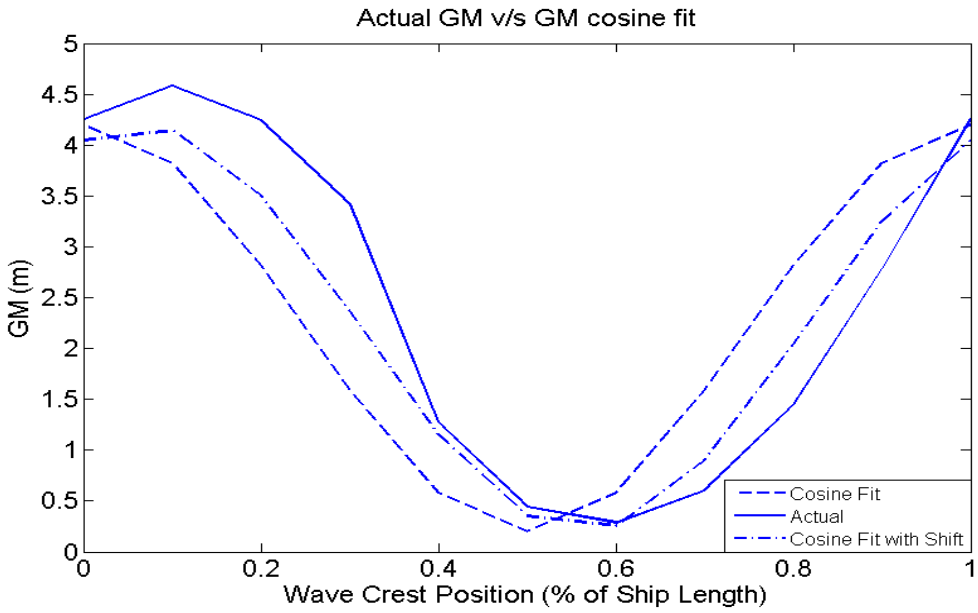

Figure 15. Actual GM variation v/s cosine approximation

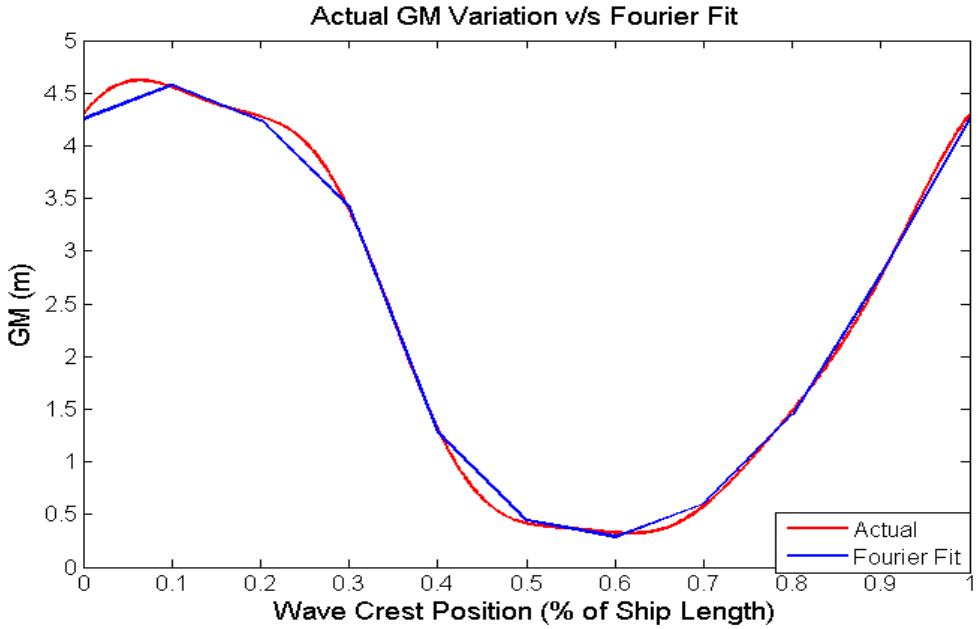

Figure 16. Actual GM variation v/s Fourier fit

Since the cosine approximation does not reproduce the actual variation with good accuracy we use a Fourier approximation for the GM variation. This is shown in Figure

16. The accuracy of the Fourier fit is clearly evident. The corresponding Ince-Strutt diagram for Mathieu and Hill's equation are shown below for comparison.

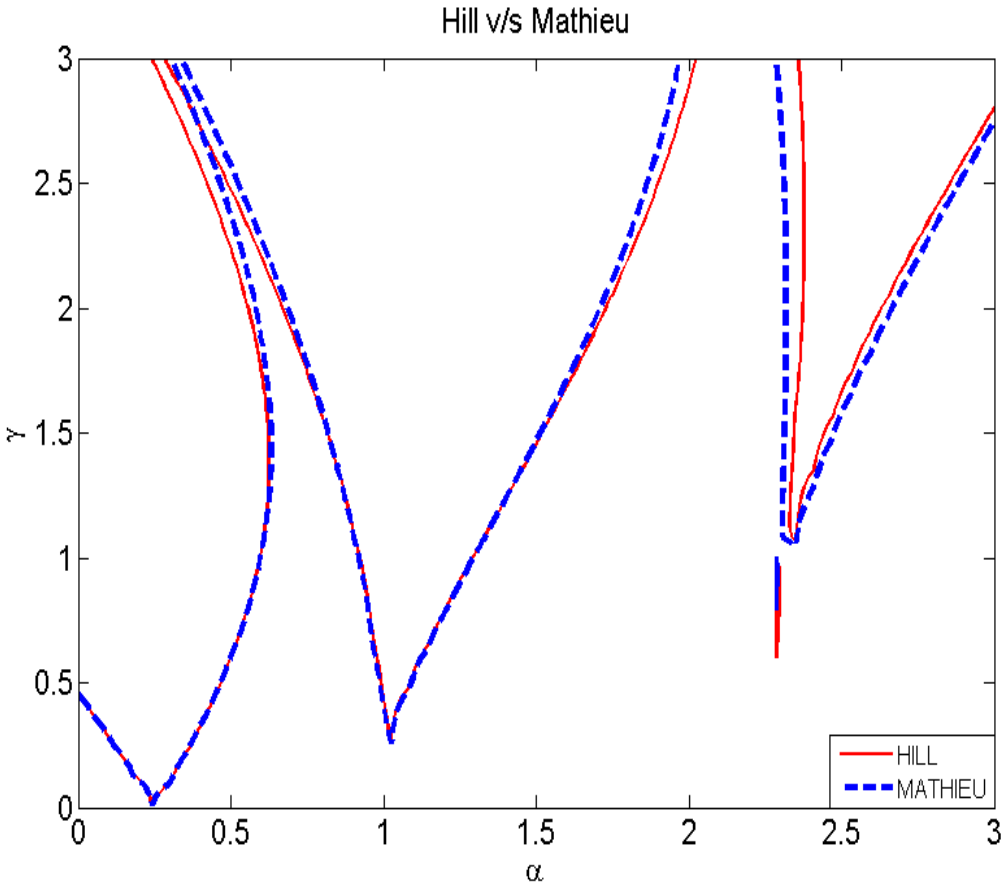

Figure 17. Ince-Strutt diagram comparison for Mathieu's and Hill's equation (H_w=L/40)

Not much difference is seen in the first instability zone, but as we move to higher instability zones the difference even though very little tends to show up. For other wave height cases the difference will be large, since the parametric parameters will be different for Mathieu's form and Hill's form. One of the reasons to use Hill's form is to aid the roll amplitude prediction method. The method is discussed in following sections.

3.10.3 GM variation in waves

In order to study the effects of wave height on the stability chart for Hill's equation GM, variation for different wave heights are developed. The wavelength is kept equal to the ship length for all the waves. Table 3 shows the wave heights used in the analysis. All the analysis are done for zero speed condition in the following analysis.

Table 3
List of waves used in parametric roll analysis

SL. No	1	2	3	4	5
Wave Length (m)	262	262	262	262	262
Wave Height (m)	6.55	5.24	4.367	2.62	1.87
H/L	1/40	1/50	1/60	1/100	1/140

The GM variation obtained for the free trim condition for different cases are shown in Figures 18 and 19.

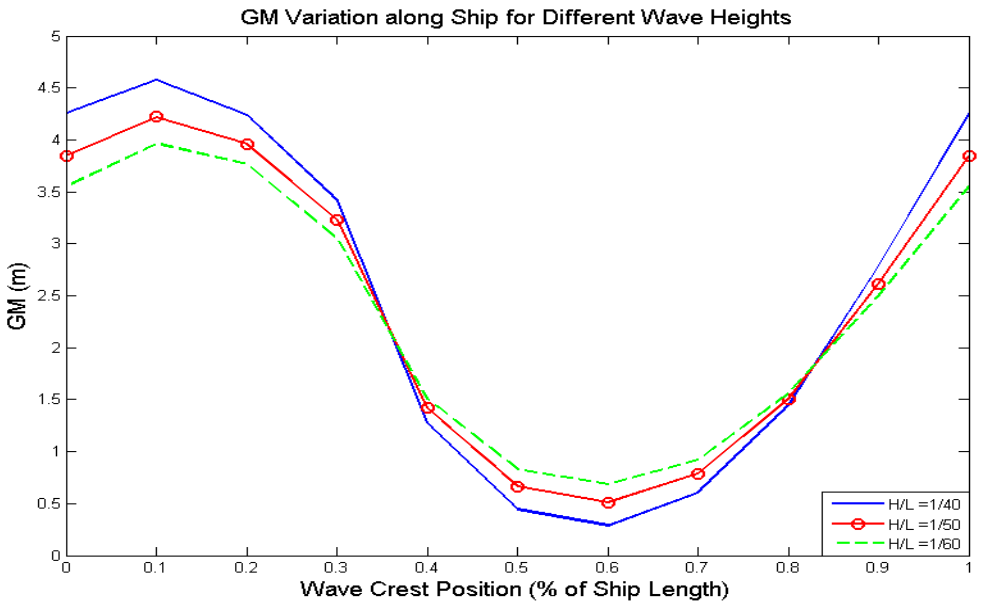

Figure 18. GM variation for different wave heights, wave length=ship length (free trim) (1/2)

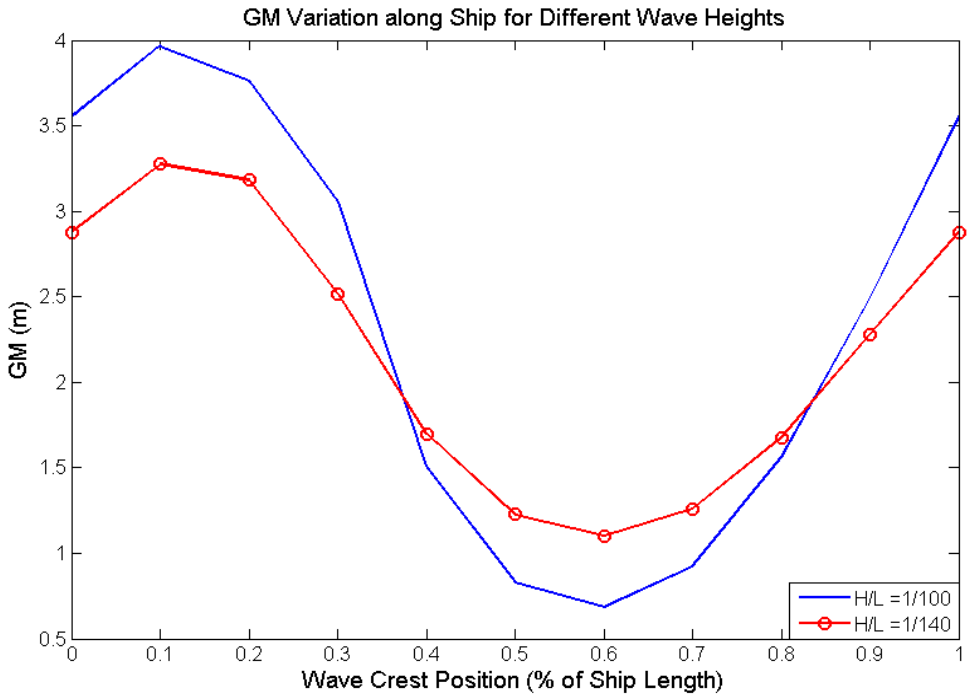

Figure 19. GM variation for different wave heights, wave length=ship length (free trim) (2/2)

The reduction in the amplitude of GM variation can be clearly seen from Figures 18 and 19. An important observation from the GM variation is the mean GM value for each observation. Some of researchers assume that the GM variation occurs about the still water GM. But the analysis shows that the mean value of GM variation is different from that of the still water GM. The mean value of GM for each of the GM variation is reported in Table 4.

Table 4
Mean GM for different wave heights

H/L	1/40	1/50	1/60	1/100	1/140
Still Water GM (m)			1.967		
Mean GM (m)	2.339	2.273	2.232	2.108	2.043

As expected, the mean GM approaches the still water GM as the wave height approaches zero, i.e the still water level. Due to this change in the mean GM, the natural frequency at which the vessel rolls will also be different. But due to the square root dependence of the natural frequency on the GM, the variation is very small.

The Ince-Strutt diagram for each of the wave cases corresponding to the Hill's form of parametric roll equation was developed. The stability charts for each wave height are plotted on the same plot to are shown in Figure 20.

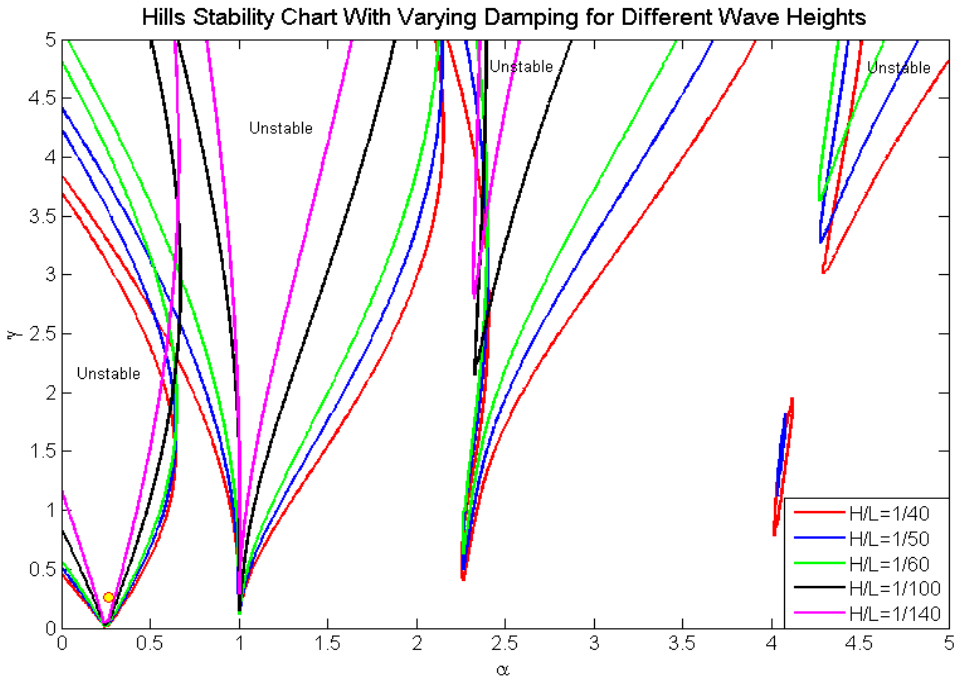

Figure 20. Ince-Strutt diagram of Hill's equation for different wave height (yellow dot (α, γ))

The effect of wave height is clearly evident from the stability chart. As expected, the variation in GM reduces which further reduces the probability of parametric roll or decreases the amplitude of parametric roll. This reduction is reflected in the chart in

terms of reduction in the unstable region leading to an increase in the stable region as the wave height decreases. Also the ship parameter (α,γ) moves closer to the neutral boundary between the stable and unstable region. As a result, the eigenvalues of the response tend to decrease and approach one. The bounded amplitude of the resulting motion will be smaller in comparison to higher wave height cases. Also the ship parameter is found to be in the unstable region for all the wave heights meaning parametric roll is to be expected for all the wave heights.

Numerical simulation results for different wave heights considering only linear damping is shown below in Figures 21 and 22.

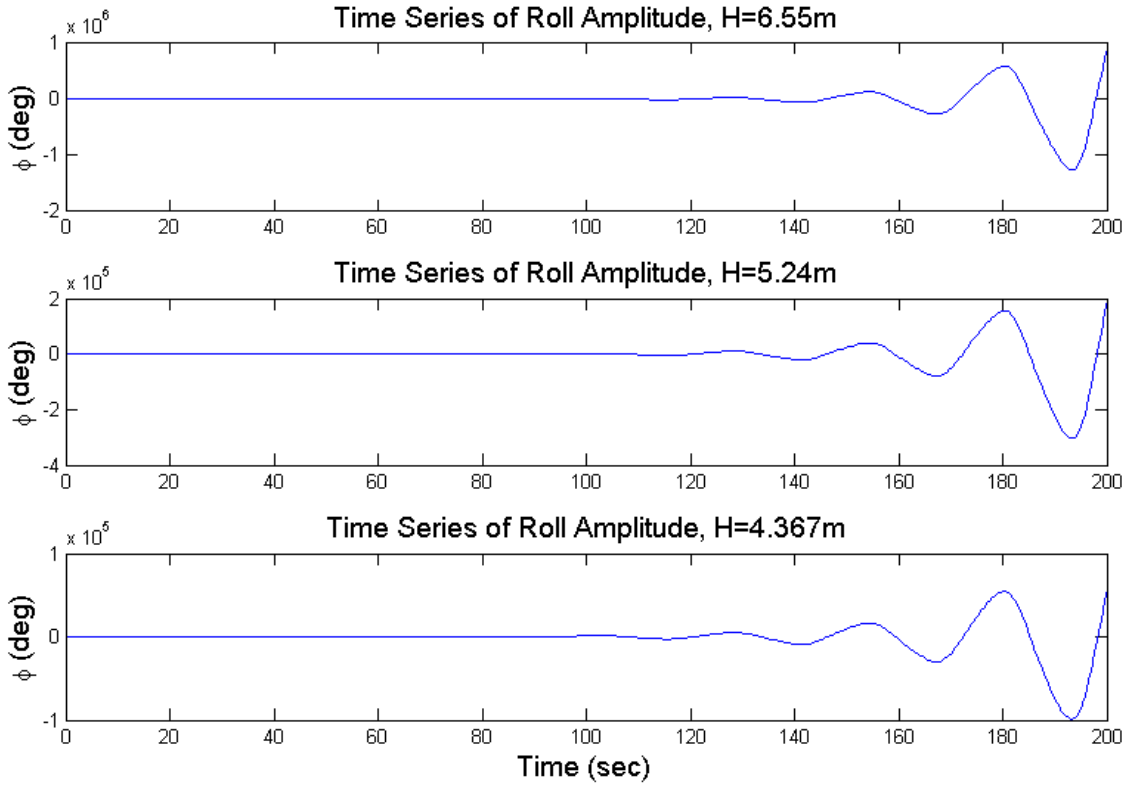

Figure 21. Time series of roll motion with linear damping (1/2)

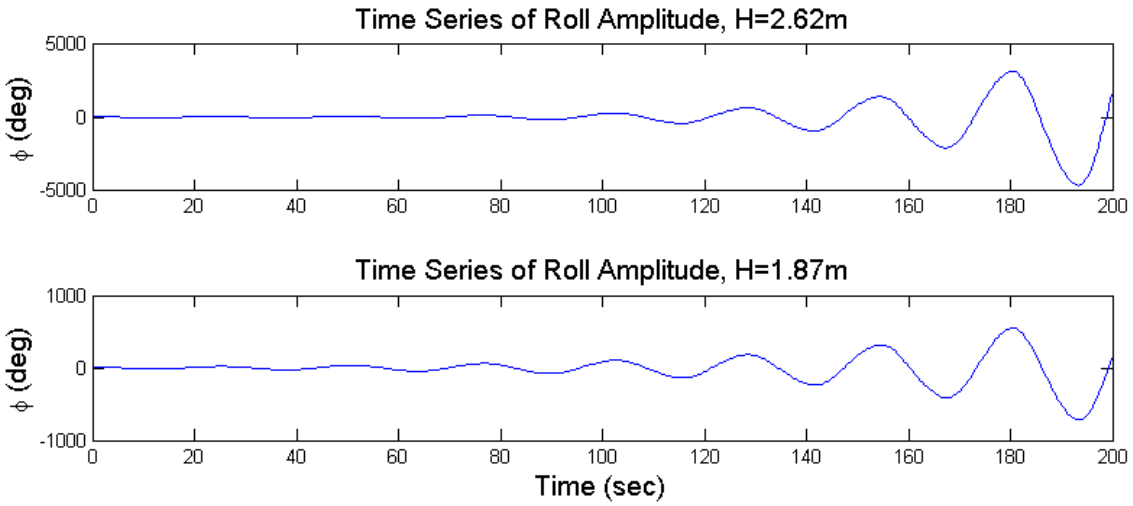

Figure 22. Time series of roll motion with linear damping (2/2)

The findings from the stability charts are clearly supported by the numerical simulations. The decrease in roll amplitude is much higher in comparison to the decrease in the wave height an indication of the non-linear behavior of the system.

3.10.4 Effects of non-linear damping on stability charts

In the previous section the parametric roll motion was analyzed considering the effects of the linear damping and time varying GM. The resulting time series showed a very large unrealistic roll motion amplitude. However such a scenario never happens in the actual situation since non-linear damping becomes predominant with an increase in roll motion amplitude. The effect of non-linear damping can be seen in Figure 13 where the effective damping ratio increases significantly with an increase in roll amplitude. In this section we will incorporate non-linear damping into the stability chart in the form of equivalent damping. Equivalent damping ratio Eq. (3-45) is used in place of the linear damping in the Hill's determinant corresponding to Hill's equation to develop the

stability chart for each roll angle. This results in a three dimensional stability chart as shown in Figure 23.

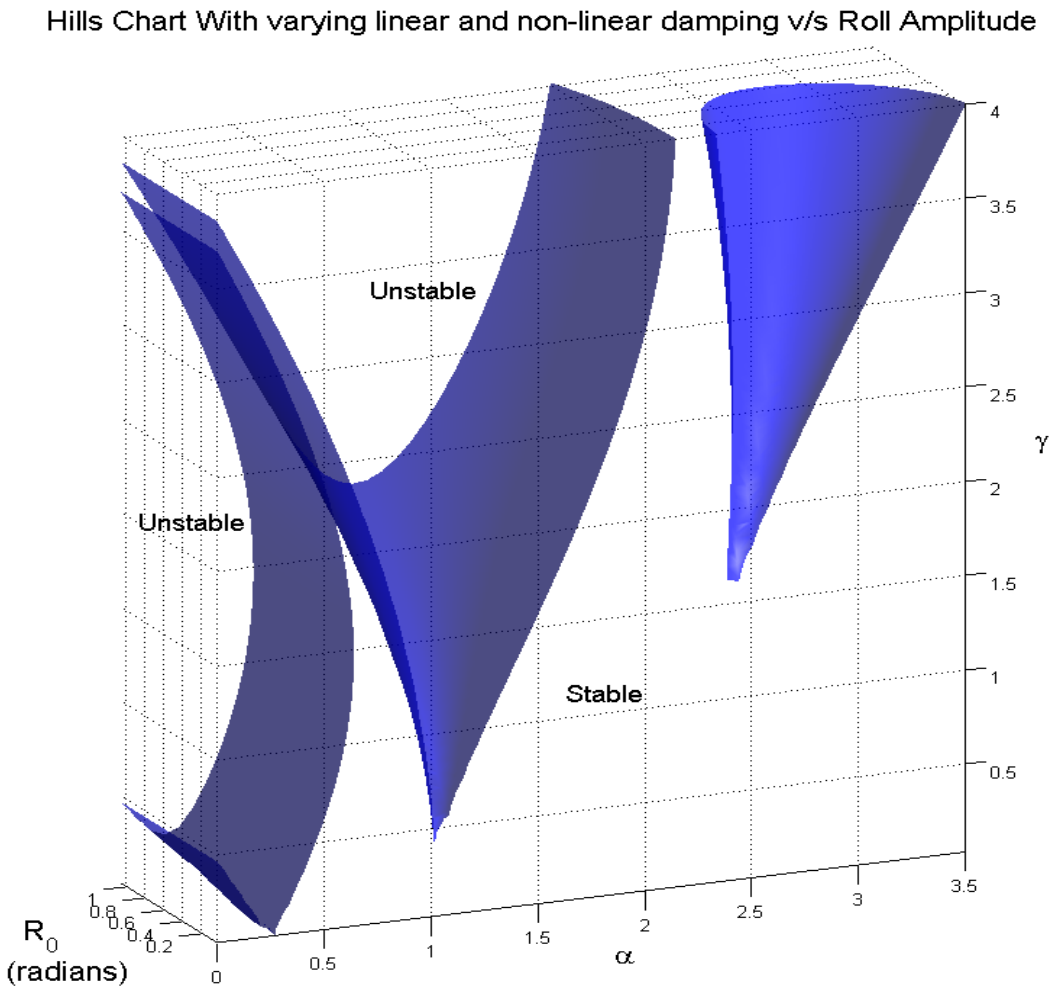

Figure 23. Stability diagram for Hill's equation with linear and non-linear damping (R_0 is bounded roll motion amplitude)

The advantage of developing such a chart is that once the ship parameter for the particular wave is plotted we can project the point onto the surface and the roll amplitude at which the projection intersects with the surface is the resulting bounded roll motion amplitude due to non-linear damping. In terms of energy balance, the energy in the

parametric system is much larger initially in comparison to the damping, which at the start of the motion is mainly linear in character. Due to parametric instability, the roll amplitude increases with time. Due to this increase in amplitude, the non-linear damping terms become important and dissipate more energy. As a result the unstable region in the stability chart decreases until the energy balance takes place. The boundary at that instant represents the neutral region. The corresponding roll amplitude of equivalent damping system represents the bounded amplitude since there is no further increase or decrease of energy in the system. The method discussed above was used to find the bounded roll amplitude for H=6.55 m with forward speed =10 m/sec in following sea condition. The roll amplitude was found to be 20 deg and this is confirmed by Figure 24. The ship parameter falls right on the boundary of the curve.

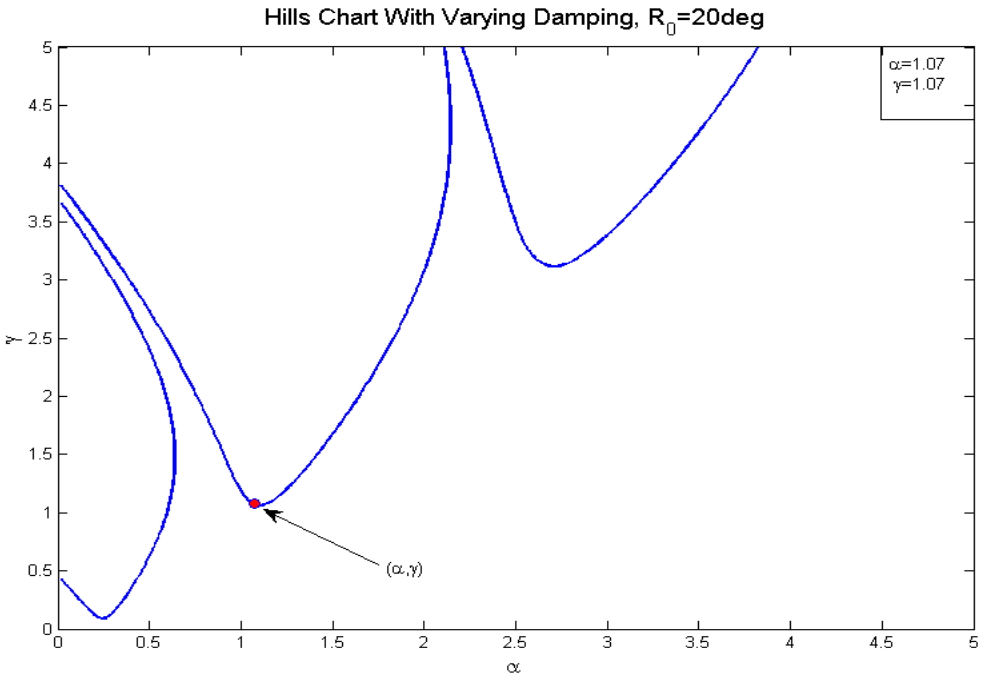

Figure 24. Stability chart with equivalent damping for R_0 = 20 deg, H=6.55 m(U=10 m/sec)

Numerical simulation considering linear and non-linear damping with time varying GM was used to verify the results of the method discussed above. Figure 25 shows the time series of roll amplitude and roll velocity for wave height H=6.55 m with U=10 m/sec . The Roll amplitude was found to be 23.5 deg from the time simulation. The error in the roll amplitude estimated using the 3D chart is about 3.5 deg (< 15%) which is good considering the fact that no simple methods are available to predict the roll motion amplitude.

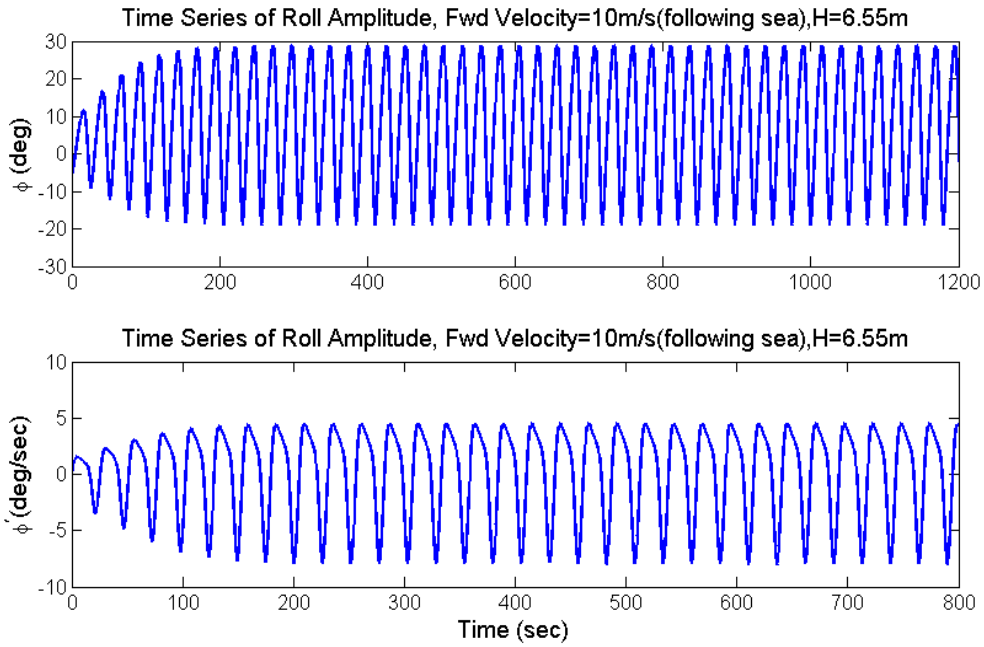

Figure 25. Time series of roll amplitude and roll velocity for H= 6.55 m, Fwd speed =10 m/sec, following sea condition (considering non linear damping)

In a similar manner the bounded roll motion amplitude can be predicted for different wave cases with some amount of accuracy. This simple method can act as the basis for predicting roll motion amplitude for any wave whose GM variation is known and a

linear approximation of GM is valid. The method mentioned above can be very useful in the stability analysis of the vessel in waves during the preliminary design stage .

3.10.5 Parametric roll amplitude prediction using Floquet theory

Floquet theory is a powerful tool for analyzing parametric systems. The theory can be used in the case of a parametric roll as well. The properties of the monodromy matrix is used to develop a tool to predict the roll motion amplitude. The periodic matrix of Eq. (3-1) considering an equivalent damping for the Hill's form of parametric roll equation is given by

$$B(\tau)=\begin{bmatrix} 1 & 0 \\ \left(\alpha+\gamma\sum_{n=1}^{4}\left(A_n\cos(n\tau)+B_n\sin(n\tau)\right)\right) & -(\mu_1+\mu_2 R_0) \end{bmatrix} \tag{3-46}$$

Substituting Eq. (3-46) into Eq. (3-5) we get

$$[\phi]'=[\bar{F}][\phi] \tag{3-47}$$

where,

$$[\bar{F}]=\begin{bmatrix} 0 & 1 & 0 & 0 \\ 0 & 0 & 1 & 0 \\ -f(\tau) & 0 & -(\mu_1+\mu_2 R_0) & 0 \\ 0 & -f(\tau) & 0 & -(\mu_1+\mu_2 R_0) \end{bmatrix} \tag{3-48}$$

And $f(\tau)=\left(\alpha+\gamma\sum_{n=1}^{4}\left(A_n\cos(n\tau)+B_n\sin(n\tau)\right)\right)$

Eq. (3-47) is integrated over the forcing period with the matrizant matrix as the initial condition to obtain the monodromy matrix. The eigenvalues of the monodromy matrix is analyzed for each roll amplitude. The roll amplitude at which the magnitude of the

eigenvalues become one is the bounded roll motion amplitude. The results of the analysis are shown in Figure 26. The variation of both the eigenvalues with roll amplitude are shown.

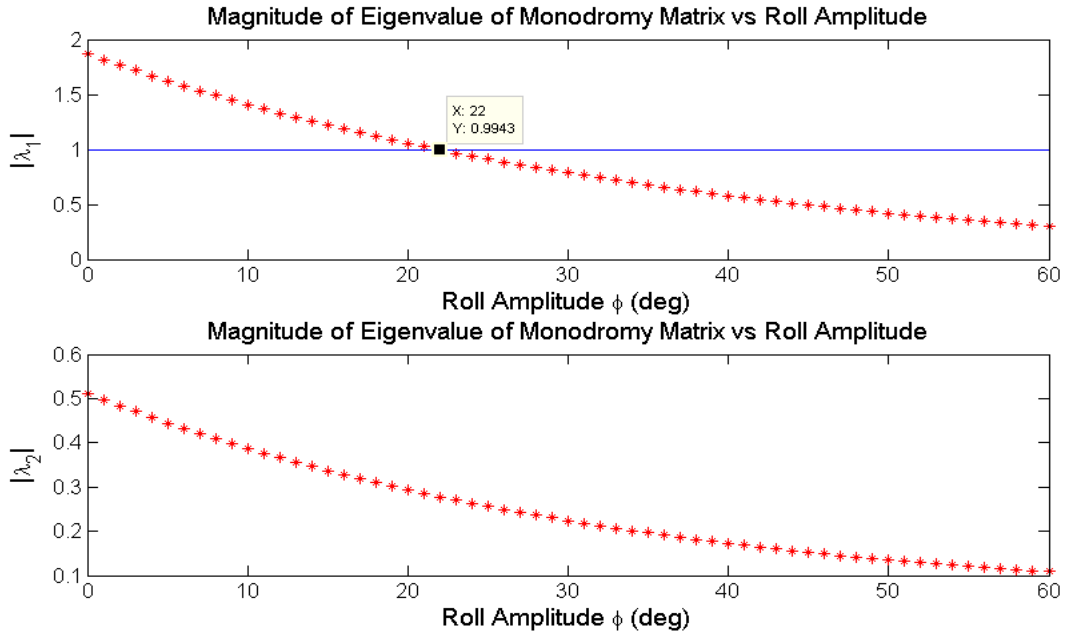

Figure 26. Eigenvalues of monodromy matrix for wave height H=6.55 m (considering equivalent damping)

The roll amplitude estimated using the above method was found to be about 22 deg, very close to the value estimated using the stability chart and within a good accuracy level of the value obtained from the numerical simulation.

3.10.6 Parametric roll with forward speed

In the previous sections we discussed methods to estimate the variation of GM without forward speed. Couple of methods were also discussed to predict the occurrence of roll motion and also estimate bounded roll motion amplitude with reasonably

accuracy. The influence of forward speed (following sea) on the vessel parametric roll characteristics were analyzed based on section 3.8. The list of forward speeds analyzed is shown in the Table 5. The encounter frequencies are shown for the following sea wave condition.

Table 5
List of forward speeds and encounter frequency (following sea)

Wave Frequency (rad/sec)			0.485			
Forward Speed (m/sec)	0.00	2.00	4.00	6.00	8.00	10.00
Encounter Frequency	0.485	0.437	0.389	0.341	0.293	0.245
α	0.274	0.338	0.426	0.554	0.751	1.073

The GM variation will be the same for all the forward speed cases since the wave frequency is the same. The encounter frequency will be different and thus the frequency of variation of GM will be different.

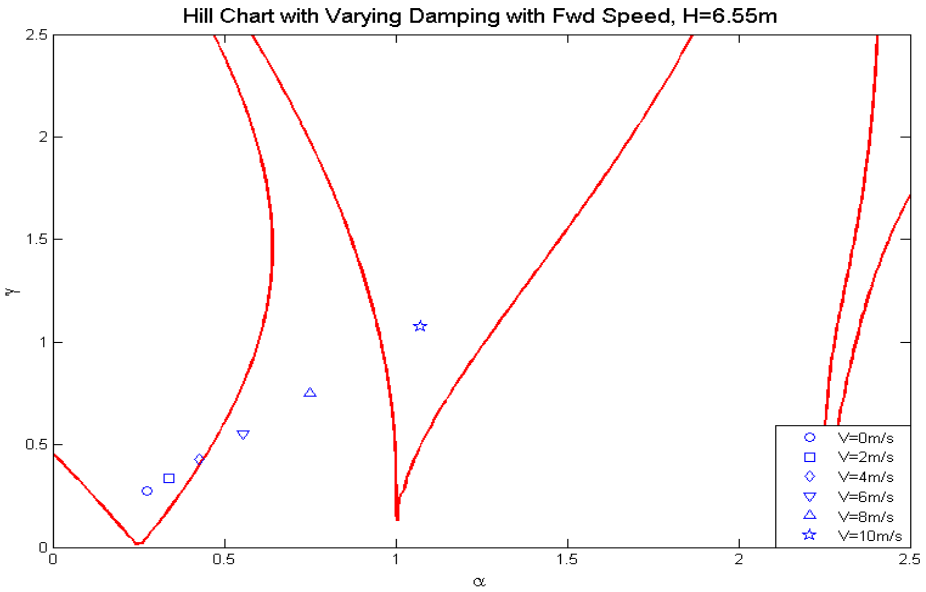

Figure 27. Hill's stability chart for different forward speed, H=6.55 m (following sea condition)

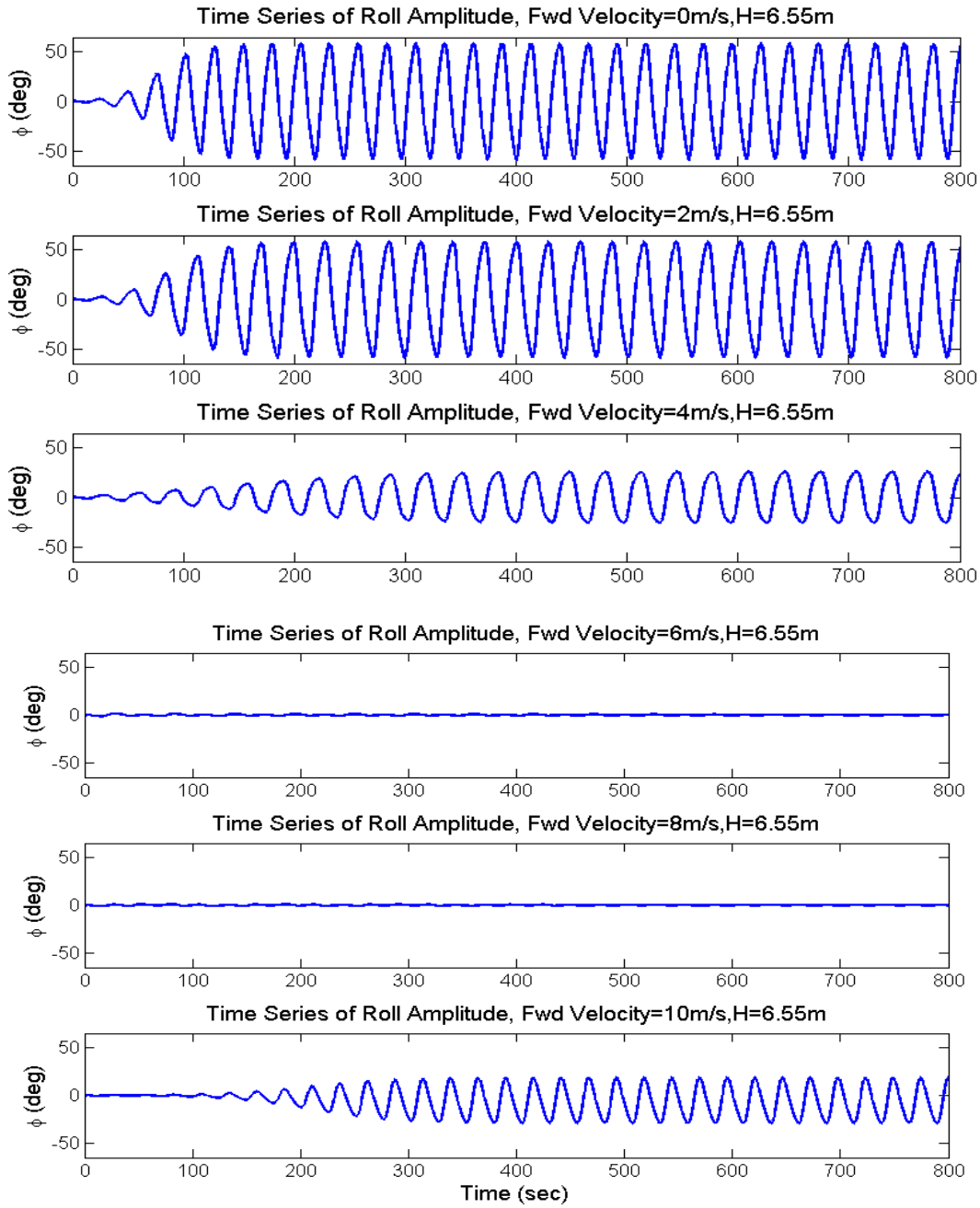

Figure 28. Time series of roll amplitude for different forward speed, H=6.55 m

The results from the chart in Figure 27 are supported by the results of numerical simulations shown in Figure 28, indicating that the charts provide a simple and accurate method for predicting the occurrence of parametric roll. The method discussed in section

3.10.4 and 3.10.5 can be used to predict the roll motion amplitude without running time consuming numerical simulations. Correlating the numerical simulations and the stability chart for Hill's equation, one can infer that the closer the ship parameter is to the neutral boundary, the lower the bounded roll motion amplitude. The Floquet approach can be used to explain this characteristic of parametric roll. The eigenvalues of the monodromy matrix for each forward speed is shown in Table 6. The eigenvalues reported are considering linear and non-linear damping.

Table 6
Eigenvalues of monodromy matrix for different forward speeds (following sea)

Wave Frequency (rad/sec)		0.485	0.485	0.485	0.485	0.485	0.485
Forward Speed (m/sec)		0.00	2.00	4.00	6.00	8.00	10.00
Eigen Value (mag)	$\lvert\lambda_1\rvert$	2.064	1.952	1.263	0.925	0.914	0.451
	$\lvert\lambda_2\rvert$	0.435	0.454	0.691	0.925	0.914	1.786

The magnitude of the unstable eigenvalues for forward speed equal to 4 m/sec is very close to 1. As a result, the damping energy contribution from the non-linear damping required to balance the parametric instability is less leading to lower bounded roll amplitude. For zero forward speed and 2 m/sec the magnitude of the eigenvalues is large resulting in large roll amplitude (in these cases the linear approximation is not valid). For cases with forward speed of 6 m/sec and 8 m/sec both the eigenvalues are less than one and stable and hence no parametric roll. For speed =10 m/sec parametric roll re-surfaces since one of the eigenvalues is greater than 1. The same can be inferred from the stability chart, the ship parameter in this case falls in the 2nd instability zone.

An important finding from this study is that forward speed of a vessel may lead to multiple parametric resonances. This property of forward speed has its own advantages and disadvantages. Depending on where the vessel parameter is with respect to the neutral boundary, the vessel forward speed can be changed to avoid parametric roll. It is well known that in high waves, which is an ideal environment for parametric roll, the vessel speed often fluctuates due to added resistance in waves and also due to voluntary reduction in speed. This can be dangerous since the vessel can dive into large amplitude roll motion without any indication. Thus it is suggested that such stability charts be kept onboard a sea going vessel and the vessel speed so adjusted so as to avoid parametric roll. Similar analysis were carried out for different wave heights and the resulting stability charts are shown in Figures 29 to 32.

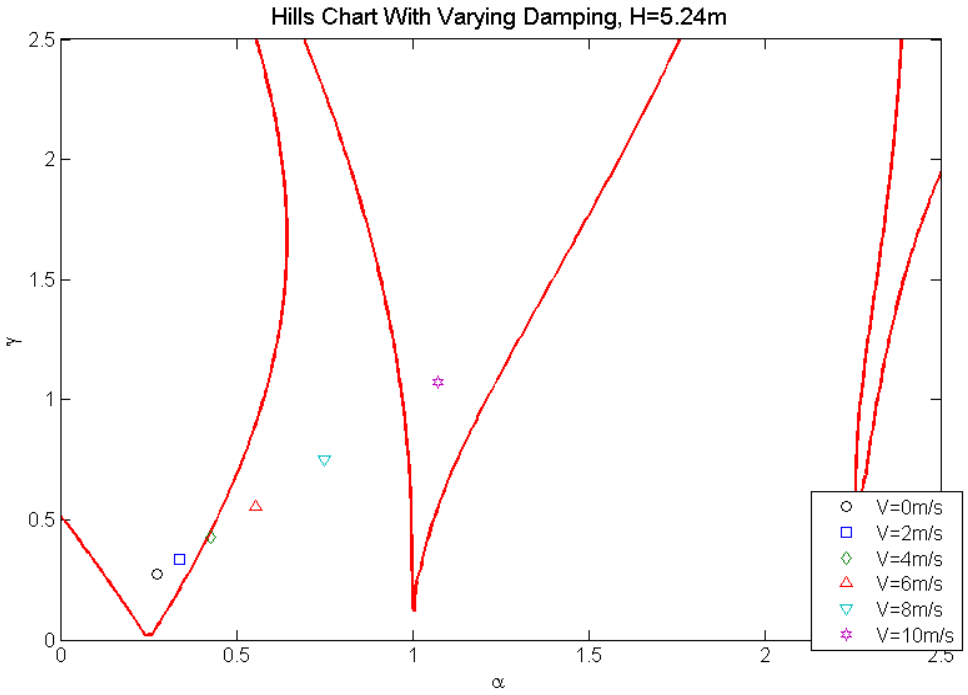

Figure 29. Hill's stability chart for different forward speeds, H=5.24 m(following sea condition)

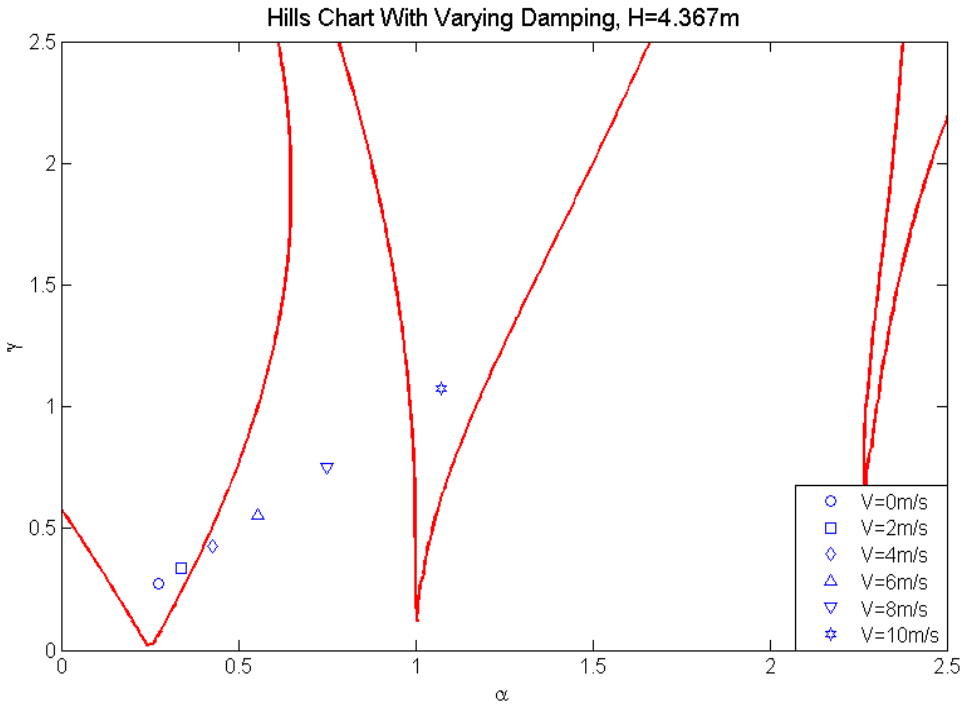

Figure 30. Hill's stability chart for different forward speeds, H=4.37 m (following sea condition)

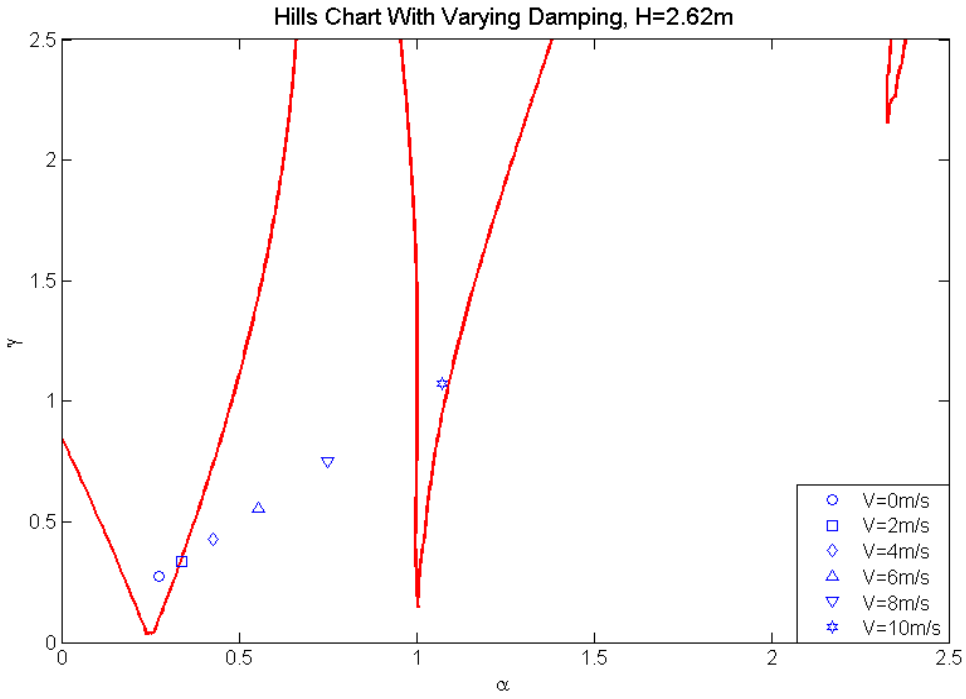

Figure 31.Hill's stability chart for different forward speeds, H=2.62 m (following sea condition)

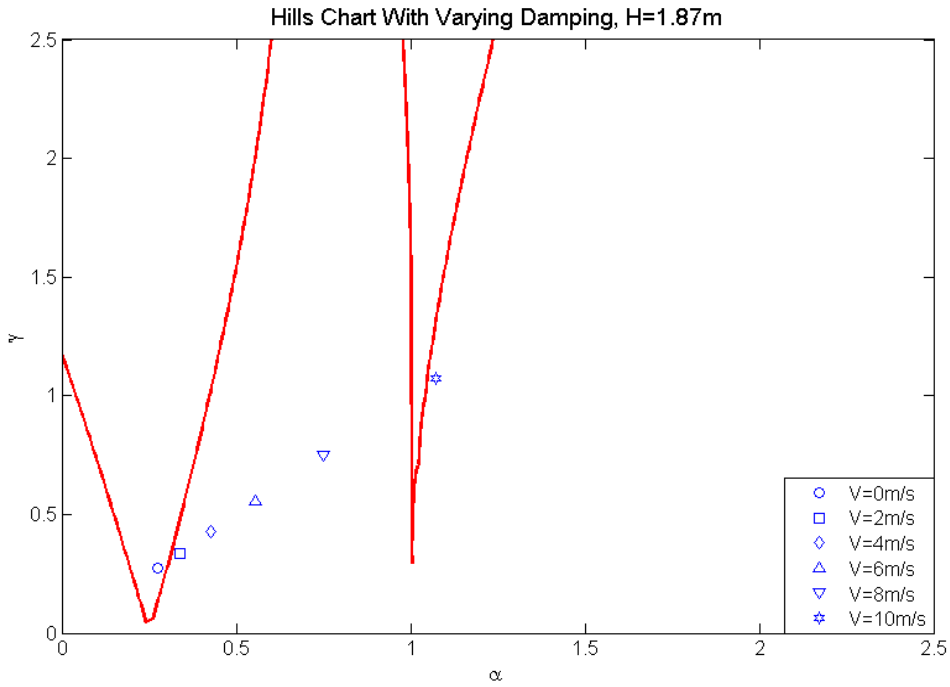

Figure 32.Hill's stability chart for different forward speeds, H=1.87 m, (following sea condition)

As expected with a decrease in wave height the unstable area decreases resulting in a change of stability for different forward speed. As a result less parametric roll is observed in such cases.

Quite often ships move head on into large waves so as to avoid large roll moments in the beam sea. In such a case the vessel forward speed can lead to higher encounter frequency of .waves. The heading angle for head sea condition will be 180 deg as per convention. Table 7 shows the encounter frequency for different forward speeds.

The ship parameters for different forwards speeds in the head sea condition were plotted on the stability chart for Hill’s equation corresponding to wave height H=6.55 m is shown in Figure 33.

Table 7
List of forward speeds and encounter frequencies (head sea condition)

Wave Frequency (rad/sec)	0.485	0.485	0.485	0.485	0.485	0.485
Forward Speed (m/sec)	0.00	2.00	4.00	6.00	8.00	10.00
Encounter Frequency(rad/sec)	0.485	0.533	0.581	0.629	0.677	0.725
α	0.274	0.227	0.191	0.163	0.141	0.123

.

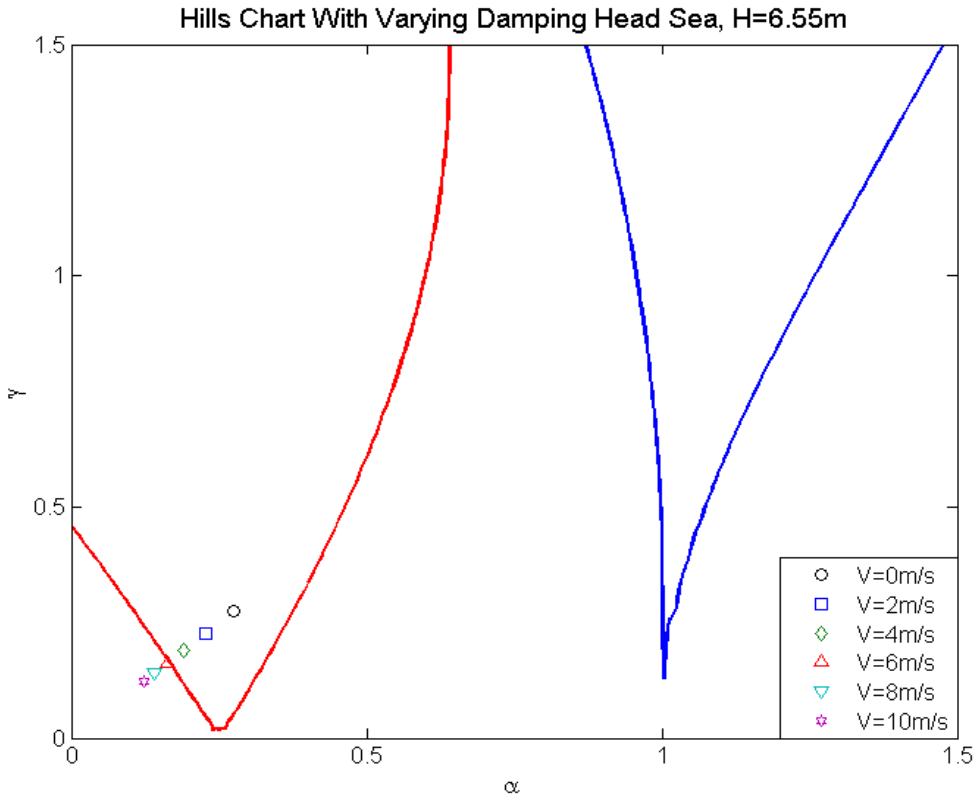

Figure 33.Hiil's stability chart for different forward speeds, H=6.55 m, (head sea condition)

From the stability chart we see that in the head sea condition with the vessel forward speed equal or greater than 6 m/sec no parametric roll is expected. For speeds lower than that the vessel is expected to experience parametric roll motion. Time domain simulations with non-linear damping and time varying linear stiffness were carried out

for the head sea condition to correlate the findings from the stability chart. The method of using the 3D stability chart to predict roll amplitude can be employed to predict the roll amplitude within the range of validity of linear righting arm approximation.

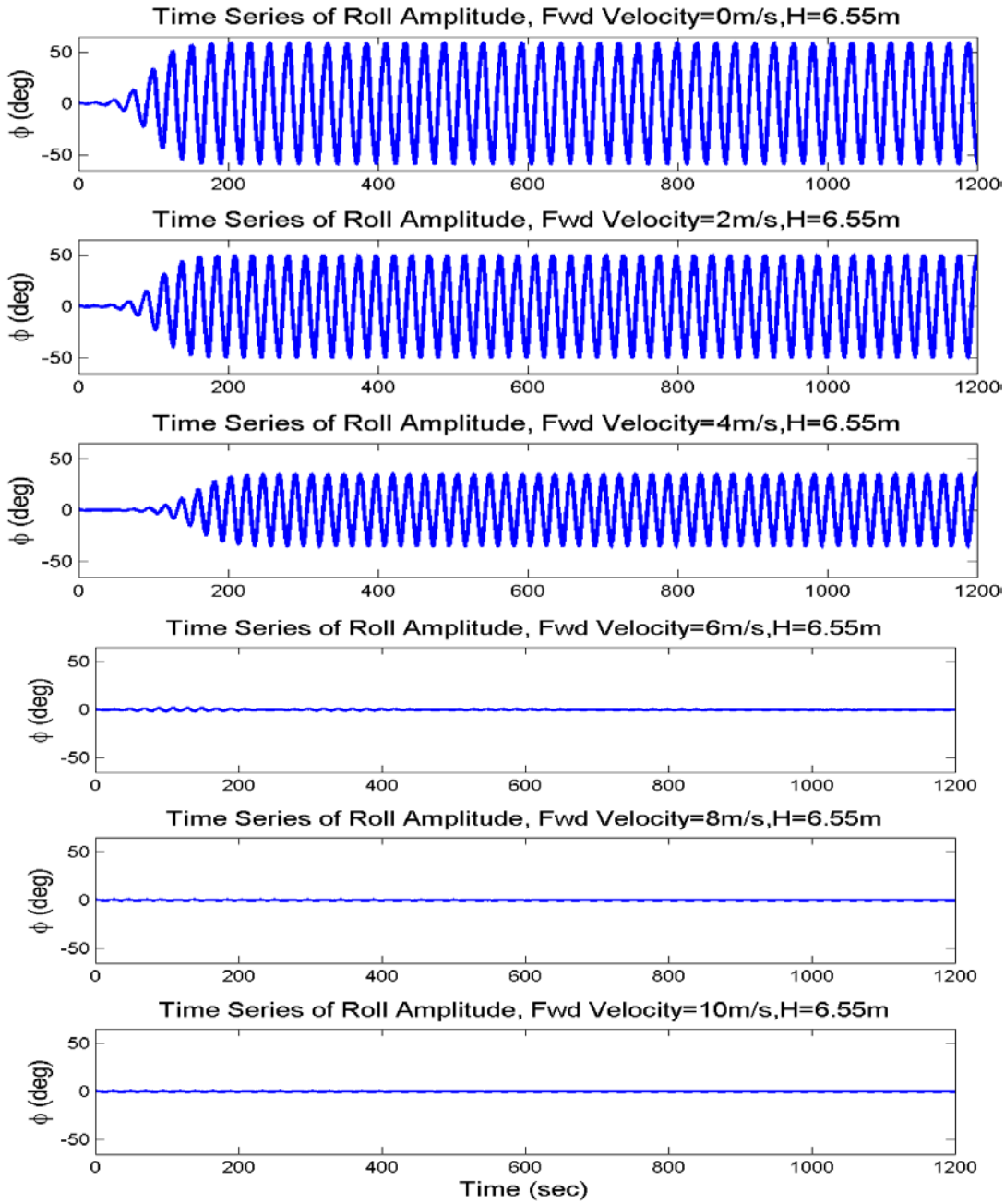

Figure 34.Time series of roll amplitude for different Fwd speeds, H=6.55 m, Head sea condition

Figure 34 shows clearly supports the findings from the stability chart. Here we see that as the forward speed increases the ship parameter moves towards the stable region on the right of primary parametric resonance region. This is due to the increase in the encounter frequency in the head sea condition during which waves are encountered at higher frequency. As a result the frequency ratio square parameter (α) decreases. No parametric roll was observed at forward speed of 10 m/sec in head sea case whereas in the case of following sea condition we saw parametric roll resurface when the forward speed was 10 m/sec as a result of the ship parameter in the 2nd instability zone. Thus the wave heading and forward speed are critical to occurrence of parametric roll and can be used as a tool to avoid parametric roll.

Looking at the plots above we see that forward speed can be a considered as a bifurcation parameter since a slight change in the forward speed can lead to large amplitude motion from zero motion. Forward speed is considered positive in following sea and negative in head sea condition. The bifurcation chart for the roll amplitude with H=6.55 m is shown in Figure 35. Projecting on to plane for particular time we observe a Hopf type bifurcation. Three bifurcation points can be clearly seen from the bifurcation diagram. One of the bifurcation point is the point at which the ship parameter crosses the left boundary of the 1st instability zone (head sea condition) the second one when the parameter crosses the right boundary of the 1st instability zone (following sea). The third bifurcation point is the value of forward speed at which the ship parameter crosses into the 2nd instability region. The bifurcation points are dependent on the wave amplitude since the boundaries are dependent on the Fourier coefficients of GM variation.

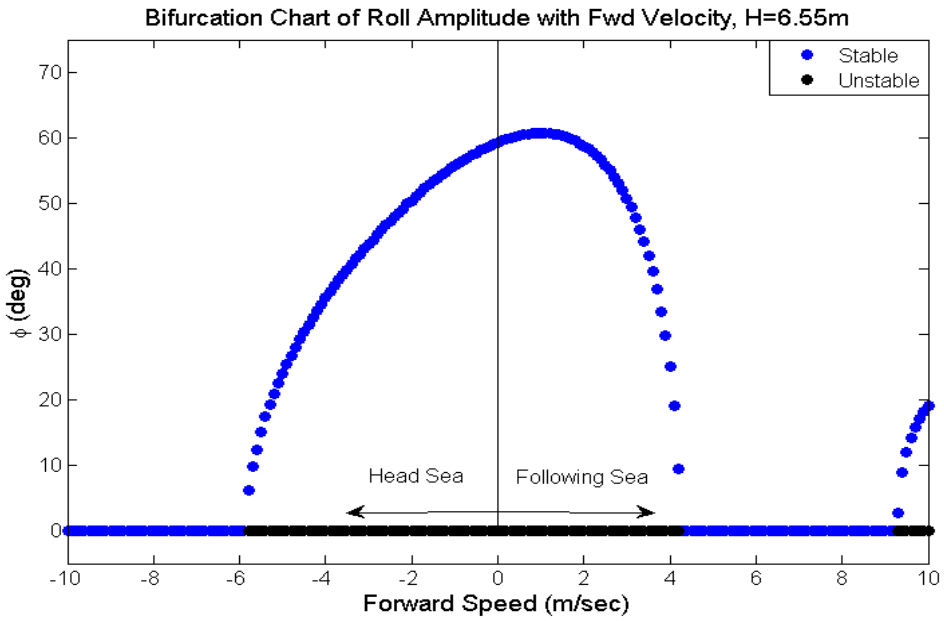

Figure 35. Bifurcation chart of roll amplitude with forward speed

3.10.7 Effect of time varying non-linear righting arm

So far we studied parametric roll considering the linear part of time varying righting arm. In this section we will discuss the effect of time varying non-linear righting arm on the parametric roll motion. The parametric roll equation of motion with time varying non-linear righting arm is a complex equation and not many tools are available to tackle the problem. All the tools available at the time of research dealt with linear time varying stiffness. The method used to incorporate the effects of non-linear damping to predict the roll motion amplitude has provided some insight into modeling non-linear time varying stiffness into the stability chart and predict the bounded roll motion amplitude. One approach will be to reproduce the time varying non-linear righting arm using a combination of Fourier fits and least square fits (Bulian, 2005). The method of Hill's infinite determinant method can be extended to further include the Hill's coefficients of

each of the time varying coefficients of the least square fit. This method is very laborious and beyond the scope of this work. Another approach as in the case of non-linear damping, the non-linear part of the righting arm may be replaced by an equivalent term and the effects of the equivalent term incorporated in the Hill's determinant. Since the non-linear shape of the right arm is very sensitive to the wave profile due to the variation in the hull geometry along the length of the vessel this approach will not give very accurate predictions. In this section we will study the effects of non-linear time varying restoring force on the roll motion using time simulations. The cases analyzed considering linear time varying stiffness will be studied considering the non-linear stiffness variation. The method of simulating the varying righting arm in time domain is used to carry out numerical simulations. Figure 36 shows the comparison between the actual and Fourier fitted time varying righting arm.

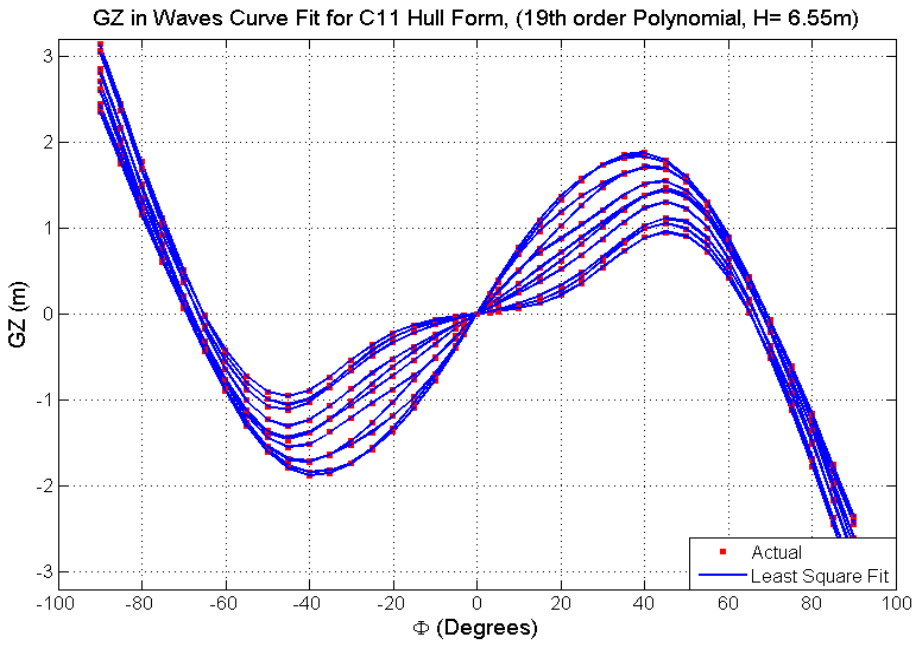

Figure 36. Comparison of actual GZ in waves with least square fit

The variation in GZ in waves can be clearly seen from Figure 36. A 19th order polynomial is used to fit the GZ. This was done so as to match variation of GM which is the primary driving factor of parametric roll. As in the case of GM each of the coefficients of the least square fits vary with time for different positions of the wave with a frequency equal to the wave frequency. This enables us to use the same approach used for time varying GM to reproduce them in a time domain. The results of numerical simulation considering non-linear damping and non-linear time varying stiffness for H=6.55m are shown in Figures 37 and 38.

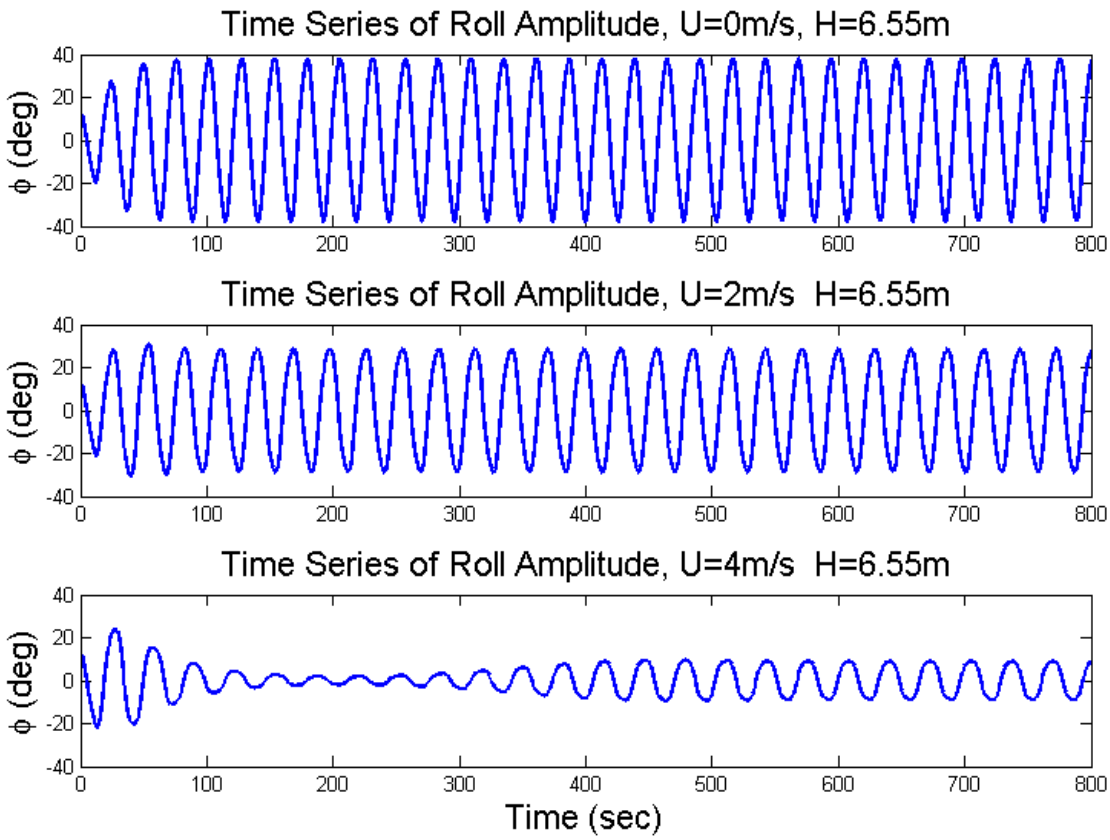

Figure 37. Time series of roll amplitude for different forward speeds (considering non- linear damping and time varying GZ, following sea condition), H=6.55 m (1/2)

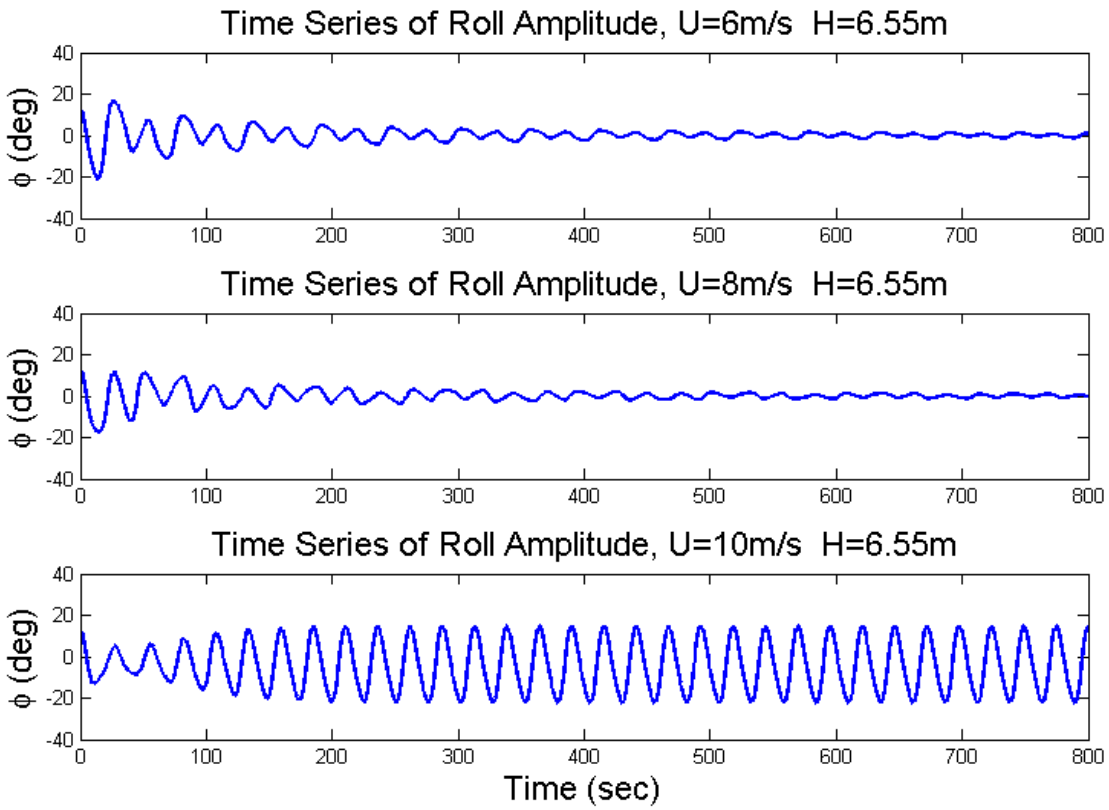

Figure 38. Time series of roll amplitude for different forward speeds (considering non- linear damping and time varying GZ, following sea condition), H=6.55 m (2/2)

As seen from the time simulation parametric roll behavior is similar to the study done with non-linear damping and linear time varying stiffness. However the resulting bounded roll amplitude has decreased considerably (especially where the linear approximation was not valid). The contribution from higher order terms of the non-linear stiffness towards the restoring moment increases as the roll amplitude increases. As a result a balance between the energy of parametric excitation is matched by the restoring force and damping at a lower amplitude. In general the bounded amplitude was found to be very close to the results with linear time varying system (which the linear approximation was true). For forward speed of 10 m/sec the effect of non-linear

restoring force was not significant since the roll angle was within the range of linear approximation.

Thus we can conclude that non-linear time varying GZ tends to reduce the bounded parametric roll motion amplitude. The reduction are depended on the wave height and frequency and cannot be generalized. As a conservative design approach 60% of the bounded roll motion amplitude considering non-linear damping maybe used as the bounded roll motion amplitude outside the linear range. Using the methods developed for predicting roll amplitude considering non-linear damping we can avoid time consuming numerical simulations to predict the amplitude of roll motion.

With this we come to the end of section regarding the analysis of parametric roll in regular waves. Real seaway is stochastic and there is a need to study parametric roll behavior in irregular seaway. Chapter IV discusses the method to analyze parametric roll in irregular seaway and the results and observations made from the analysis.

CHAPTER IV

IRREGULAR WAVE ANALYSIS

4.1 GM Variation as Volterra System

In this section we will discuss a method developed by (Hua et al., 1994) who represented the GM of a vessel in waves as a Taylor series expansion and used the Volterra systems approach to obtain GM variation in irregular waves. This section will highlight the important mathematical formulations to explain the concept developed by the authors. All the formulas reported in this section are extracted from the paper, please refer the paper for further details. Previously, we discussed the parametric roll properties of the C11 hull form in idealized regular waves. The methods developed in previous chapters are only applicable for regular waves or periodic variation of GM. Real seaway is irregular and all the methods developed so far are not applicable. The stability charts and Floquet theory are only useful for systems with periodically varying stiffness. Thus predicting the occurrence of parametric roll in irregular seaway is a difficult task and estimating the roll amplitude in irregular waves is not easy. The initial GM of a vessel can be represented by the following well known relation

$$GM = KB + BM - KG \tag{4-1}$$

The idea was to develop a function that would estimate GM based on the wave elevation along the vessel. Important parameters that affect GM such as breadth, sectional moment about keel and sectional area were represented as Taylor series expansion about the mean draft $T(x)$ given by

$$B\left(x,T\left(x\right)+z\right)=B\left(x,T\left(x\right)\right)+\frac{\partial B}{\partial z}z+\frac{1}{2!}\frac{\partial^2 B}{\partial z^2}z^2+....\tag{4-2}$$

$$M\left(x,T\left(x\right)+z\right)=M\left(x,T\left(x\right)\right)+\frac{\partial M}{\partial z}z+\frac{1}{2!}\frac{\partial^2 M}{\partial z^2}z^2+....\tag{4-3}$$

$$A\left(x,T\left(x\right)+z\right)=A\left(x,T\left(x\right)\right)+\frac{\partial A}{\partial z}z+\frac{1}{2!}\frac{\partial^2 A}{\partial z^2}z^2+....\tag{4-4}$$

Here, z is the variable for sectional draft change.

Once the draft at each station is known, the sectional properties for different sections along the length of the ship can be estimated using the Taylor series expansion and thus the GM. Using the following substitutions

$$\begin{aligned}
&c_1\left(x\right)=\frac{\partial B}{\partial z}, \quad c_2\left(x\right)=\frac{1}{2!}\frac{\partial^2 B}{\partial z^2}, \quad ...\\
&d_1\left(x\right)=\frac{\partial M}{\partial z}, \quad d_2\left(x\right)=\frac{1}{2!}\frac{\partial^2 M}{\partial z^2}, \quad ...\\
&e_1\left(x\right)=\frac{\partial A}{\partial z}, \quad e_2\left(x\right)=\frac{1}{2!}\frac{\partial^2 A}{\partial z^2}, \quad ...
\end{aligned}\tag{4-5}$$

The Taylor series expansion appear as polynomials in z. Each of these coefficients can be numerically estimated using the least square fit (or similar method) of the sectional area, breadth and sectional moment about keel for different draft points. Using the above approach, different terms that make up GM can be evaluated as

$$KB=\frac{\int_L M\left(x,T\left(x\right)\right)dx}{\nabla}\tag{4-6}$$

$$BM=\frac{1}{12}\frac{\int_L B^3\left(x,T\left(x\right)\right)dx}{\nabla}\tag{4-7}$$

The variation of initial GM in regular and irregular waves neglecting Smith effect is given by

$$\partial GM = \frac{1}{\nabla}\begin{bmatrix} \frac{B^3\left(x,T\left(x\right)+r\left(x\right)\right)}{12} + M\left(x,T\left(x\right)+r\left(x\right)\right) \\ -A\left(x,T\left(x\right)+r\left(x\right)\right)KG\left(x\right) \end{bmatrix} - GM_0 \tag{4-8}$$

where $KG(x)$ is the section mass centre above the keel, $r(x)$ is the relative wave position at each section and GM_0 is still water GM.

Using Eq. (4-2) to (4-5) in Eq. (4-8) we get

$$\partial GM = \sum_i \partial GM_i \tag{4-9}$$

where,

$$\begin{aligned} \partial GM_1 &= \frac{1}{\nabla}\int_L [\frac{B^2\left(x,T\left(x\right)\right)c_1\left(x\right)}{4} + d_1\left(x\right) - KGe_1\left(x\right)]r\left(x\right)dx, \\ \partial GM_2 &= \frac{1}{\nabla}\int_L [\frac{3B^2\left(x,T\left(x\right)\right)c_1\left(x\right)+3B\left(x,T\left(x\right)\right)c_2{}^2\left(x\right)}{12} + d_2\left(x\right) \\ &\qquad - KGe_2\left(x\right)]r^2\left(x\right)dx - \frac{1}{\nabla}\int_L xe_1\left(x\right)\eta_5 r\left(x\right)dx \end{aligned} \tag{4-10}$$

and so on.

From Eq. (4-10) we can define the following geometry functions

$$G_1\left(x\right) = \frac{1}{\nabla}[\frac{B^2\left(x,T\left(x\right)\right)c_1\left(x\right)}{4} + d_1\left(x\right) - KGe_1\left(x\right)] \tag{4-11}$$

$$G_2(x) = \frac{1}{\nabla}\int_L [\frac{3B^2(x,T(x))c_1(x) + 3B(x,T(x))c_2{}^2(x)}{12} + d_2(x) - KGe_2(x)] \quad (4\text{-}12)$$

$$R_2(\omega, x) = \frac{xe_1(x)\eta_5}{\nabla} = -\frac{xB(x,T(x))\eta_5}{\nabla} \quad (4\text{-}13)$$

And so on $G_3(x), R_3(\omega, x)\ldots$

From the above equations for geometry functions we see that each geometry function is made up of three terms in general. The 1st term is depended on the breadth variation, the second term on the sectional moment variation and the third term the sectional area variation along the length of the vessel. The contribution of each term towards the geometry function for C11 Hull form can be seen in the Figures 39 and 40.

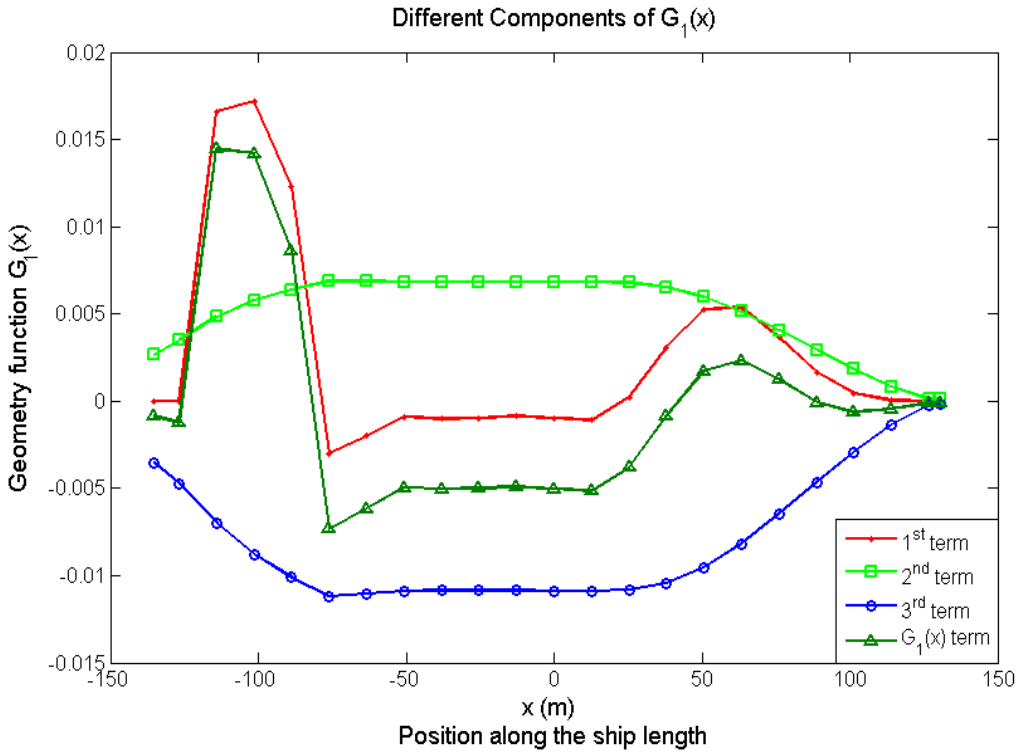

Figure 39. Different components of 1st order geometry function $G_1(x)$ for C11 hull form

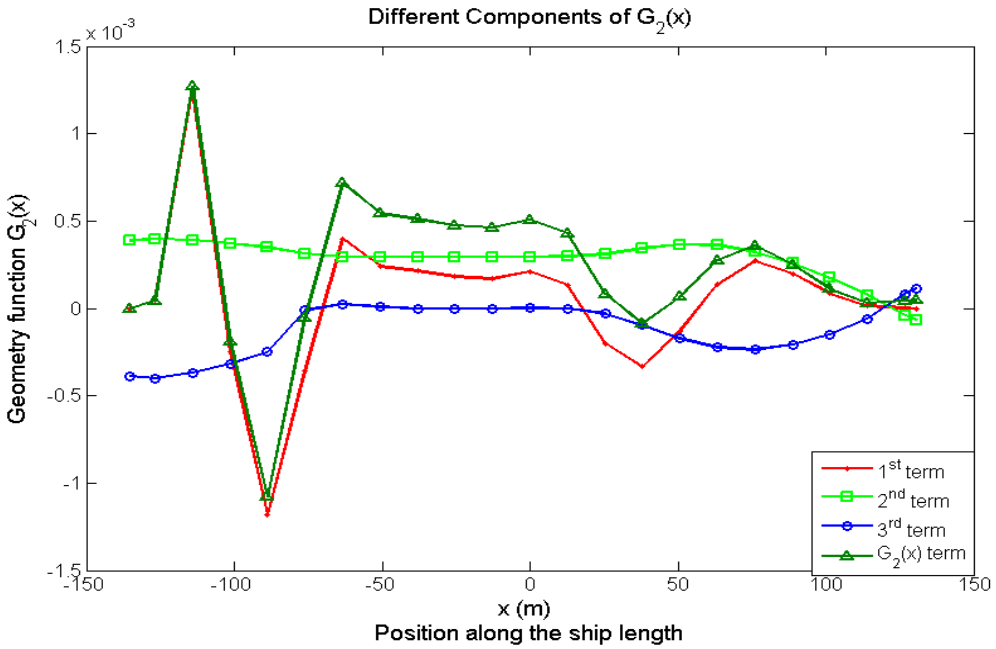

Figure 40. Different components of 2nd order geometry function $G_2(x)$ for C11 hull form

From the shape of the geometry functions one can clearly notice that the variation in the geometry function is large close to the ends of the vessel. This is expected since the variation in the hull section is significant at the ends of the vessel. The relative importance of various orders of the geometry functions are shown in the Figure 41. The contribution of the 1st order geometry function is significant. As one would expect, the contributions from higher order geometry functions tend to decrease as the order increases. In this analysis we will limit ourselves up to 2nd order transfer function in the estimation of GM variation in irregular sea. Total GM variation is evaluated as the sum of 1st and 2nd order GM variation as given by Eq. (4-9). This method has the added advantage of being an analytical method with the vessel geometry as the input. In comparison to the method followed in the regular wave analysis where the GM variation

for each wave case had to be evaluated based on large angle stability, this method helps us evaluate the GM variation based on transfer functions for any wave frequency.

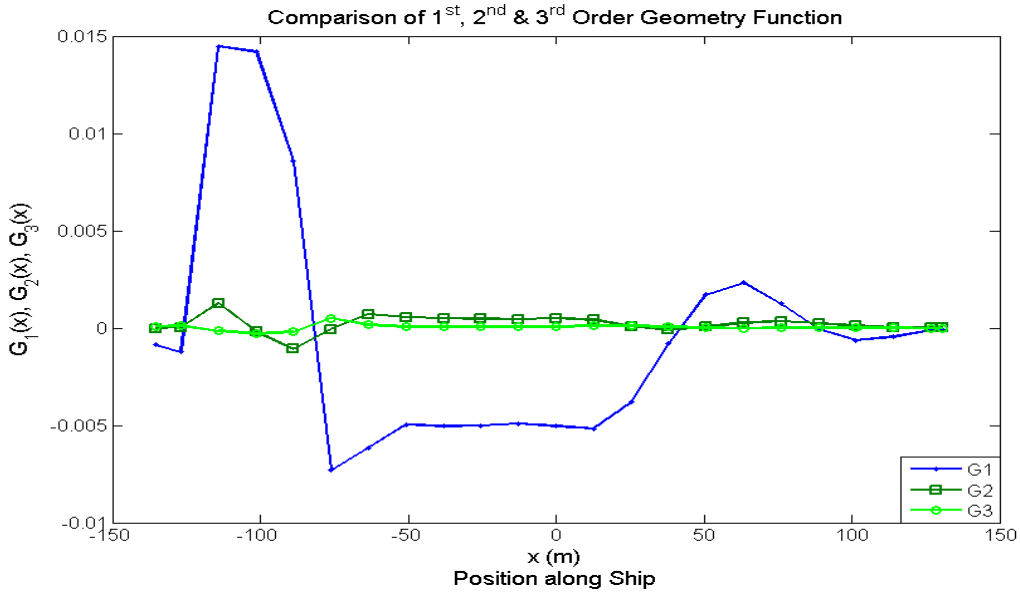

Figure 41. Comparison of different orders of geometry functions of C11 hull form

In the regular wave analysis we neglected the effects of heave and pitch motion during the estimation of GM in waves. With this model the effects of heave and pitch motions are captured in the relative wave elevation. The wave elevations are modified for each frequency based on the heave and pitch RAO's. An irregular wave train can be represented as sum of sinusoidal waves with random phase given by

$$\eta(x,t) = \frac{1}{2}\left\{\sum_{n=1}^{N} a_n \cdot [e^{i(k_n x - \omega_n t + \beta_n)} + e^{-i(k_n x - \omega_n t + \beta_n)}]\right\} \tag{4-14}$$

where, a is the wave amplitude of an individual wave, k the wave number, ω the wave frequency and N is the number of waves

Assuming a linear relation of heave and pitch motion to the wave amplitude the relative wave elevation can be written as

$$r(x,t)=\frac{1}{2}\left\{\sum_{n=1}^{N}a_n\cdot[e^{ik_n x}-\eta_3(\omega_n)+x\cdot\eta_5(\omega_n)]e^{-i(\omega_n t+\beta_n)}]\right\}+ \frac{1}{2}\left\{\sum_{n=1}^{N}a_n\cdot[e^{-ik_n x}-\overline{\eta}_3(\omega_n)+x\cdot\overline{\eta}_5(\omega_n)]e^{i(\omega_n t+\beta_n)}]\right\} \tag{4-15}$$

Here $\eta_3(\omega)$ and $\eta_5(\omega)$ are the heave and pitch RAO, where the over bars represent the complex conjugate.

The terms in the square brackets in Eq. (4-15) are complex conjugates of each other and can be considered as the transfer function of relative motion. These terms can be represented by $\nu(\omega,x)$ and $\overline{\nu}(\omega,x)$. Using Eq. (4-10),(4-11) and (4-15) the 1st order transfer function for GM variation can be represented as

$$f(\omega)=\int_L G_1(x)\cdot\nu(\omega,x)\cdot dx \tag{4-16}$$

And the complex conjugate is given by

$$\overline{f}(\omega)=\int_L G_1(x)\cdot\overline{\nu}(\omega,x)\cdot dx \tag{4-17}$$

The transfer function for the second order GM variation is dependent on the sum and difference frequency components of the relative motion. Apart from the sum and difference frequency component, the 2nd order GM variation also depends on $R_2(\omega,x)$. As in the case of 1st order transfer functions the 2nd order transfer functions are also obtained by integrating the product of the geometric function and the relative motion

transfer function of each section over the length of the vessel. The 2nd order transfer functions of GM variation are given by

$$
\begin{aligned}
u_2(\omega_m,\omega_n) &= \int_L [G_2(x)\cdot v(\omega_m,x)\cdot v(\omega_n,x) + R_2(\omega_m,x)\cdot v(\omega_m,x)]dx \\
\overline{u}_2(\omega_m,\omega_n) &= \int_L [G_2(x)\cdot v(\omega_m,x)\cdot \overline{v}(\omega_n,x) + R_2(\omega_m,x)\cdot \overline{v}(\omega_m,x)]dx \\
v_2(\omega_m,\omega_n) &= \int_L [G_2(x)\cdot \overline{v}(\omega_m,x)\cdot v(\omega_n,x) + \overline{R}_2(\omega_m,x)\cdot v(\omega_m,x)]dx \\
\overline{v}_2(\omega_m,\omega_n) &= \int_L [G_2(x)\cdot \overline{v}(\omega_m,x)\cdot \overline{v}(\omega_n,x) + \overline{R}_2(\omega_m,x)\cdot \overline{v}(\omega_m,x)]dx
\end{aligned}
\tag{4-18}
$$

From the definition of transfer function we can see that $u_2(\omega_m,\omega_n)$ and $\overline{v}_2(\omega_m,\omega_n)$ are conjugates of each other as well $\overline{u}_2(\omega_m,\omega_n)$ and $v_2(\omega_m,\omega_n)$.

The transfer functions discussed above have the form of transfer functions based on the Volterra system. The Volterra system is a very well known method of response analysis in frequency domain in marine hydrodynamics. The same methodology is applied to obtain the GM variation in frequency domain. Based on the transfer functions the 1st and 2nd order GM variation in irregular wave can represented as

$$
\partial GM_1(t) = \sum_{n=1}^{N} a_n \cdot [f(\omega_n)\cdot e^{-i(\omega_n t+\beta_n)} + \overline{f}(\omega_n)\cdot e^{i(\omega_n t+\beta_n)}]
\tag{4-19}
$$

$$
\begin{aligned}
\partial GM_2(t) = &\sum_{m=1}^{M}\sum_{n=1}^{N} a_m a_n \cdot \{u_2(\omega_m,\omega_n)\cdot e^{-i((\omega_m+\omega_n)t+\beta_m+\beta_n)} + \\
&\qquad \overline{u}_2(\omega_m,\omega_n)\cdot e^{-i((\omega_m-\omega_n)t+\beta_m-\beta_n)}\} + \\
&\sum_{m=1}^{M}\sum_{n=1}^{N} a_m a_n \cdot \{\overline{v}_2(\omega_m,\omega_n)\cdot e^{i((\omega_m+\omega_n)t+\beta_m+\beta_n)} + \\
&\qquad v_2(\omega_m,\omega_n)\cdot e^{i((\omega_m-\omega_n)t+\beta_m-\beta_n)}
\end{aligned}
\tag{4-20}
$$

The real part of the 1st order transfer function for C11 hull form is shown in Figure 42 with the origin at midship.

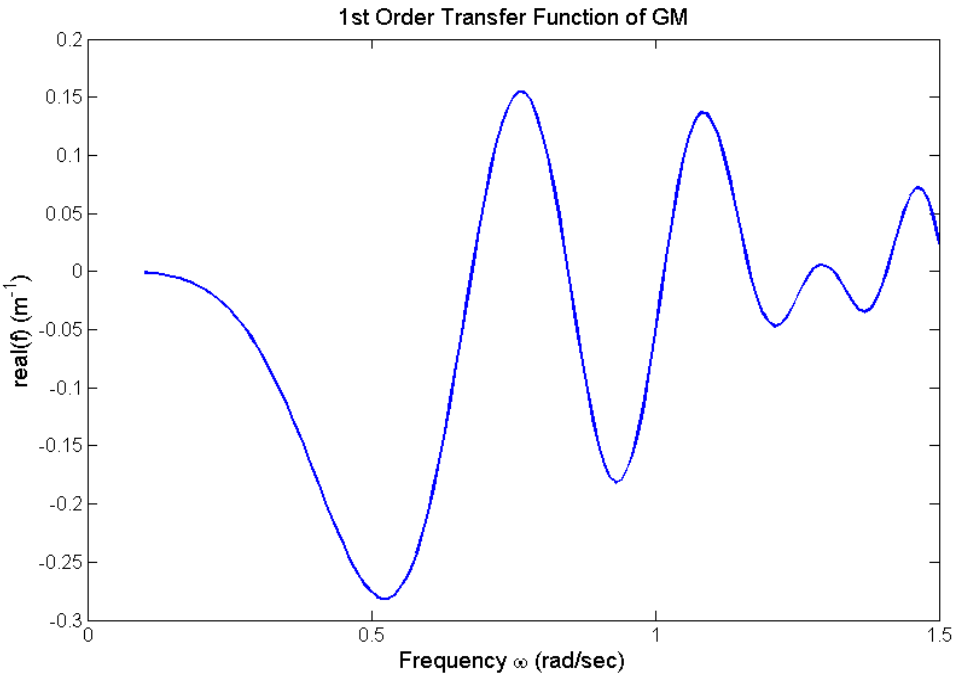

Figure 42. 1st order transfer function of GM variation (C11 hull form)

Figure 42 shows that the magnitude of the 1st transfer function is significant at lower frequencies and reduces as the frequency increases. As a result, one would expect a reduction in the variation of GM for waves at higher frequencies.

The real and imaginary parts of the 2nd order transfer functions are shown in Figure 43 to Figure 46. Only the real and imaginary part of $u_2(\omega_m, \omega_n)$ and $v_2(\omega_m, \omega_n)$ are shown since the other two transfer functions are complex conjugates of each other. The transfer functions are plotted in the sum and difference frequency domain.

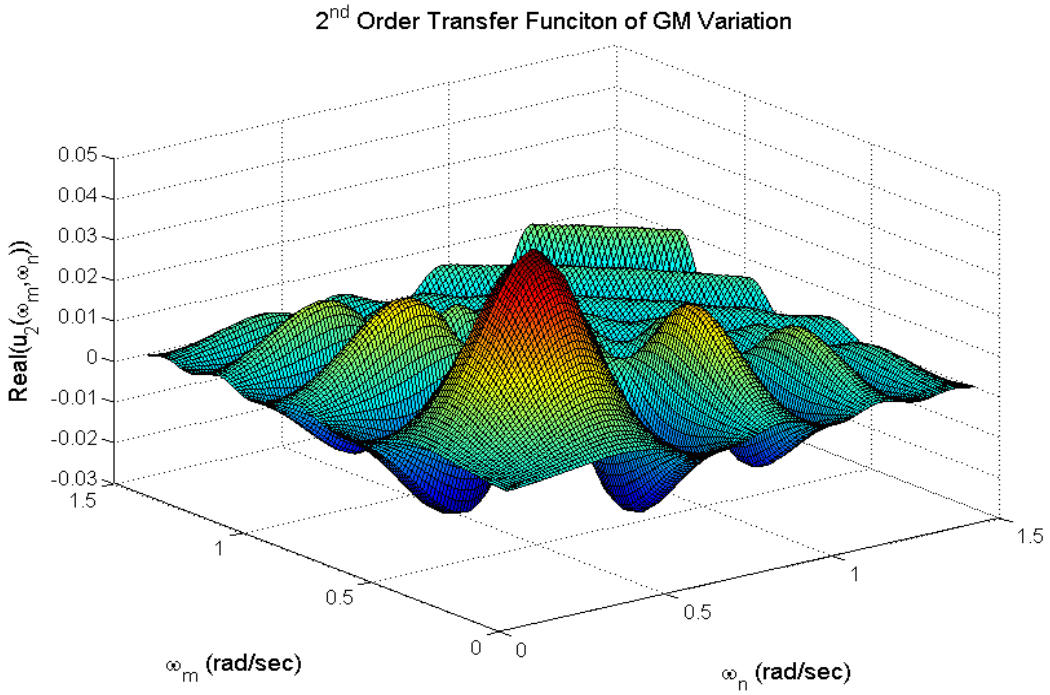

Figure 43. Real part of $u_2(\omega_m, \omega_n)$ (2nd order transfer function of GM variation)

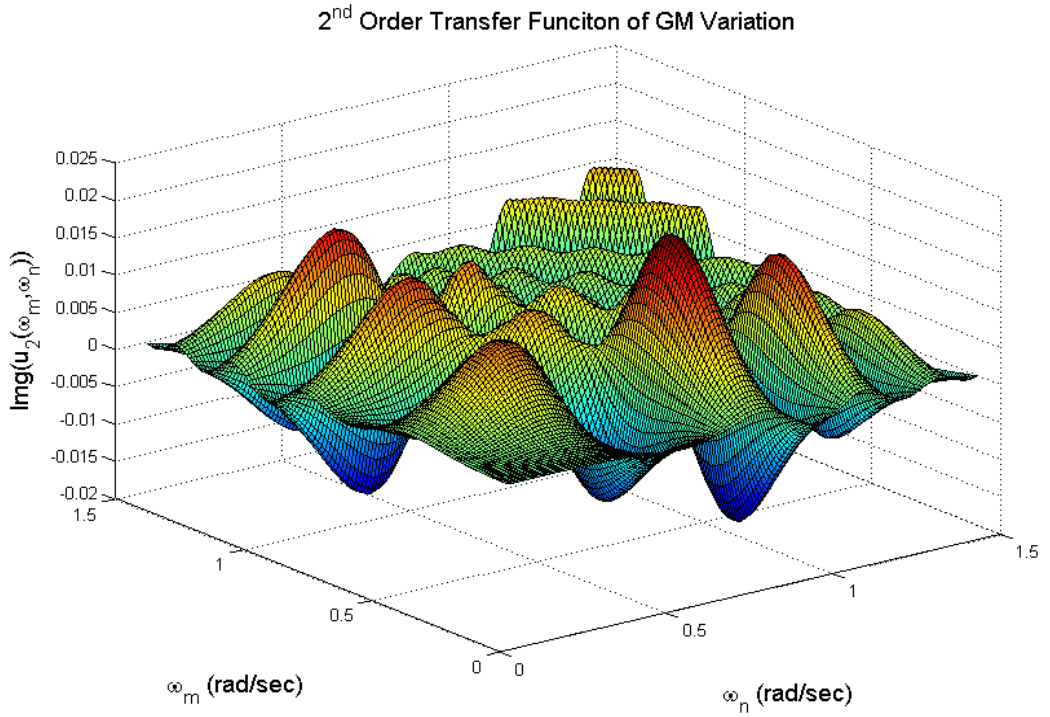

Figure 44. Imaginary part of $u_2(\omega_m, \omega_n)$ (2nd order transfer function of GM variation)

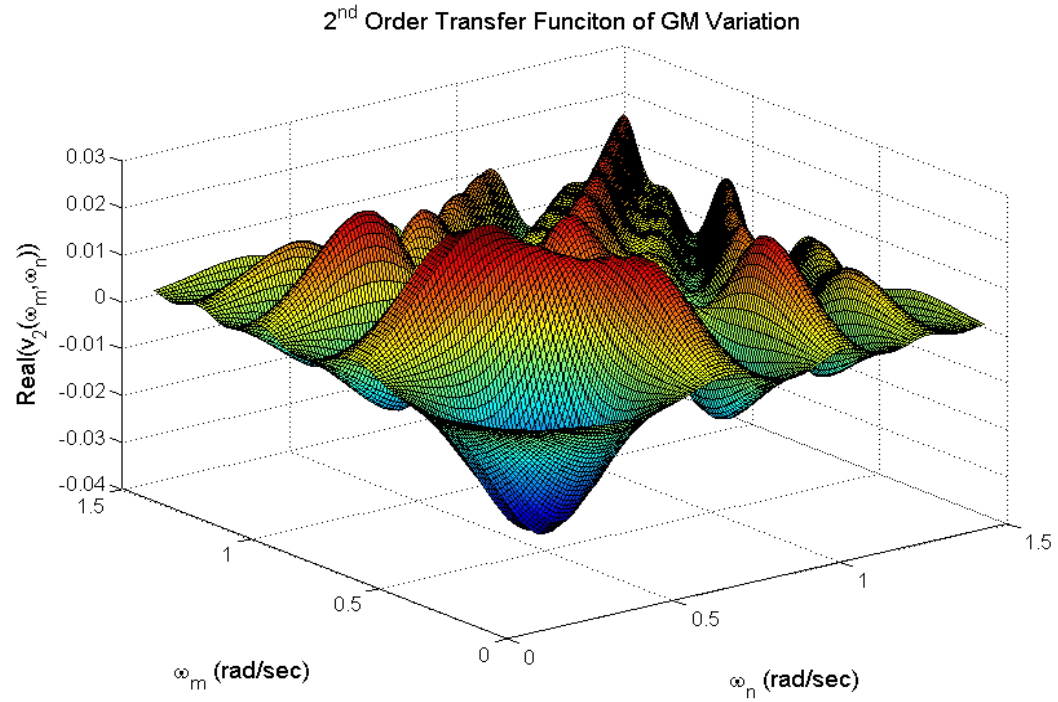

Figure 45. Real part of $v_2(\omega_m, \omega_n)$ (2nd order transfer function of GM variation)

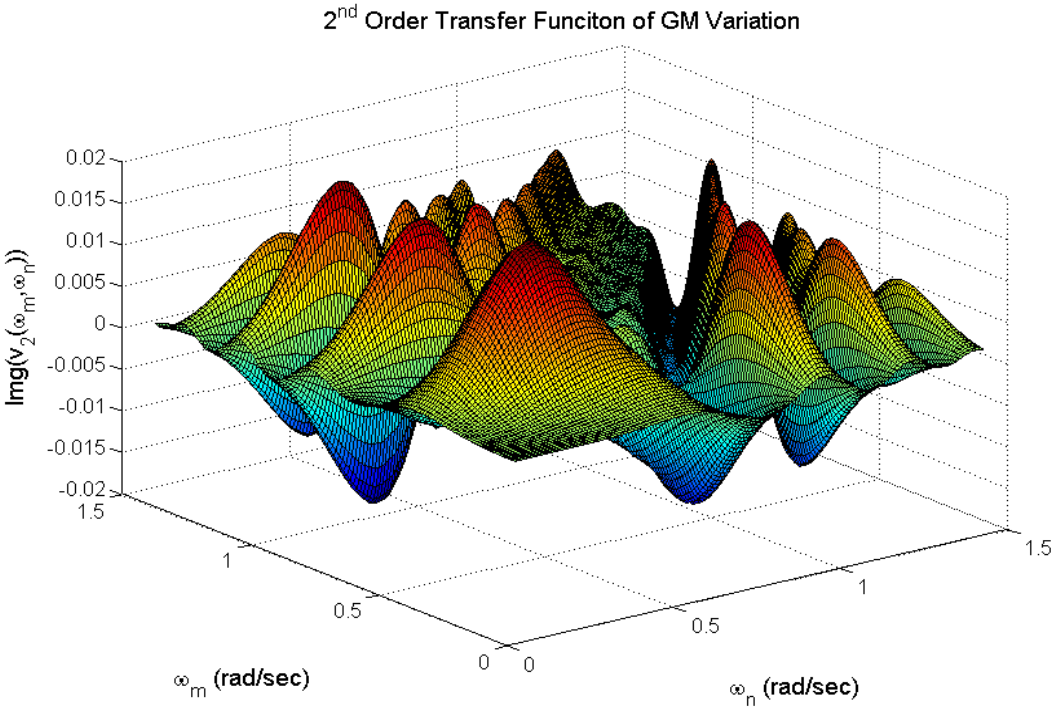

Figure 46. Imaginary part of $v_2(\omega_m, \omega_n)$ (2nd order transfer function of GM variation)

The contributions of various orders of GM variation to the total variation of GM in waves are shown in Figure 47.

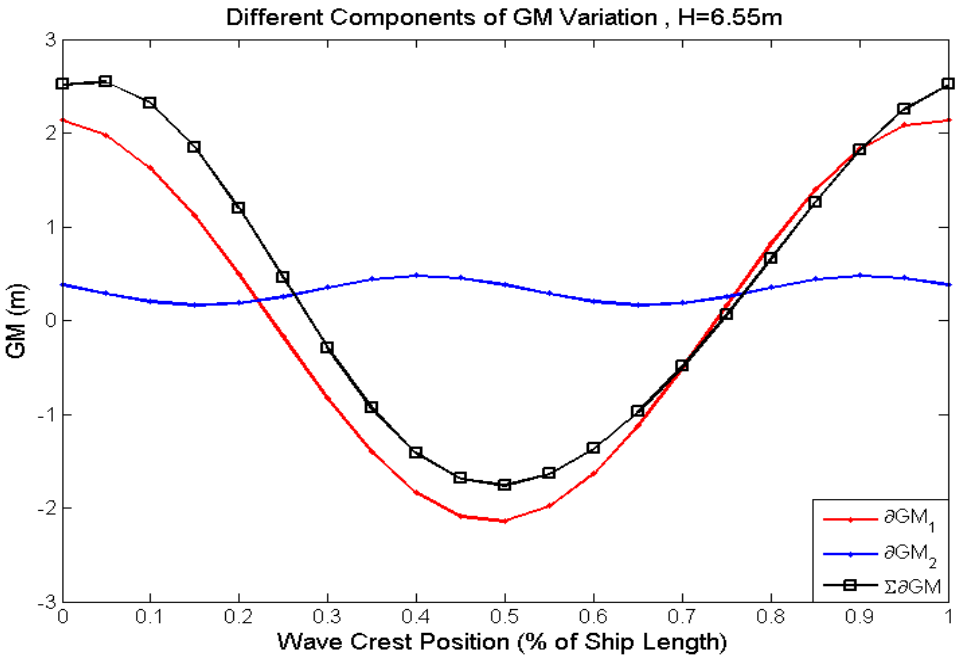

Figure 47. Different components of GM variation of C11 hull form

From the figure we see that the contribution to total GM variation decreases as the order of GM variation increases. Similar behavior is seen in marine hydrodynamics. The second order forces are found to be very small in magnitude in comparison to the 1st order forces. Also the 2nd order GM varies with a frequency equal to the twice the 1st order frequency. In this study we will consider only 1st and 2nd order GM variation.

4.2 Effects of Heave and Pitch Coupling on GM Variation

In the regular wave analysis method hydrostatic balance was assumed and GM variation estimated from the underwater vessel geometry based on the wave profile. The

method discussed here is capable of evaluating the effects of heave and pitch motions on the wave geometry and the associated GM variation. In this section we will compare the GM variation obtained using hydrostatic software and the Volterra method.

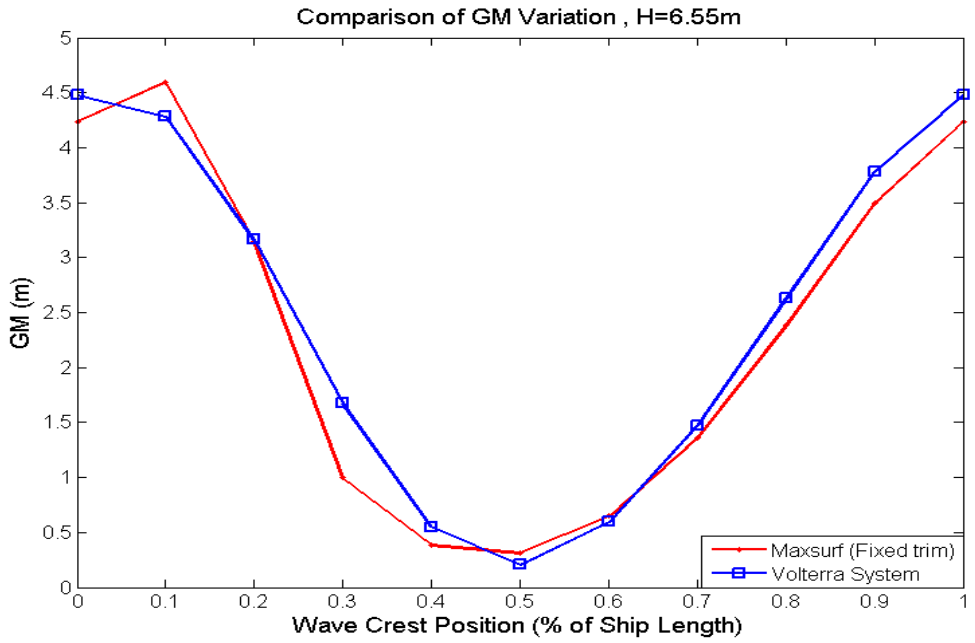

Figure 48. Comparison of GM variation estimated using Maxsurf and Volterra system

Figure 48 shows the comparison of GM estimated for different position of wave crest along the length of the ship using Maxsurf© and Volterra approach. The figure shows that the Volterra approach, which is an approximate method, does estimate GM variation with good accuracy. In this case the heave and pitch effect on the GM variation is not taken into account in the Volterra system method. The effects of heave and pitch motions are incorporated through the transfer functions for relative motion as given by Eq. (4-15). The heave and pitch effects are incorporated through their RAO's. Figure 49 shows the Heave and Pitch RAO's estimated using SHIPMO©.

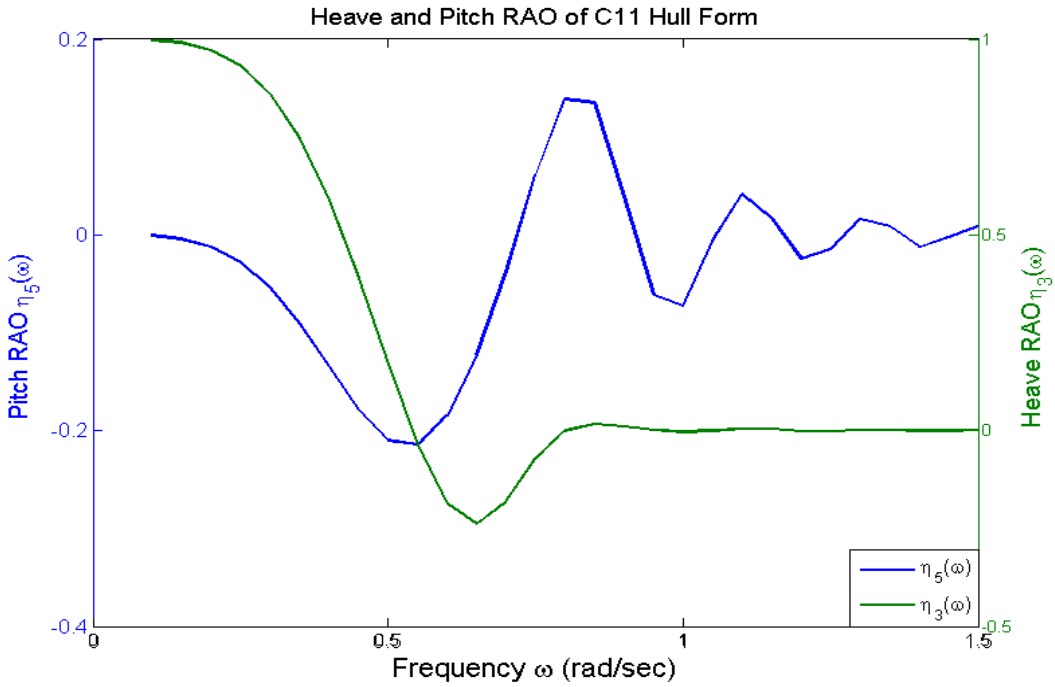

Figure 49. Heave and pitch RAO of C11 hull form

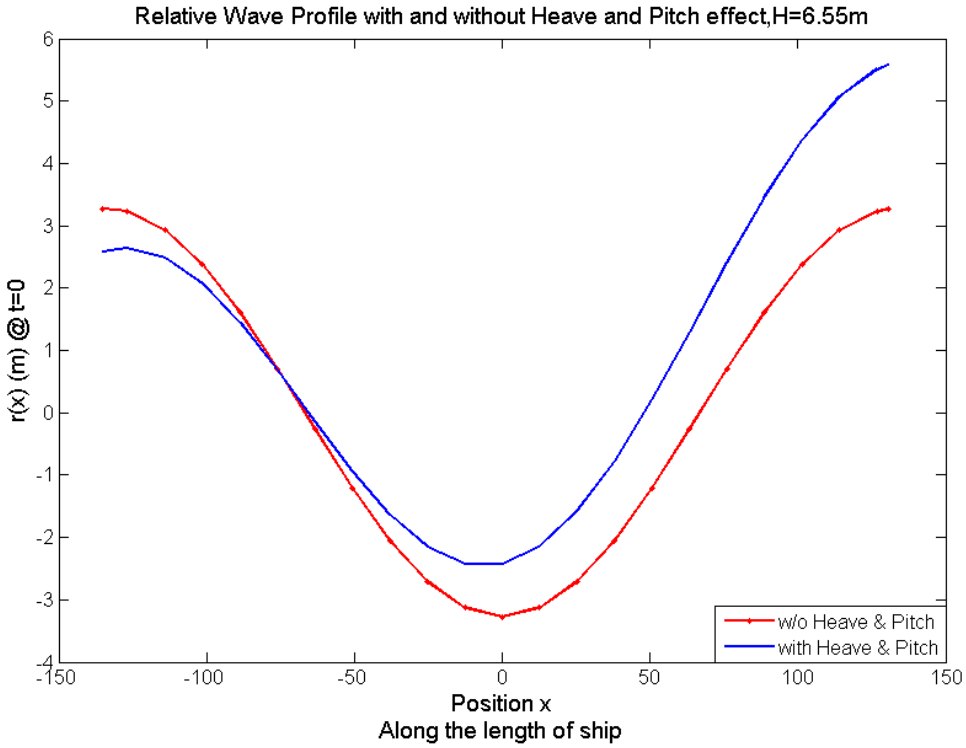

Figure 50. Effect of heave and pitch motion on relative wave profile

Figure 50 shows the relative wave profile with and without considering the heave and pitch motion effects. We see that the relative wave profile is considerably different from the actual wave profile and this can lead to different sectional properties and GM. Figure 51 shows the effect of heave and pitch motions on the GM variation. The GM variation obtained using MAXSURF© is shown for comparison purpose. We see that the GM variation considering heave and pitch is considerably different in comparison to cases without considering heave and pitch. The volume displacement in the Volterra model is assumed constant which is not true in the case of large pitch and heave motion. The magnitude of heave RAO is very small at the forcing frequency of 0.485 rad/sec whereas the pitch RAO is significant at the forcing frequency. Thus the relative wave profile is controlled by pitch motion of the vessel. Figure 51 supports the same.

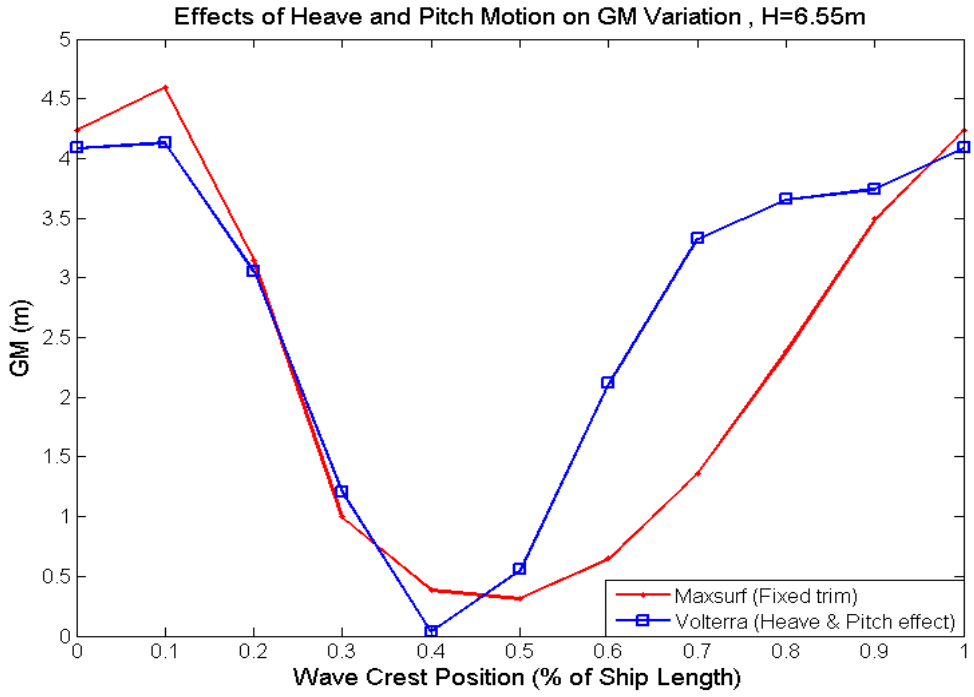

Figure 51. Effects of heave and pitch motion on GM variation of C11 hull form

The time series of the roll and pitch motion for the corresponding wave frequency and wave height are shown in Figure 52. From the time series we see that the pitch motion is very small and has frequency twice that of roll. This is due to the fact that pitch is under direct excitation of wave frequency which is twice the natural frequency of roll.

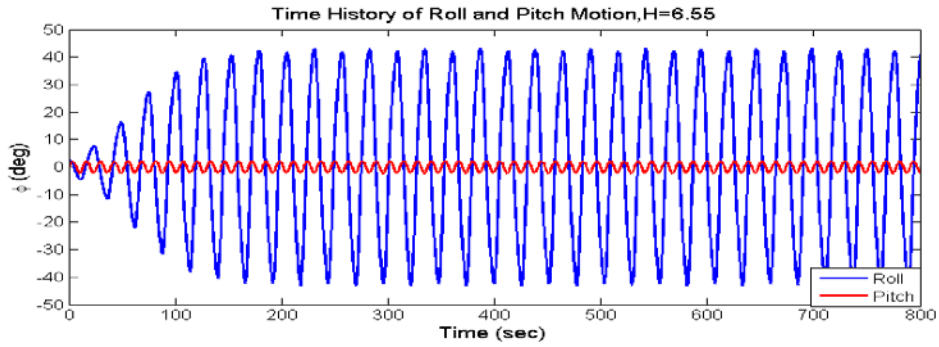

Figure 52. Time series of roll and pitch motion for H=6.55m (λ =L_{PP})

Comparison between the roll motion with and without the heave and pitch coupling is shown in Figure 53. In this case a reduction in the bounded roll amplitude is observed. However depending on the frequency of excitation and vessel hydrodynamics the bounded roll motion amplitude may increase or decrease. Thus it is important to consider heave and pitch coupling in estimating parametric roll motion.

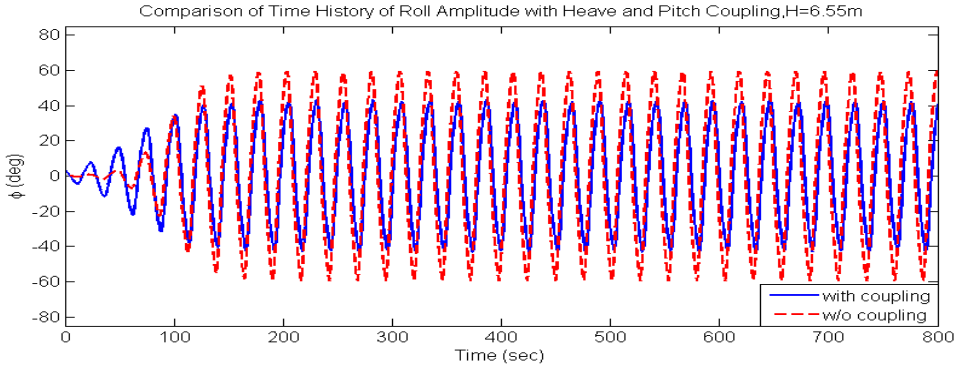

Figure 53. Comparison of roll time series with and without considering heave and pitch coupling.

4.3 Results

4.3.1 GM variation and parametric roll in irregular seaway

In order to estimate the GM variation in irregular seaway an irregular wave profile is generated from a wave spectrum. A two parameter unidirectional Bretschneider spectrum is used in this study. The two inputs to the spectrum are the significant wave height H_S and peak period T_P.

The spectral density of the Bretschneider spectrum is given by

$$S(\omega) = \frac{5}{16} H_s{}^2 \omega_m{}^4 \omega^{-5} \exp\left(-1.25 \left(\frac{\omega_m}{\omega} \right)^4 \right) \tag{4-21}$$

where ω_m is the modal frequency given by

$$\omega_m = \left(\frac{3}{5} \right)^{\frac{1}{4}} \frac{2\pi}{T_P} \tag{4-22}$$

In order to study sensitivity of roll motion to peak period and significant wave height GM variation is estimated for a range of H_S and T_P. Details regarding the same are given in Table 8.

Table 8
Range of spectrum parameters

Spectrum	Bretschneider				
Hs (m)	2	3	4	5	6
Tp (sec)	8,9,10,12,14	8,9,10,12,14	8,9,10,12,14	8,9,10,12,14	8,9,10,12,14

Random phase method is used to develop the irregular wave profile. The wave amplitude of individual waves obtained from the spectral density is given by Eq. (4-23)

$$a_i = \sqrt{2 \cdot S(\omega_i) \cdot \Delta\omega} \qquad i=1,2...n \tag{4-23}$$

Taking into consideration simulation time and accuracy, frequencies in the range of 0.1 rad/sec to 1.5 rad/sec with a frequency resolution of 0.01 is used in the analysis to generate random time series of wave elevation.

The Bretschneider spectrum for H_S = 3.0 m and T_P=12 sec is shown in Figure 54.

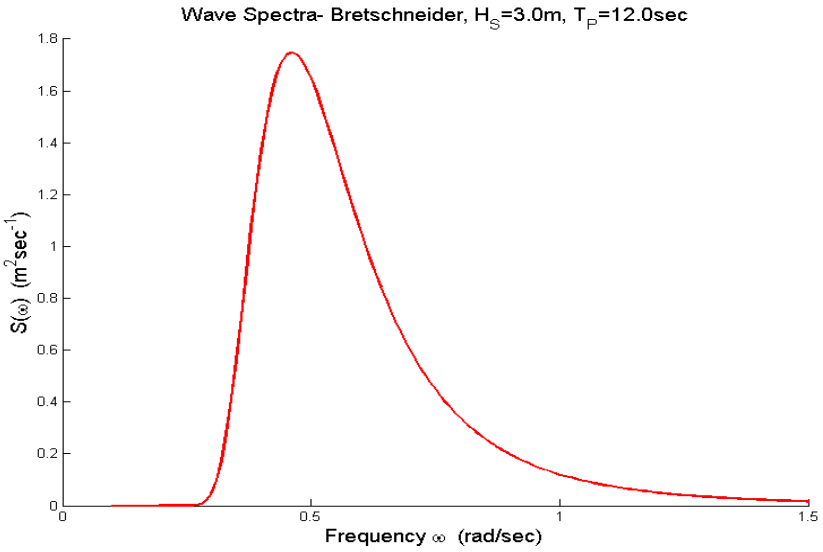

Figure 54. Wave spectra (Bretschneider), Hs=3.0 m, Tp=12 sec

In order to obtain a statistically relevant estimate of parametric roll motion in irregular seaway, different realizations of wave elevation are made using a different set of random phase angles for each realization. Also due to the non-linear characteristics of the system different realizations are required to obtain a good statistical estimate of roll amplitude. Figure 55 shows one realization of the irregular wave profile for Hs=3.0 m.

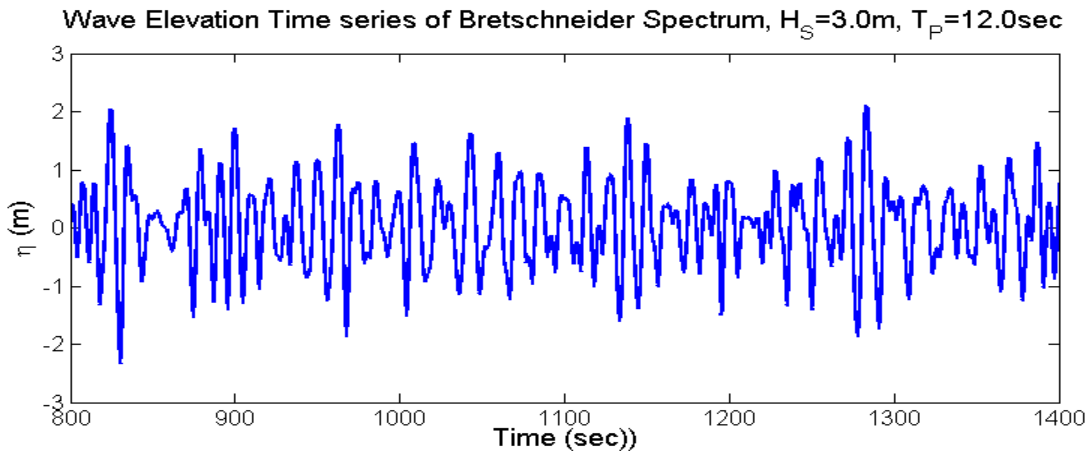

Figure 55. A realization of wave elevation time series of Bretschneider spectrum, H_S=3.0 m, T_P=12 sec

The GM variation of the C11 Hull form was estimated using the Volterra system approach described above. The 1st and 2nd order GM variation and total GM variation of one of the realization in irregular seaway for Hs=3.0 m and Tp=12 sec is shown in Figure 56. The second order variation is found to be positive almost all the time and seems to follow first order GM variation.

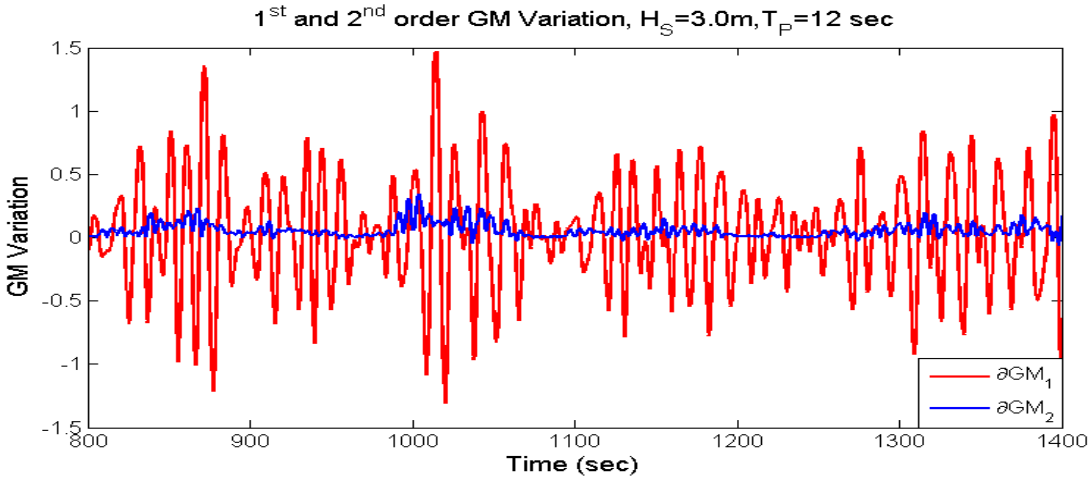

Figure 56. 1st and 2nd order GM variation of C11 hull form, Hs=3.0 m, Tp=12 sec

The GM variation and the corresponding roll motion time series of C11 hull form obtained by numerical simulation for head sea condition with zero forward speed are shown in Figure 57. Non-linear damping is considered in the numerical simulations.

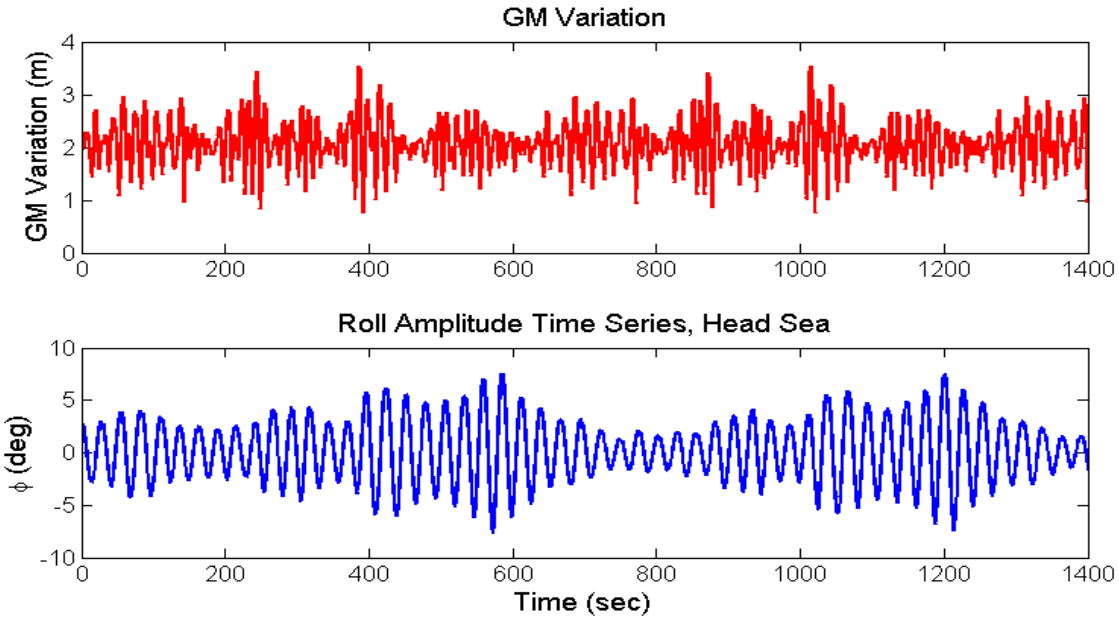

Figure 57. GM time series (Top) and roll amplitude time series (bottom) for Hs=3.0 m, Tp=12 sec

From the roll time series in Figure 57 it is clearly evident that parametric roll is observed for Hs=3.0m with Tp=12sec. From the time series we can see intermittent bursts of large amplitude roll motion. This behavior is different in comparison to the roll response in regular wave where a harmonic response with constant roll amplitude was observed. Another observation that can be made from Figure 57 is that parametric roll is observed right after a peak in the GM variation in general. Thus whenever there is a large variation in GM the system develops sufficient parametric excitation to overcome the

threshold value resulting in parametric rolling motion. Different realization of the Hs=3 m with Tp=12 sec are shown in Figure 58.

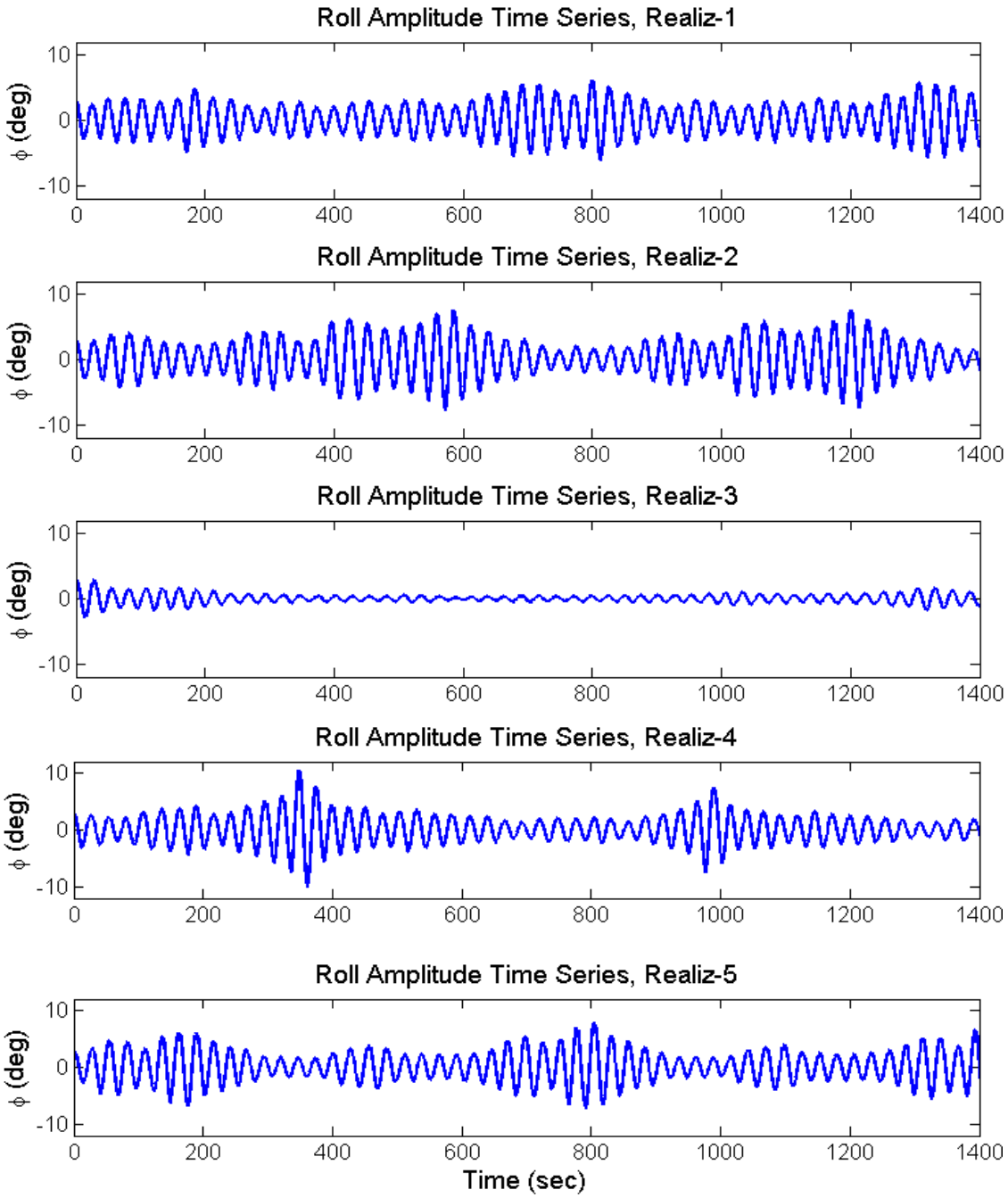

Figure 58. Different realizations of time series of roll amplitude for Hs=3.0 m, Tp=12 sec

From Figure 58 we see that roll motion is non-erogodic. Different realizations have different statistical properties. Another interesting observation is the position of intermittent bursts of parametric roll. The positions of these bursts are different for each observation. In some realization we see no parametric roll e.g Realiz-3. Thus parametric roll may or may not occur in irregular sea. This behavior can be attributed to the non-linear (time varying) characteristics of the system. The irregularity in the GM variation makes the response highly random and the non-linearity of the parametric system makes the response highly unpredictable.

The spectrum of GM variation of different realization is shown in Figures 59 and 60.

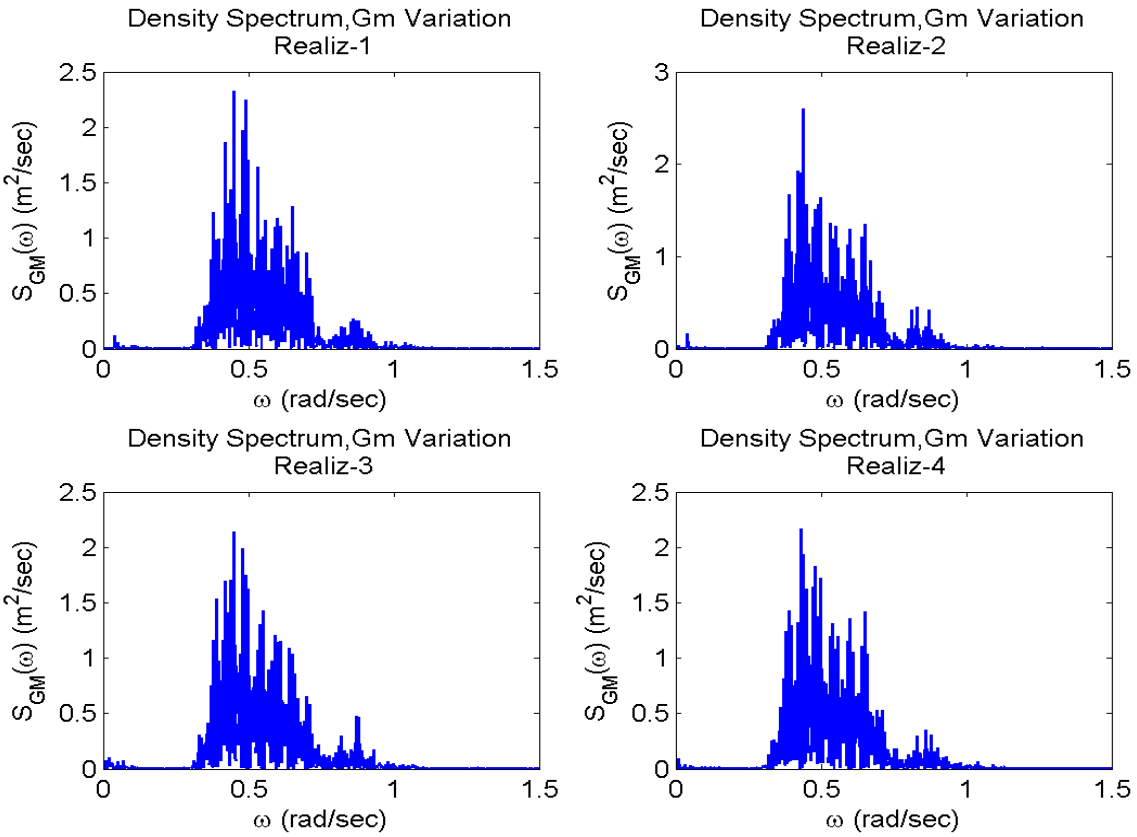

Figure 59. Spectrum of GM variation, Hs=3.0 m, Tp=12 sec (1/2)

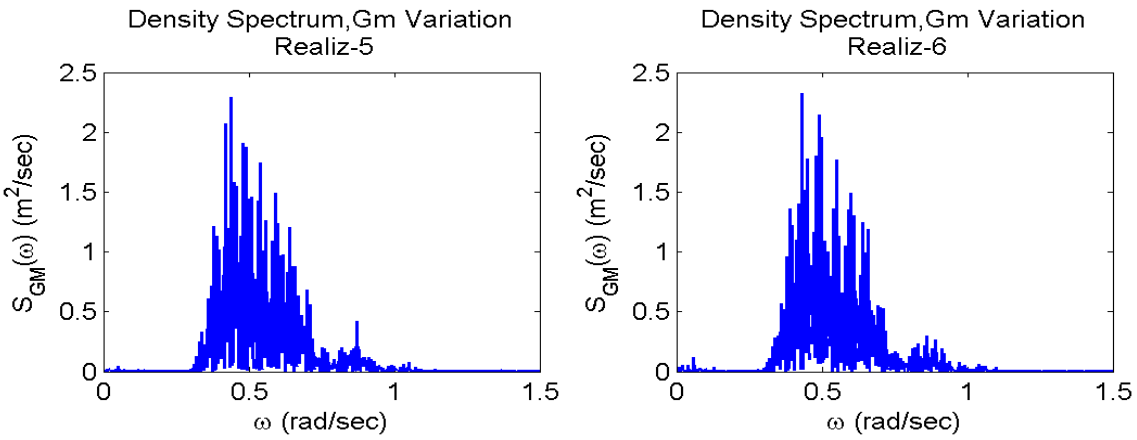

Figure 60. Spectrum of GM variation, Hs=3.0 m, Tp=12sec (2/2)

The spectrums of GM variations for different realizations look very similar. The sum frequency components seems to be dominant in comparison to the difference frequency components of the 2nd order GM variation. Most of the contribution to GM variation comes from the 1st GM variation. The peak period of the GM variation is close to the peak period of the wave spectrum clearly indicating the influence of 1st order GM variation on the overall nature of GM variation in irregular sea. The spectrum does not give much insight as to why no parametric roll was observed for Realiz-3. Thus we may conclude that parametric roll is highly random and non-erogodic in nature and it is difficult to predict the occurrence of parametric rolling of ships in irregular seaway. Since the roll angles in these simulations are small, the non-linear terms of the righting arm are not important. Use of GM variation is good enough to give reasonable estimate of parametric roll amplitude. Hence we may conclude that a vessel found to be prone to parametric roll in regular waves is highly susceptible to parametric roll in irregular seaway. In this chapter we shall resort to utilizing statistical measures rather than absolute values to represent the response properties.

4.3.2 Effect of peak period on parametric roll

We know that parametric roll does occur in irregular seaway. But its occurrence is difficult to predict. In this section we shall investigate the influence of spectral peak period (Tp) on parametric roll behavior. The results of simulation for Hs=3.0 m for Tp=8,9,10,12 and 14 sec are shown Figures 61 to 65.

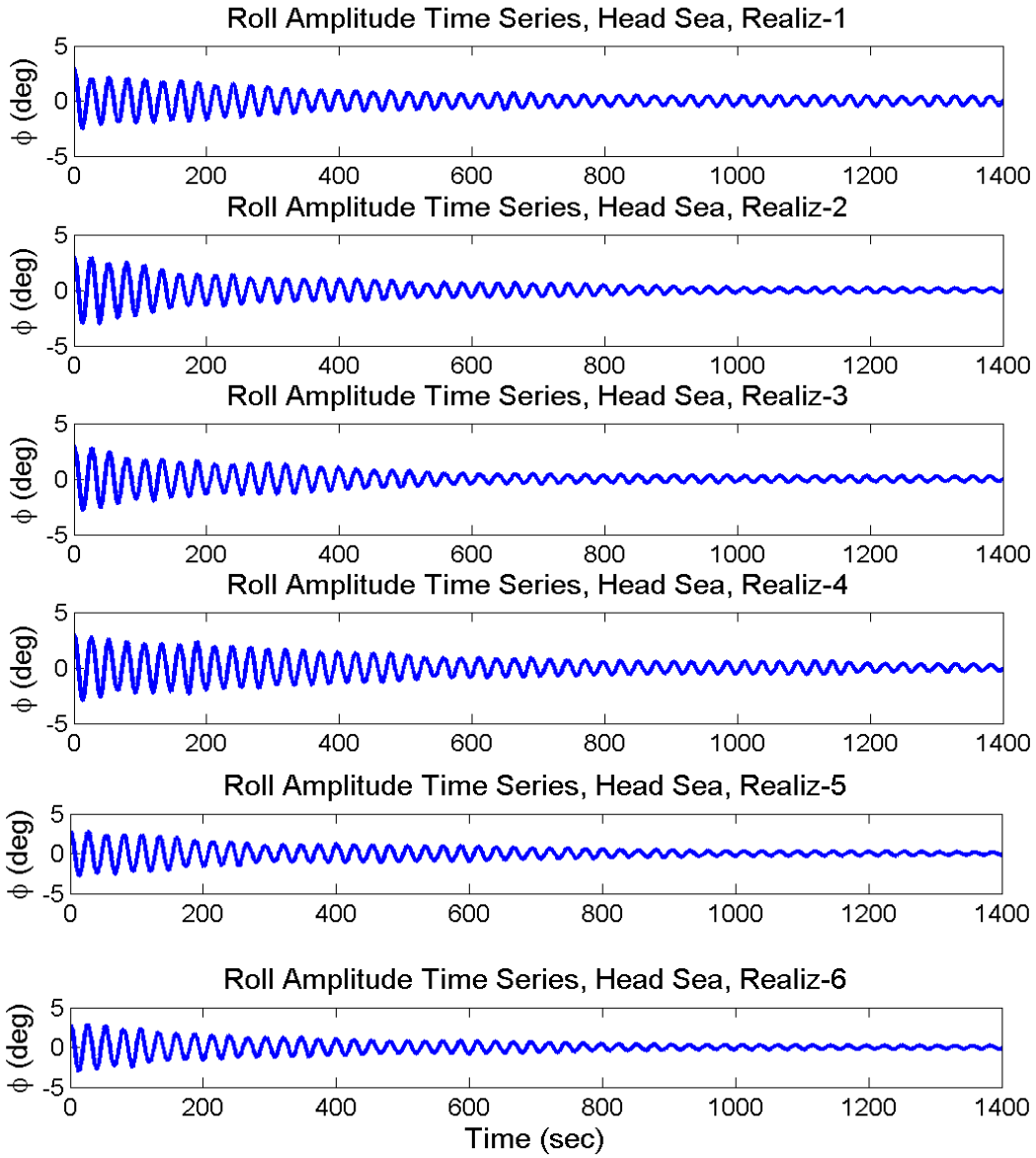

Figure 61. Different realizations of time series of roll amplitude, Hs=3.0 m, Tp=8 sec

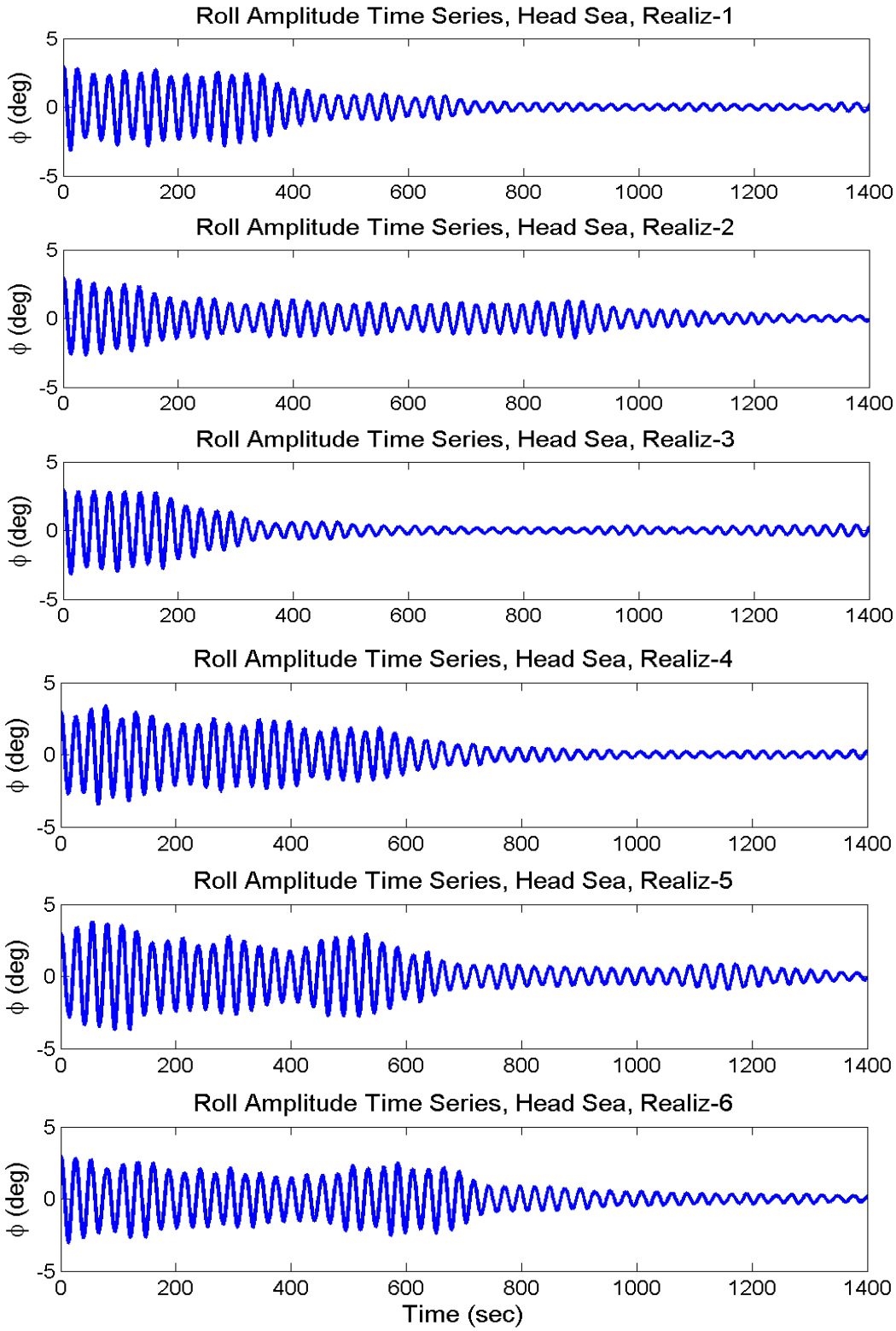

Figure 62. Different realizations of time series of roll amplitude, Hs=3.0 m, Tp=9 sec

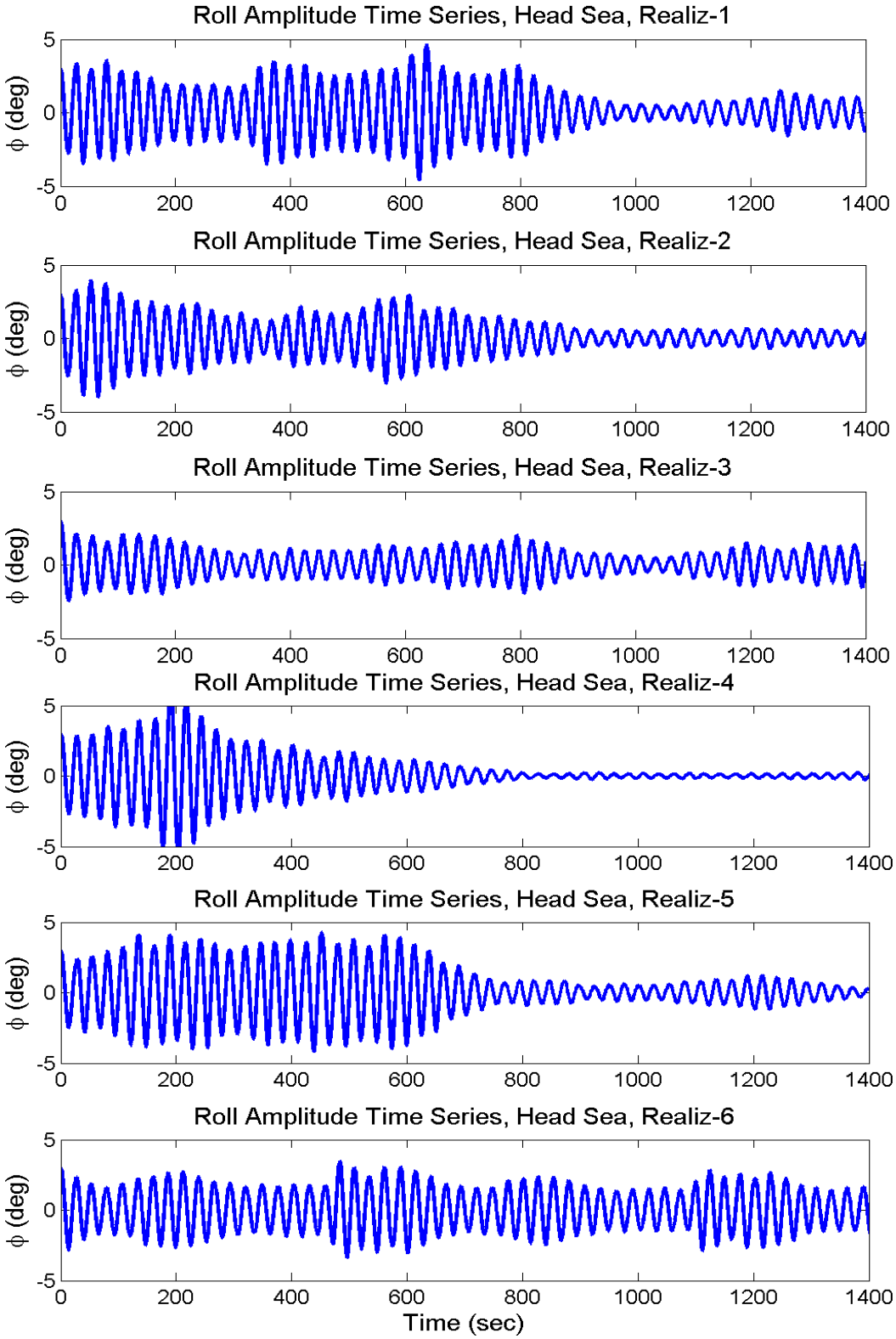

Figure 63. Different realizations of time series of roll amplitude, Hs=3.0 m, Tp=10 sec

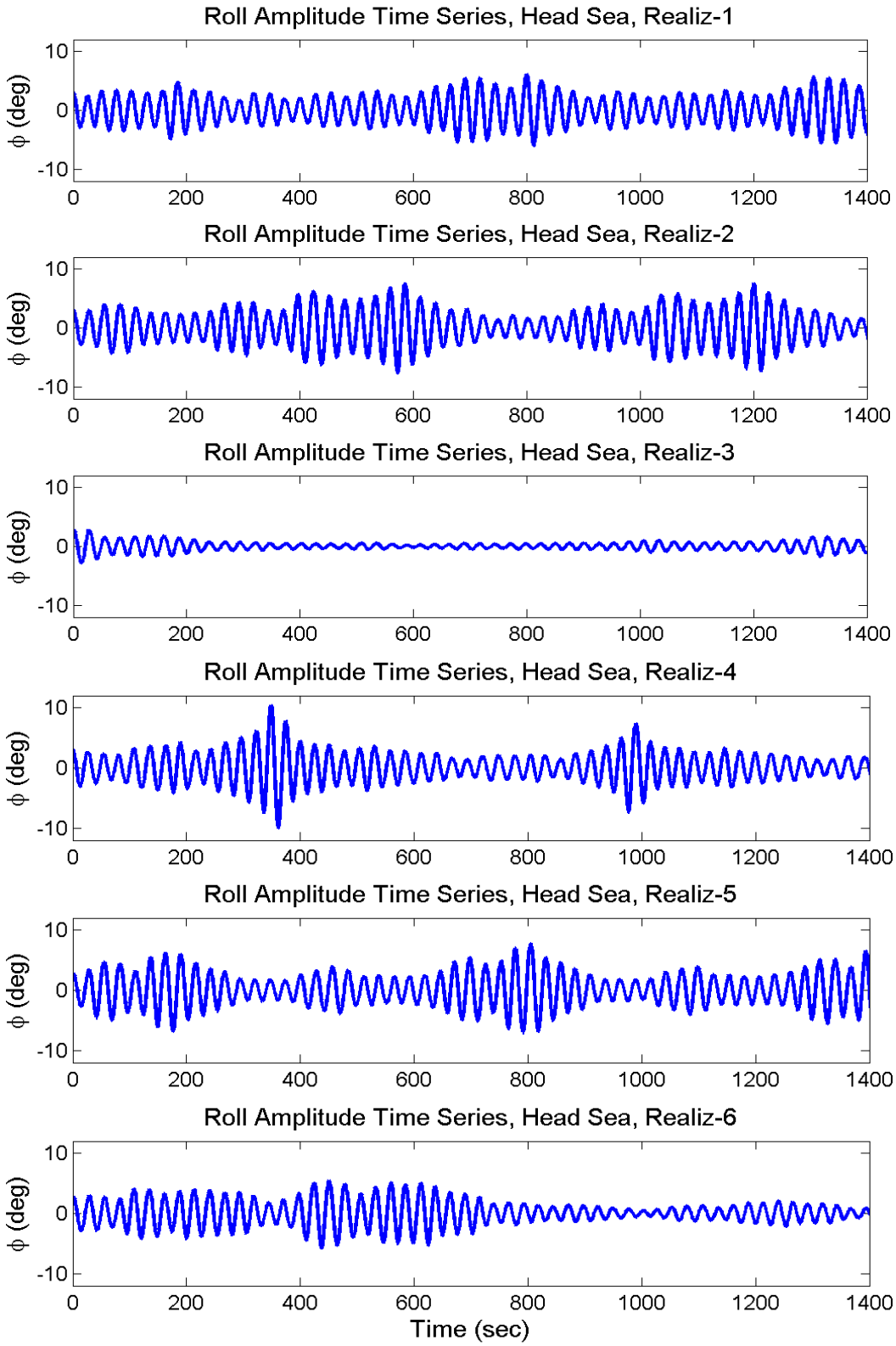

Figure 64. Different realizations of time series of roll amplitude, Hs=3.0 m, Tp=12 sec

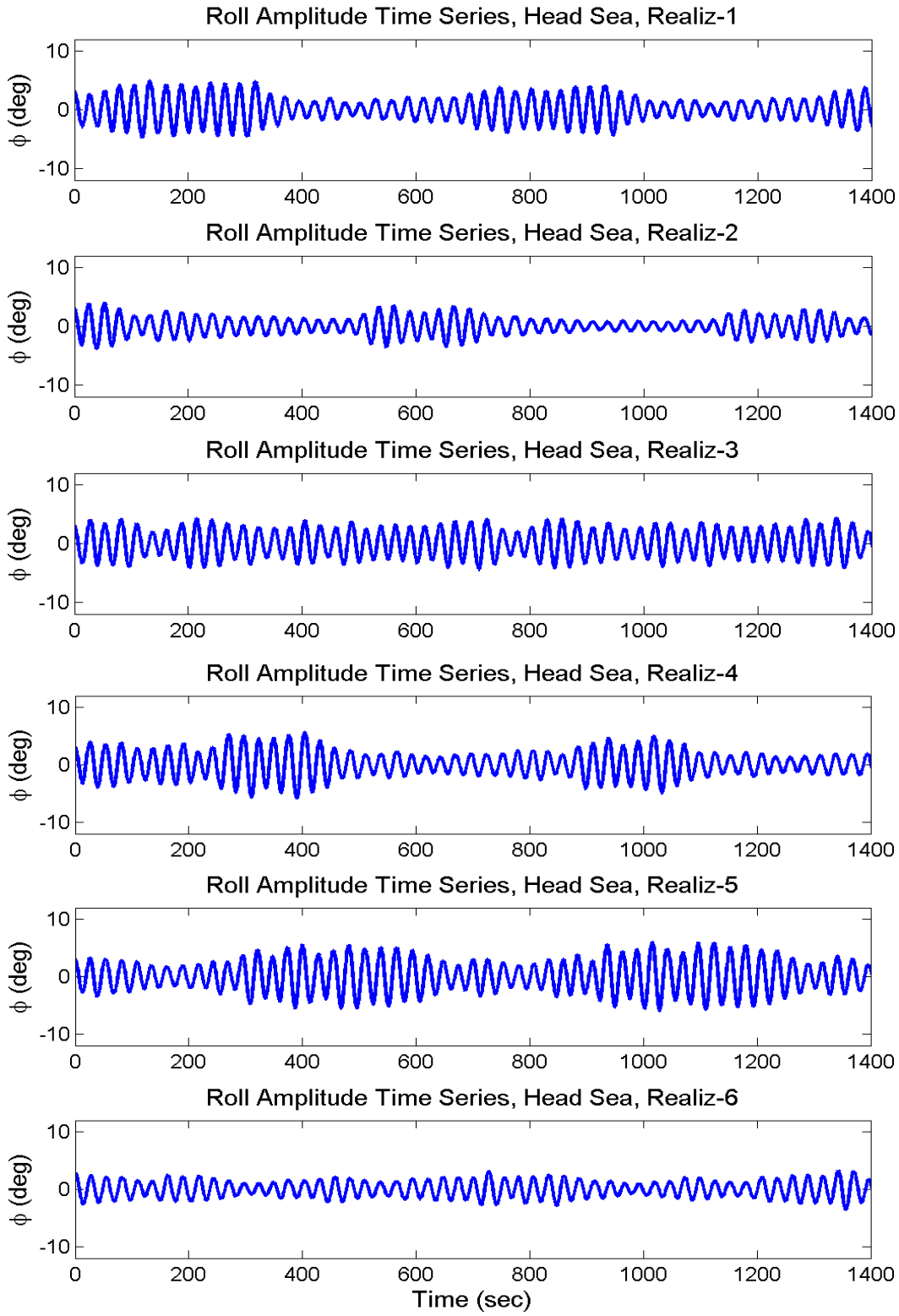

Figure 65. Different realizations of time series of roll amplitude, Hs=3.0 m, Tp=14 sec

From the numerical simulation results of parametric roll for different peak periods of the wave spectrum, we see that the parametric roll increases with an increase in the peak period. The roll motion seems to have increased significantly when the peak period was increased to 12 sec. The roll amplitude was found to decrease in general as the peak period was increased beyond 12 sec. The modal period of the spectrum with peak period of 12 sec is equal to 13.6 sec. If we look back at regular wave analysis, we found that the critical period of 12.96 sec was found to produce significant parametric roll motion. The corresponding frequency of 0.485 rad/sec is twice the natural frequency of roll for C11 Hull form. When the modal period is close to the critical period or the frequency ratio parameter α is close to the first instability zone of the stability chart we see a significant increase in the roll response. This is because the energy in the spectrum is concentrated around the modal period and there is sufficient wave energy (wave height) at the modal frequency that can lead to large variation in the GM resulting in large amplitude roll motion. Now that we have identified the critical peak period of the spectrum that can result in significant parametric roll, we shall investigate the effect of wave height on the parametric roll behavior of C11 hull form for Tp=12 sec. The effect of significant wave height on parametric roll behavior will be discussed in the next section.

As we are dealing with irregular wave time series and irregular roll motion it would be better to estimate statistical peaks rather than absolute maximum. A Weibull fit was carried over the time series for each peak period in order to estimate the Weibull maximum. Combined data of all the 6 realization was used in the Weibull estimate.

Table 9 shows the important statistical properties corresponding to each peak period. Figure 66 shows the roll amplitude and the corresponding probability of exceedence .for different spectral peak period for Hs=3.0m.

Table 9
Statistical properties of roll amplitude of C11 hull form for different peak period in irregular sea Hs=3.0 m, Fwd speed=0 m/sec

Hs (m)		3.0	3.0	3.0	3.0	3.0
Tp (sec)		8.0	9.0	10.0	12.0	14.0
Roll Amplitude (deg)	**Max**	1.86	2.77	5.07	10.19	6.01
	Min	0.09	0.07	0.06	0.18	0.61
	Weibull Estimate	1.89	2.93	4.82	9.24	6.10

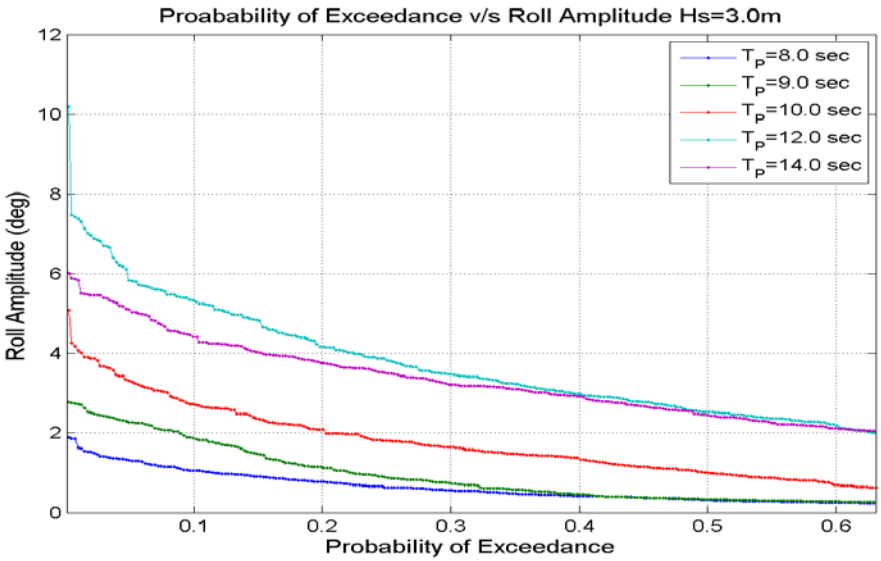

Figure 66. Effect of peak period on roll motion of the C11 hull form in irregular seaway, Hs=3.0m, Fwd speed =0m/sec

From the above analysis we can conclude that a wave spectrum with its modal period close to the critical period of the vessel can lead to large amplitude roll motion in longitudinal irregular sea due to parametric resonance in the 1st instability zone.

4.3.3 Effect of Hs on parametric roll in irregular seaway

From the sensitivity study of peak period of the spectrum on the parametric roll motion of the vessel, the critical peak period was found to be 12sec.. In this section we will study the effect of Hs on the parametric roll behavior with Tp=12sec. Numerical simulations for different Hs are shown in Figures 67 to 71.

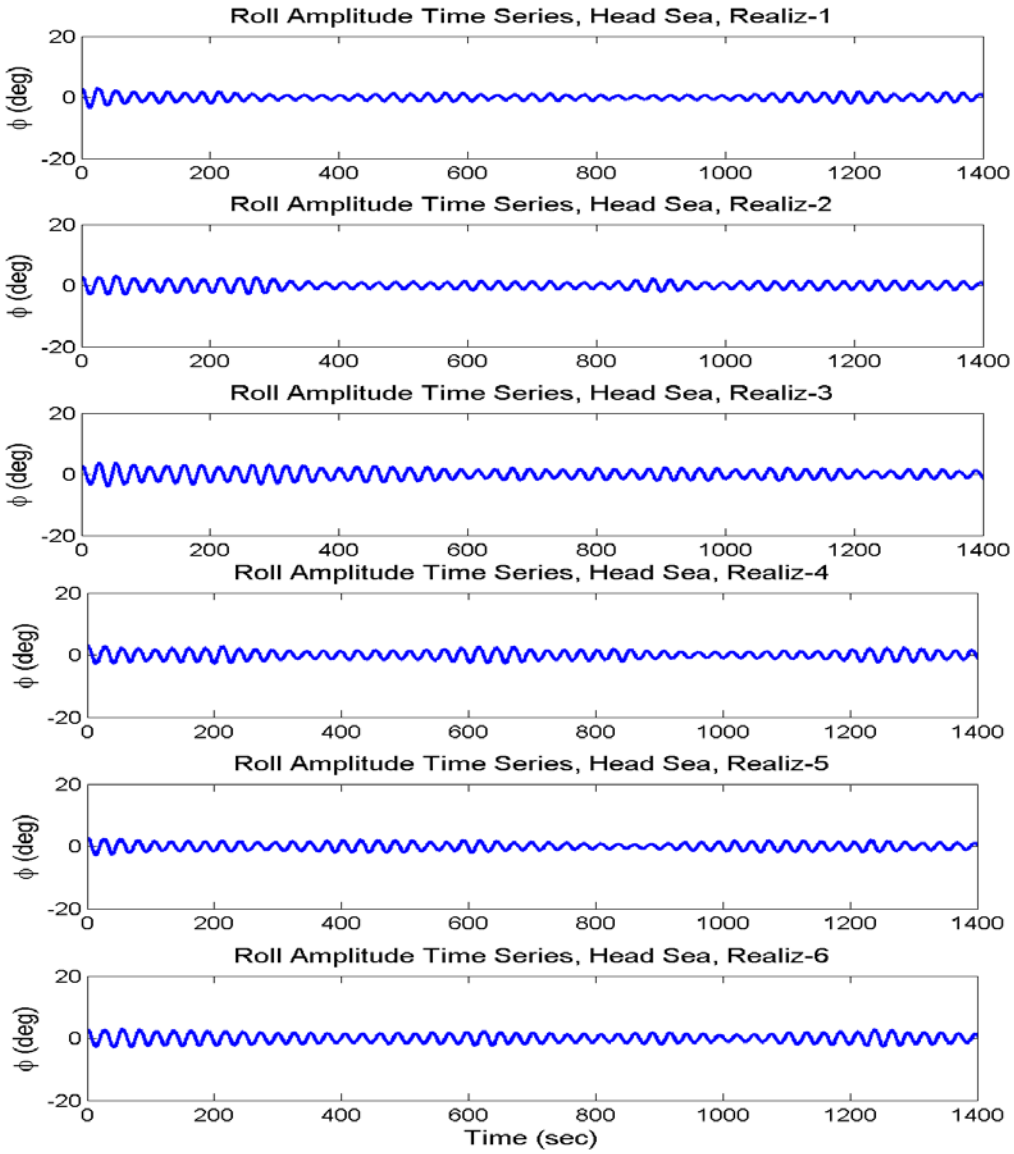

Figure 67. Different realizations of time series of roll amplitude, Hs=2.0 m, Tp=12 sec

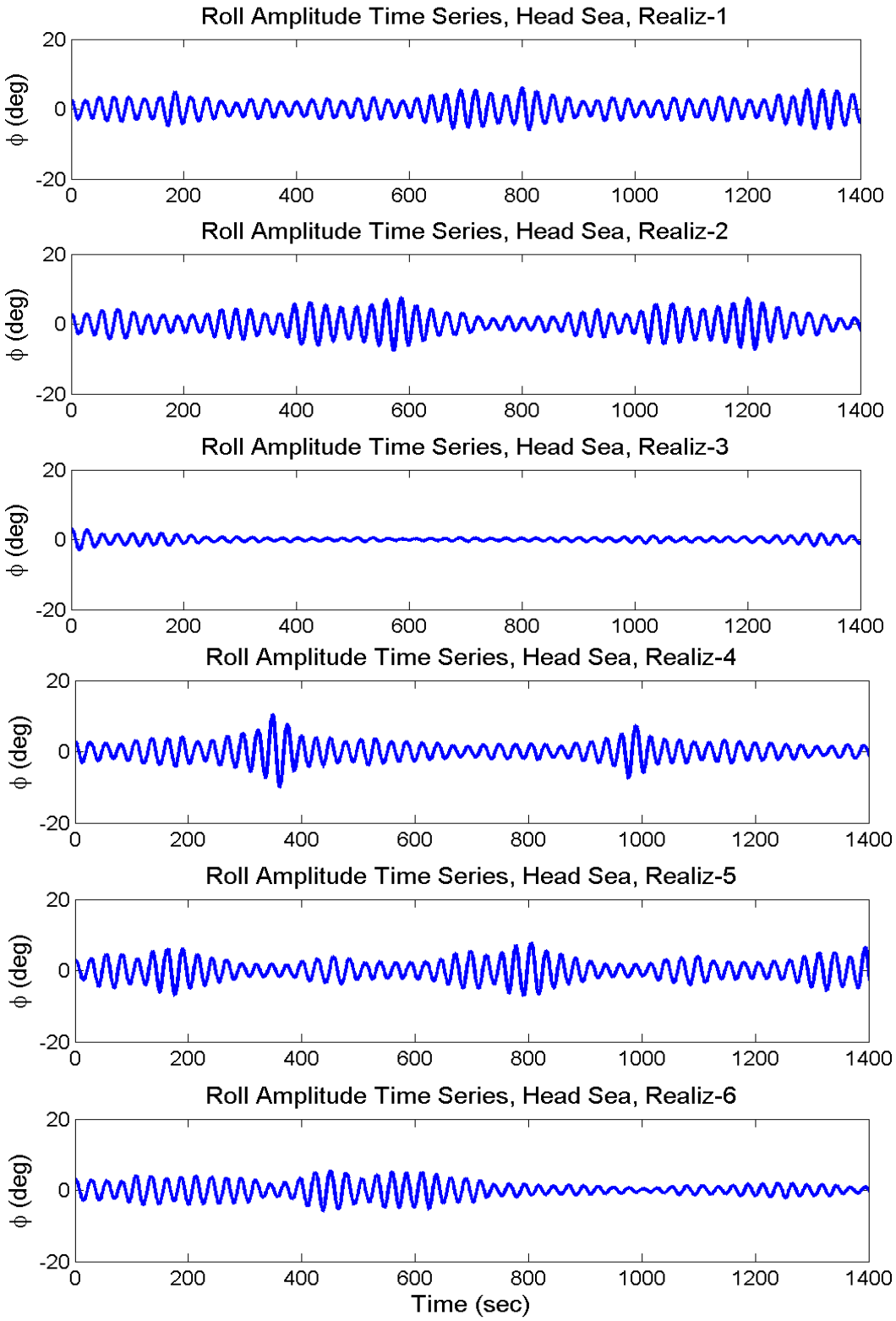

Figure 68. Different realizations of time series of roll amplitude, Hs=3.0 m, Tp=12 sec

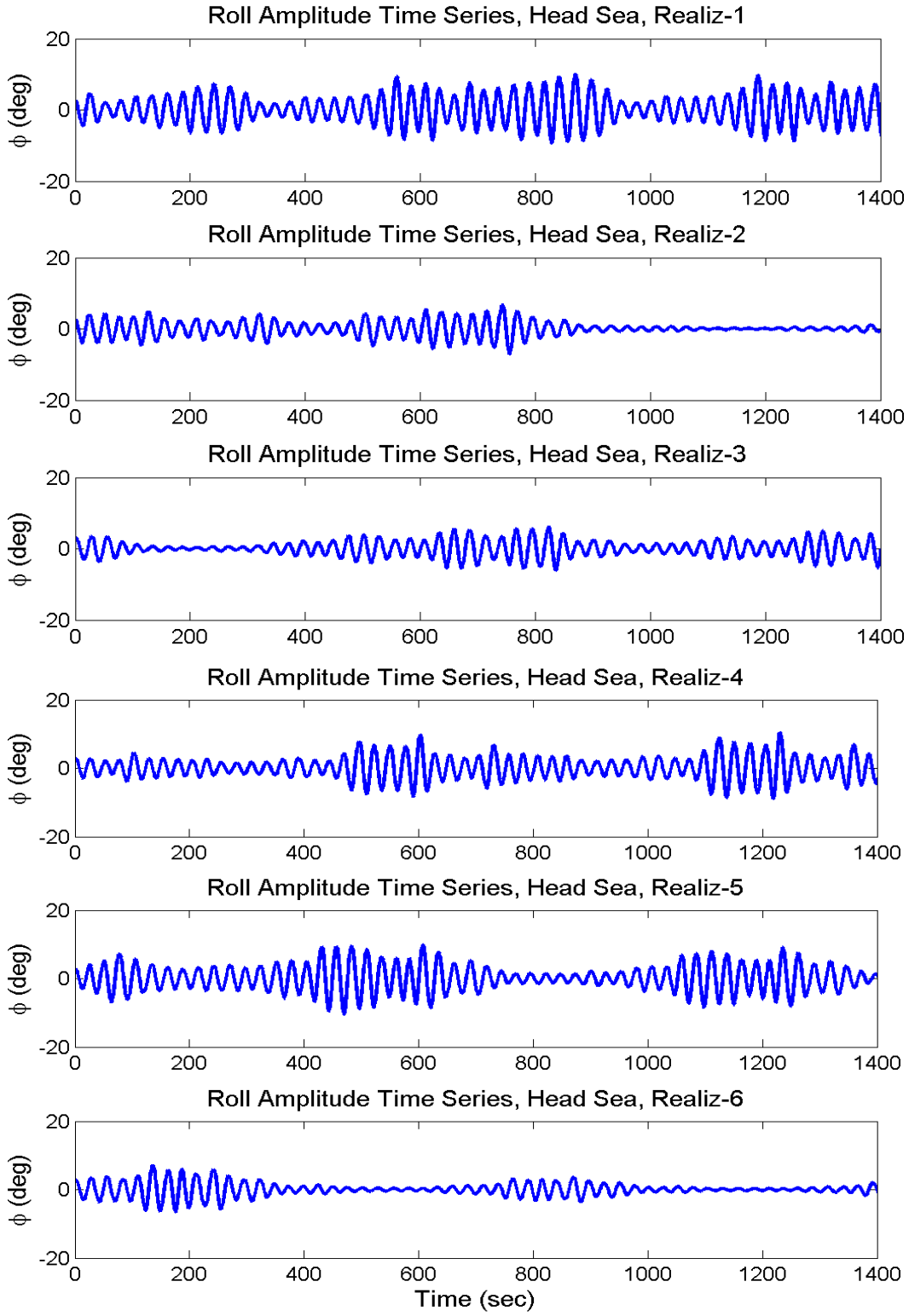

Figure 69. Different realizations of time series of roll amplitude, Hs=4.0 m, Tp=12 sec

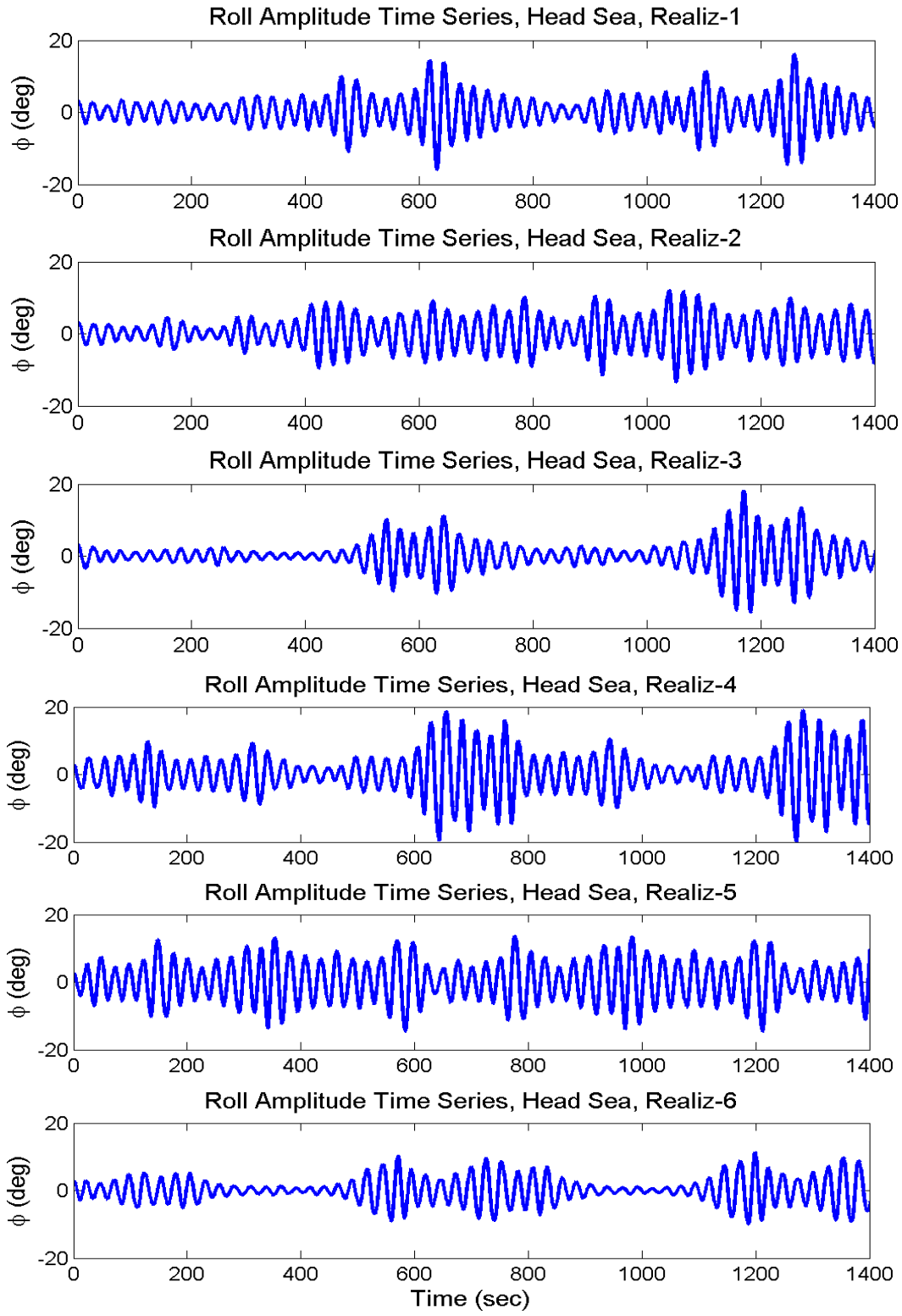

Figure 70. Different realizations of time series of roll amplitude, Hs=5.0 m, Tp=12 sec

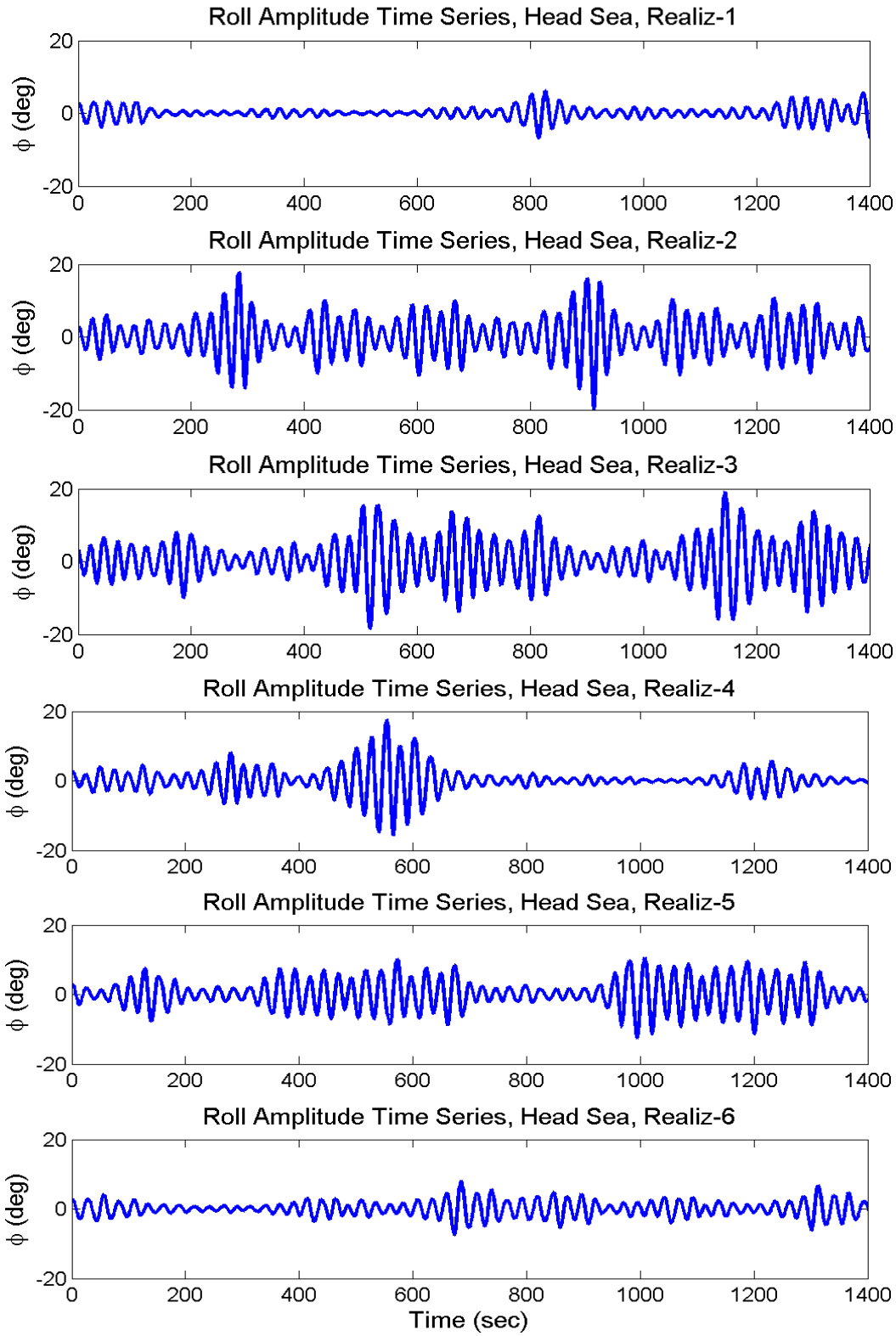

Figure 71. Different realizations of time series of roll amplitude, Hs=6.0 m, Tp=12 sec

The statistical properties of the roll motion for different significant wave height are shown in Table 10. Weibull fit is carried over the combined data over 6 realizations.

Table 10
Statistical properties of roll amplitude of C11 hull form for different significant wave heights in irregular sea, Tp=12 sec, Fwd speed=0 m/sec

Hs (m)		2.0	3.0	4.0	5.0	6.0
Tp (sec)		12.0	12.0	12.0	12.0	12.0
Roll	**Max**	3.23	10.19	9.95	17.83	18.18
Amplitude	**Min**	0.65	0.18	0.07	0.59	0.34
(deg)	**Weibull Estimate**	3.15	9.24	9.91	19.95	20.38

The roll motion amplitude is found to increase with an increase in the significant wave height. The Weibull estimate of roll amplitude increases from 10 deg at Hs=4.0 m to 20 deg at Hs=5.0 m. Such a behavior is a clear indication of the non-linear character of the system. The random properties of the seaway makes it very difficult to predict the roll motion. Figure 72 shows the probability of exceedence for different roll amplitude for varying Hs.

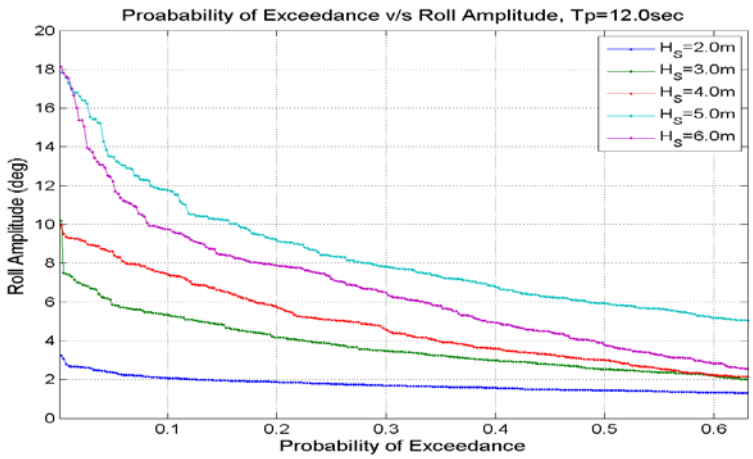

Figure 72. Effect of significant wave height on roll motion of C11 hull form in irregular seaway, Fwd Speed =0 m/sec

4.3.4 Parametric roll with forward speed

In the previous section we studied the roll motion of vessel in head sea waves with zero forward speed. In this section we shall study the effect of forward speed on the roll response in irregular seaway. As seen from regular wave analysis the effect of forward speed is to increase or decrease the encounter frequency of waves. We shall study the effect of forward speed in the head sea condition. In this case the encounter frequency of the waves increases. Figure 73 shows the wave spectrum for different forward speed with waves encountered head on.

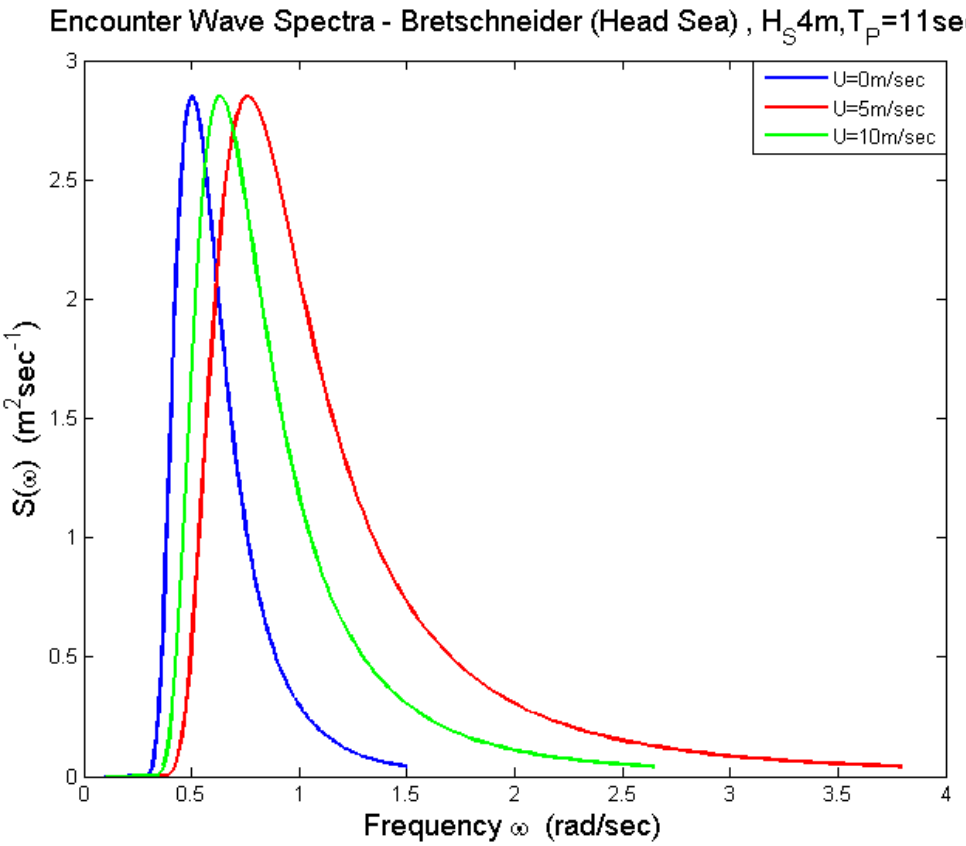

Figure 73. Encounter wave spectrum for Hs=6 m, Tp=12 sec

From Figure 73 we see that the modal frequency of the encounter spectrum increases as the forward velocity of vessel increases. This is quite expected since waves are encountered faster as the relative velocity increases in head sea condition. The GM variation for different encounter frequency are estimated using the Volterra approach. The heave and pitch motions also change with change in the encounter frequency thus affecting the GM variation. Figure 74 shows a realization of wave profile and the corresponding components of GM variation.

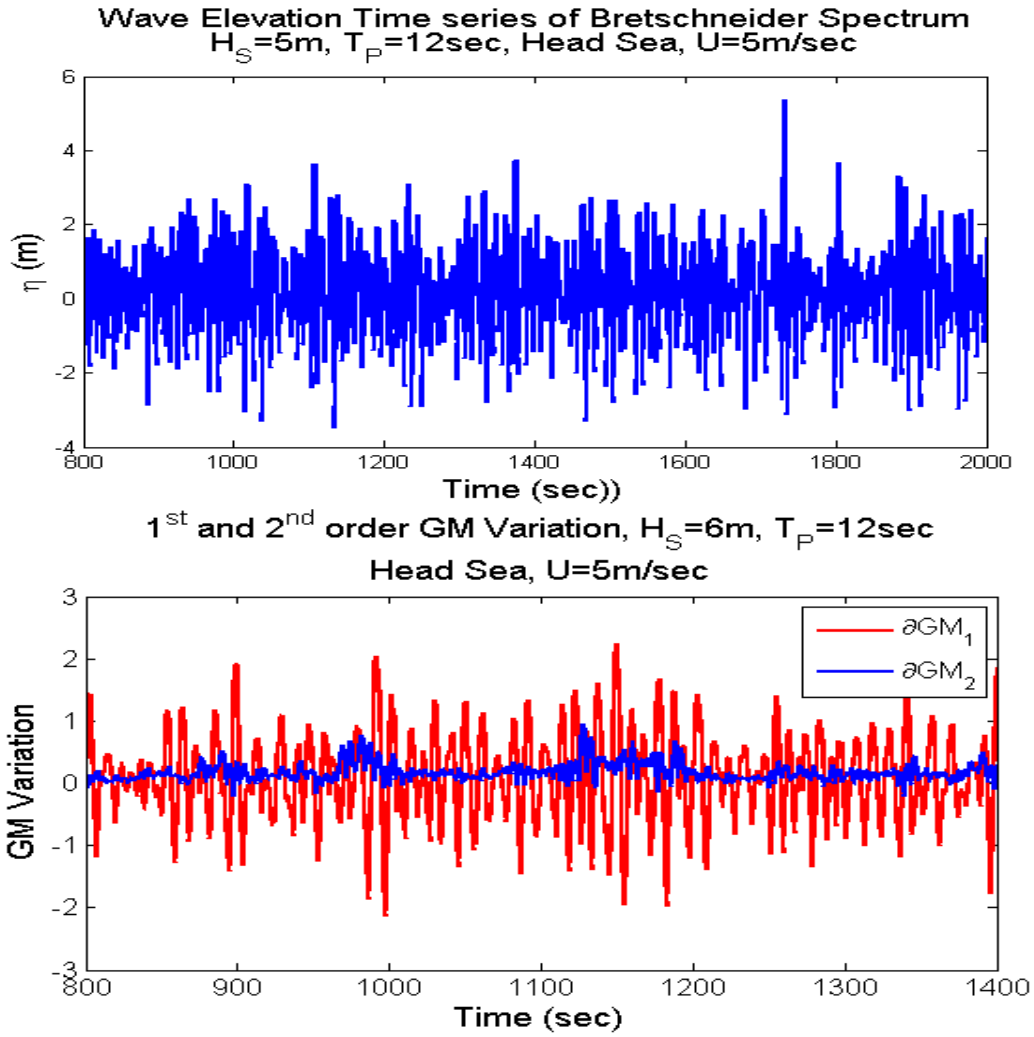

Figure 74. Wave elevation (Top) and components of GM variation, Hs=6 m, Tp=12 sec, U=5 m/sec

The spectrum of the realization for cases with and without forward speed are shown in Figure 75.

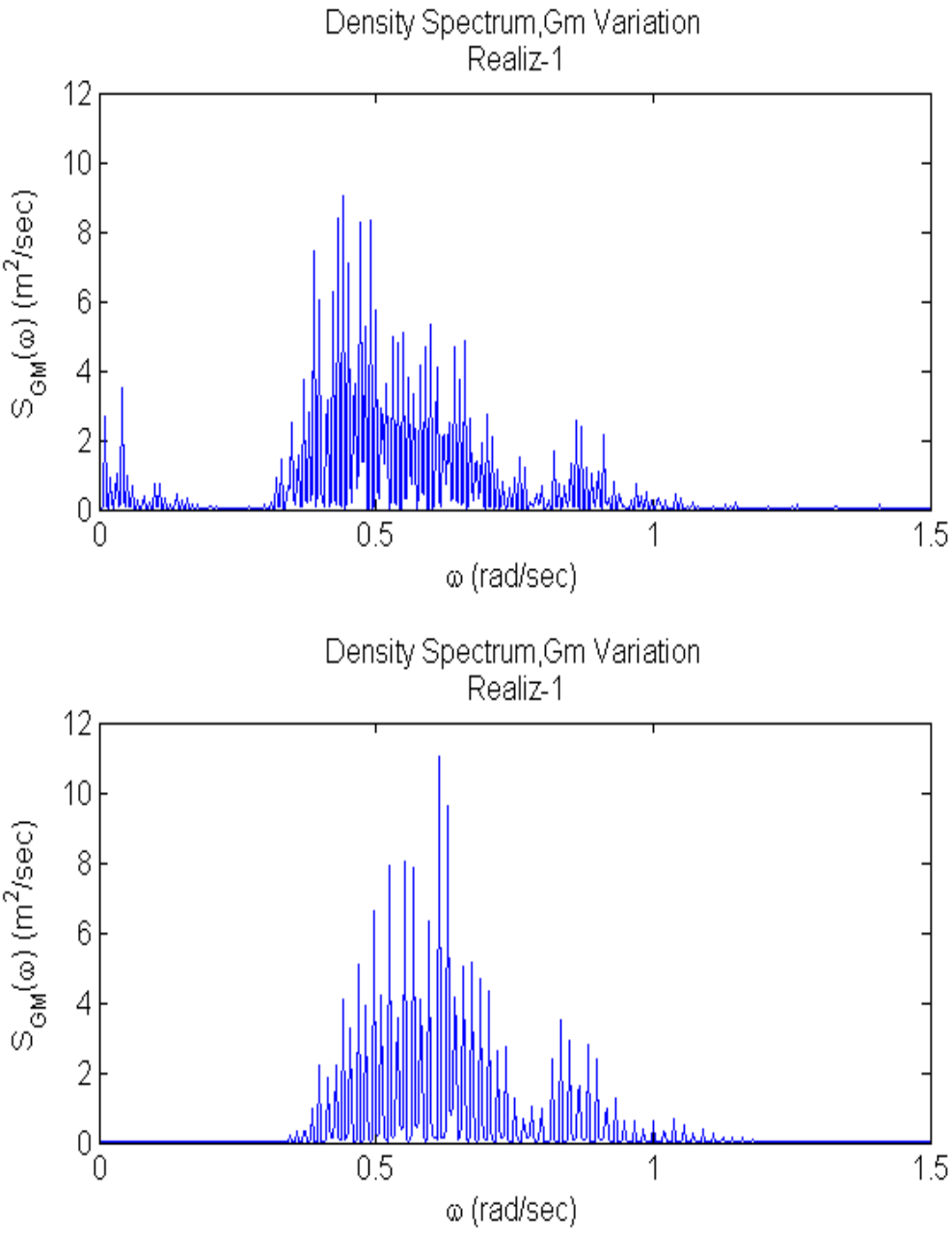

Figure 75. GM spectrum U=0 m/sec (Top), U=5 m/sec(Bottom), Hs=6 m, Tp=12 sec

From the GM spectrum we can clearly the see the shift in energy of GM variation to higher frequency due to high frequency of waves encountered. Also we notice that the GM variation in the tail near the principal resonant zone is higher in the case with forward speed. In addition the difference frequency components which was significant in the case of zero forward speed was found to be negligible in the forward speed case. Due to the shift in the energy of GM variation we would expect lower parametric excitation energy due to primary resonance. For a higher peak period the shift can result in sufficient parametric excitation at primary resonant frequency leading to large amplitude roll motion. GM spectrum for Hs=6m and Tp=14 sec is shown in Figure 76.

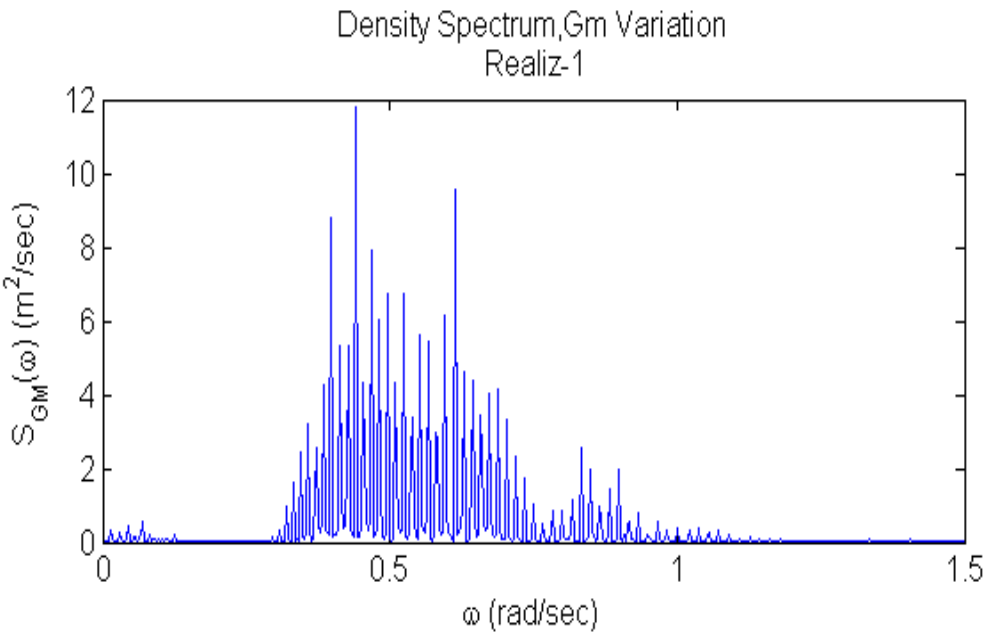

Figure 76. GM spectrum U=5 m/sec, Hs=6 m, Tp=14 sec

As expected the peak energy of GM variation is now closer to the primary resonance frequency zone which is ideal for parametric roll motion. Table 11 shows the maximum, minimum and the Weibull estimate of the roll amplitude for Hs=6m for different Tp.

Table 11
Statistical properties of roll amplitude of C11 hull for different peak period in irregular sea, Hs=6.0 m, Fwd speed =5 m/sec (head sea)

Hs (m)		6.00	6.00	6.00	6.00	6.00
Tp (sec)		8.00	9.00	10.00	12.00	14.00
Roll Amplitude (deg)	**Max**	1.94	1.87	3.50	15.34	19.20
	Min	0.11	0.09	0.06	0.09	0.44
	Weibull Estimate	1.95	1.82	3.70	15.17	18.06

The statistical properties for forward speed of 10m/sec in the head sea condition in shown in Table 12.

Table 12
Statistical properties of roll amplitude of C11 hull for different peak period in irregular sea, Hs=6.0 m, Fwd speed =10 m/sec (head sea)

Hs (m)		6.00	6.00	6.00	6.00	6.00
Tp (sec)		8.00	9.00	10.00	12.00	14.00
Roll Amplitude (deg)	**Max**	1.68	1.82	2.00	10.22	15.87
	Min	0.11	0.09	0.10	0.77	0.97
	Weibull Estimate	1.72	1.87	2.04	9.43	15.22

From the Table 11 and Table 12 we see that roll amplitude increases as the peak period increases due to the shift in the energy of the GM spectrum due to forward speed in head sea condition. The modal encounter period of the spectrum with Tp=14sec decreases to a value closer to 13sec which is the primary parametric resonant period. As a result the parametric excitation energy at primary resonant frequency is high due to which we observer large amplitude parametric roll in comparison to lower period.

In the case of following sea the encounter frequency decreases. Due to the forward speed of the vessel, waves which have speed less than that of the vessel will not catch up, as a

result less and less waves will be encountered The modal period increases due to forward speed in the following sea condition due to which we can expect more parametric roll at peak period less than 13sec in comparison to spectrums with peak period greater than 13sec.

From the above study in general we see that parametric roll may or may not occur in irregular longitudinal sea. The non-linear property of the system coupled with the random parametric excitation makes it very difficult to predict the occurrence of parametric roll in irregular seaway. But the study has helped us understand some important properties of parametric roll. In general parametric roll was found to occur when there is sufficient energy in the GM variation spectrum at twice the natural frequency. This is similar to what was observed in regular wave analysis. When the excitation frequency was equal to or close to twice the natural frequency, large amplitude roll motion was observed even in the presence of non-linear damping. An important criteria for parametric roll to occur in irregular seaway is having spectral modal period close to the primary resonant frequency of the vessel.

With this, we conclude this section of parametric roll analysis of C11 hull form in irregular seaway. The main conclusion of the section will be summarized in the next chapter.

CHAPTER V

CONCLUSIONS

Based on the studies and results of analysis of parametric roll properties of C11 hull form following conclusions can be made

5.1 Parametric Roll Analysis in Regular Waves

1. The single degree of roll equation of motion with time varying linear stiffness can be reduced to a Hill or Mathieu form and system stability evaluated.

2. The Mathieu form is very general and does not capture non-harmonic variation in stiffness. The Hill's form is capable of representing the non-harmonically varying stiffness variation

3. Based on the stability region in the Ince-Strutt diagram different resonant zones were identified. Sub-harmonic, principal and super-harmonic resonant frequencies were identified based on these resonant zones and natural frequency of roll. A Forcing frequency equal to twice the natural frequency was found to be more critical due to large unstable region around it.

4. The Hill's equation with linear damping only helps predicts the occurrence of parametric roll but does not predict the roll amplitude. Non-linear damping bounds the motion resulting in a bounded roll motion amplitude. For regions where a linear approximation of stiffness is valid, the method of equivalent linear damping is used in place of non-linear damping and the stability boundaries are

extended into a 3-dimensional surface. The bounded roll motion amplitude can thus be predicted from the surface with good accuracy.

5. Floquet theory is a very useful tool for studying stability of parametric systems and can also be extended to include non-linear damping in the form of equivalent roll amplitude depended damping. Wherever the eigenvalues become unity the corresponding amplitude represented the bounded roll motion amplitude. This method was also found to be predict roll amplitude with good accuracy.

6. The effect of forward speed was to shift the parameters (α, γ) in the Ince-Strutt diagram. The shift resulted in different response of the vessel depending upon where the parameter fell for different forward speeds (head and following sea condition). Sub and primary resonance were found to occur as a result of forward speed. Forward speed of the vessel thus gives operators an option to stabilize a vessel undergoing parametric roll provided the location of parameters (α, γ) is with respect to the neutral boundaries. This can be a very useful information from the operational point of view.

7. Forward speed of the vessel can lead to a Hopf type bifurcation in the vessel roll motion (considering only steady state response). Thus forward speed was found to be a critical bifurcation parameter which can control the roll motion.

8. The methods developed to predict roll amplitude can be put to use in early design stage to avoid parametric roll.

5.2 Parametric Roll Analysis in Irregular Waves

1. The Volterra method of representing the metacentric height variation (due to wave profile) was found to give a good estimate of the GM variation. The method can also incorporate the coupling effects of heave and pitch motion.

2. First and second order transfer functions for GM variation can be easily determined for any hull form and these functions can then be used to estimate the GM variation in a regular or irregular seaway.

3. The occurrence of parametric roll was found to be highly random in an irregular seaway making it difficult to predict their occurrence. However, we may conclude that parametric roll does occur in an irregular seaway.

4. Parametric roll was found to be significant when the modal period of the spectrum was close to twice the natural period of roll in the zero speed case. Thus when the modal period of the spectrum is close to the primary resonant frequency of the vessel parametric roll was found to occur in an irregular seaway.

5. Forward speed in the head sea condition reduced the spectral modal period and thus the roll motion was amplified at a higher spectral period than lower ones. The opposite is true for the following sea condition. A vessel experiencing parametric roll in irregular seaway should either increase or decrease the forward speed depending on the encountered modal period of the spectrum to avoid or reduce parametric roll motion. As a design guideline the vessel roll period should be kept away from the design spectral modal period to avoid parametric roll.

CHAPTER VI

FUTURE WORK

The work detailed in this thesis has its own limitations and assumptions. Based on the studies carried out as part of this work several interesting topics were brought into attention which needs further research and analysis. Some of the important topics that need further research are outlined below,

1. In this study parametric roll is studied in longitudinal sea, i.e head or following sea. The effect of wave heading on the parametric roll motions is an interesting topic. The fact that roll motion in subjected to direct and indirect excitation makes the response and damping much more complicated.

2. The Volterra model discussed in Chapter IV assumes a constant volume of displacement whereas the volume displacement of the vessel changes in an irregular seaway. This would result in instantaneous transfer functions and different GM variation. Also the natural frequency of the vessel becomes a variable. This further complicates the system and prediction, leading to more parametric resonant conditions.

3. The roll equation of motion subjected to a random excitation such as a sea spectrum qualifies as a random dynamical system. An important tool that has been used extensively to study the statistical properties of such a system in the Fokker-Plank equation. The roll equation of motion can be converted to Fokker-Plank equation assuming a white noise excitation and solved to obtain the time

varying probability density function. A stationary density function can be obtained if an equilibrium solution exists. Colored noise may be incorporated by means of a filter. The main disadvantage of the method is exponential increase in computation time with increase in the number of state variables of the system. Active research is going on to develop simpler method to tackle this problem.

REFERENCES

ABS, 2004. ABS Guide for the Assessment of Parametric Roll Resonance in the Design of Container Carriers. American Bureau of Shipping.

Beck, R.F., Troesch, A.W., 1989. SHIPMO.BM, Michigan.

Belenky, V.L., Weems, K.M., Lin, W.M., Paulling, J.R., 2003. Probabilistic analysis of roll parametric resonance in head sea, 8th International Conference on the Stability of Ships and Ocean Vehicles, pp. 325-340.

Bulian, G., 2003. Development of analytical nonlinear models for parametric roll and hydrostatic restoring variations in regular and irregular waves, Department of Naval Architecture, Ocean and Environmental Engineering (DINMA). University of Trieste,Trieste,Italy.

Bulian, G., 2005. Nonlinear parametric roling in regular waves- a general procedure for the analytical approximations of the GZ curve and its use in time domain simulations. Ocean Engineering 32, 309-330.

Bulian, G., 2008. On an improved Grim effective wave. Ocean Engineering 35 (17-18), 1811-1825.

Bulian, G., Francescutto, A., Lugni, C., 2004. On the non-linear modeling of parametric rolling in regular and irregular waves. International Shipbuilding Progress 51 (2/3), 173-203.

Chakrabarti, S., 2001. Empirical calculation of roll damping for ships. Ocean Engineering 28, 915-932.

Dunwoody, A.B., 1989a. Roll of ship in astern seas- response to GM fluctuations. Journal of Ship Research 33 (4), 284-290.

Dunwoody, A.B., 1989b. Roll of ship in astern seas - metacentric height spectra. Journal of Ship Research 33, 221-228.

Falzarano, J.M., 1990. Predicting complicated dynamics leading to vessel capsizing, Naval Architecture and Marine Engineering. The University of Michigan, Ann Arbor.

Falzarano, J.M., Shaw, S.W., Troesch, A.W., 1992. Application of global methods for analysing dynamical systems to ship rolling and capsizing. International Journal of Bifurcation Chaos 2, 101-116.

Floquet, G., 1883. Sur les équations différentielles linéaires à coefficients périodiques. Annales scientifiques de l'École Normale Supérieure 12 (2), 47-88.

France, W.N., MarcLevadou, Treakle, T.W., Paulling, J.R., 2001. An investigation of head-sea parametric rolling and its influence on container lashing systems. Marine Technology 40 (1), 1-19.

Froude, W.F., 1863. Remarks on Mr. Scott Russell's paper on rolling. Trans. Inst. Naval Res. 4, 232-275.

Grim, O., 1952. Rollschwingungen, Stabilität und Sicherheit im Seegang. Forschungshefte für Schiffstechnik 1.

Grim, O., 1961. Beitrag zu dem Problem der Sicherheit des Schiffes im Seegang. Schiff und Hafen 6, 490-497.

Hamamoto, M., Enomoto, T., Sera, W., 1996. Model experiment of ship capsize in astern seas-second report. Journal of Society of Naval Architects of Japan 179, 77-87.

Hill, G.W., 1886. On the part of the motion of lunar perigee which is a function of the mean motions of the sun and moon. Acta Math 8, 1-36.

Himeno, Y., 1981. Prediction of ship roll damping- state of the art. Department of Naval Architecture and Marine Engineering,The University of Michigan, Ann Arbor.

Hua, J., Wang, W.-H., Chang, J.-R., 1994. A representation of GM-variation in waves by the Volterra system. Journal of Marine Science and Technology 7 (2), 94-100.

Hua, J., Wang, W.-H., Chang, J.-R., 2001. Roll motion of a RoRo-ship in irregular following waves. Journal of Marine Science and Technology 9 (1), 38-44.

Kan, M., 1992. Chaotic capsizing, 20th ITTC Seakeeping Committee and Kansai Fulid-Dynamics Research Group, Osaka, Japan, pp. 155-180.

Kerwin, J.E., 1955. Notes on rolling in longitudinal waves. International Shipbuilding Progress 2, 597-614.

Koo, B.J., Kim, M.H., Randall, R.E., 2004. Mathieu instability of a spar platform with mooring and risers. Ocean Engineering 31 (17-18), 2175-2208.

Mathieu, E., 1868. Mémoire sur le mouvement vibratoire d’une membrane de forme elliptique. Journal des Mathématiques Pures et Appliquées, 137-203.

Munif, A., Umeda, N., 2006. Numerical prediction on parametric roll resonance for a ship having no significant wave-induced change in hydrostatically-obtained metacentric height. International Shipbuilding Progress 53, 183-203.

Nayfeh, A.H., 1986. Nonlinear rolling of ships in regular beam seas. International Shipbuilding Progress 33 (40-49).

Odabashi, A.Y., 1977. Ultimate stability of ships. Transactions of RINA 119, 237-263.

Palmquist, M., 1994. On the statistical properties of the metacentric height of ships in following irregular seas, STAB'94, Melbourne, Florida.

Paulling, J.R., 1961. The transverse stability of a ship in a longitudinal seaway. Journal of Ship Research 4 (1), 37-49.

Spyrou, K.J., Tigkas, I., Scanferla, G., Pallikaropoulos, N., Themelis, N., 2008. Prediction potential of the parametric rolling behaviour of a post-panamax containership. Ocean Engineering 35, 1235-1244.

Stoker, J.J., 1950. Nonlinear Vibrations in Mechanical and Electrical Systems. Interscience Publishers, New York.

Thompson, J.M.T., de Souza, J.R., 1996. Suppression of escape by resonant modal interactions in shell vibration and heave-roll capsize. Proc of Royal Society of London 452, 2527-2550.

Umeda, N., Hamamoto, M., Takaishi, Y., 1995. Model experiments of ship capsize in astern seas. Journal of Society of Naval Architects of Japan 177, 207-217.

van der Pol, F., Strutt, M.J.O., 1928. On the stability of the solutions of Mathieu's equation. Philosophical Magazine of Journal of Science 15, 18-38.

APPENDIX A

1. Effect of Sway and Yaw Coupling

So far a single degree of freedom equation of motion was considered in the analysis. However ship motion is coupled and roll motion is coupled to sway and yaw motion through the radiated wave damping and added mass/inertia terms. In this section we will study the influence of sway and yaw motion coupling on parametric roll behavior. The coupled equation of motion with time varying roll linear restoring moment in roll in head or following sea condition is given by Eq.(A-1)

$$[M]\left[\ddot{\zeta}\right]+[B]\left[\dot{\zeta}\right]+\left[B_2\right]\left[\dot{\zeta}_1\right]+[C]\zeta=0 \tag{A-1}$$

where,

$$[M]=\begin{bmatrix} M_{22} & M_{24} & M_{26} \\ M_{42} & M_{44} & M_{46} \\ M_{62} & M_{46} & M_{66} \end{bmatrix}+\begin{bmatrix} A_{22} & A_{24} & A_{26} \\ A_{42} & A_{44} & A_{46} \\ A_{62} & A_{46} & A_{66} \end{bmatrix}$$

$$[B]=\begin{bmatrix} B_{22} & B_{24} & B_{26} \\ B_{42} & B_{44} & B_{46} \\ B_{62} & B_{64} & B_{66} \end{bmatrix}$$

$$\left[B_2\right]=\begin{bmatrix} 0 & 0 & 0 \\ 0 & B_2 & 0 \\ 0 & 0 & 0 \end{bmatrix}$$

$$[C]=\begin{bmatrix} 0 & 0 & 0 \\ 0 & \nabla\rho g GM\left(t\right) & 0 \\ 0 & 0 & 0 \end{bmatrix}$$

$$[\zeta]=\begin{bmatrix} \zeta_2 \\ \zeta_4 \\ \zeta_6 \end{bmatrix} \tag{A-2}$$

Here the subscripts 2,4,6 represent the sway, roll and yaw motions and the dots represent the time derivative.

The added mass/inertia and radiated wave damping are obtained from linear hydrodynamics program SHIPMO. Non-linear roll damping is included to obtained bounded roll motion.

2. Results

Numerical simulation of the coupled equations were carried out for a wave steepness of 1/40 and wave length equal to the ship length. The sway, roll and yaw time series for zero forward speed case is shown in Figure 77.

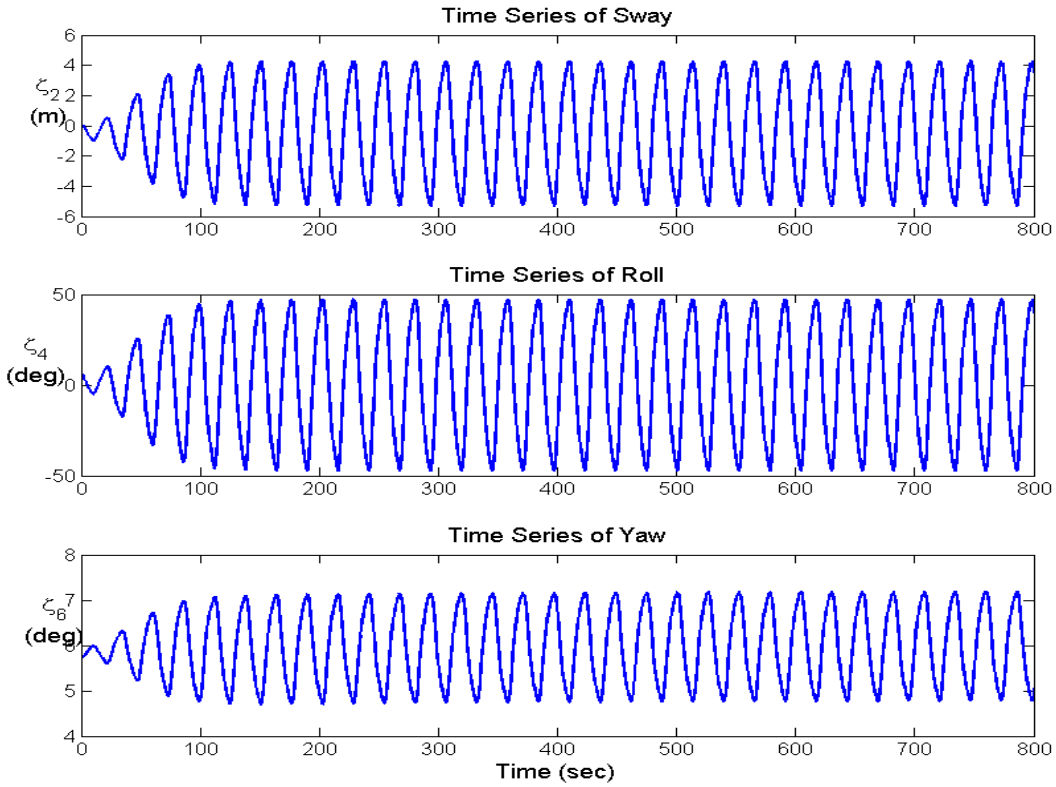

Figure 77. Time series of coupled sway, roll and yaw motions with time varying roll restoring moment, H/L=1/40, Fwd speed=0m/sec

The numerical simulation output for following sea case with a forward speed of 10m/sec is shown in Figure 78.

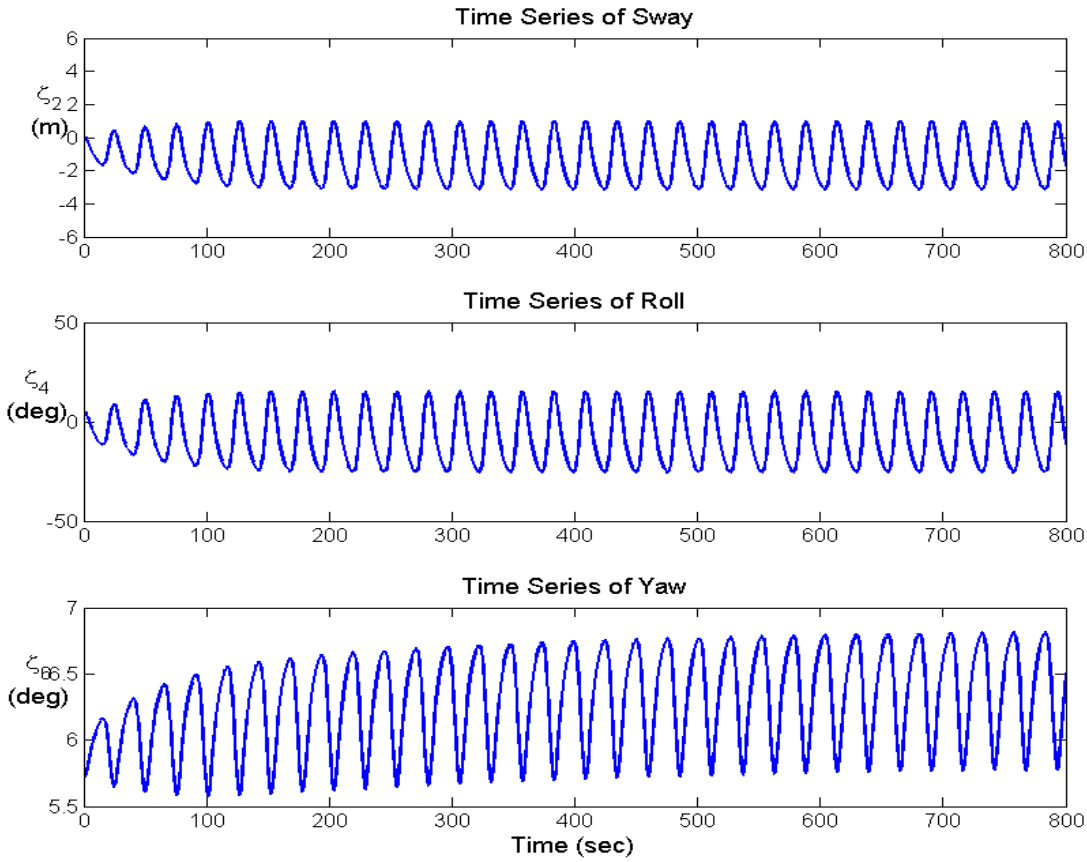

Figure 78. Time series of coupled sway, roll and yaw motions with time varying roll restoring moment, H/L=1/40, Fwd speed=10m/sec

From the results of numerical simulation we see that parametric roll does occur even if the coupling effects of sway and yaw are considered. The main effect of coupling is seen to be a reduction in the bounded roll amplitude. The damping coupling between roll and sway and roll and yaw increases the effective damping of the system and thus there is a reduction in the bounded roll motion amplitude. Also due to the coupling in the mass matrix the effective roll natural frequency will also be different.

Figure 79 shows the comparison between the roll motion with and without considering the horizontal motion coupling.

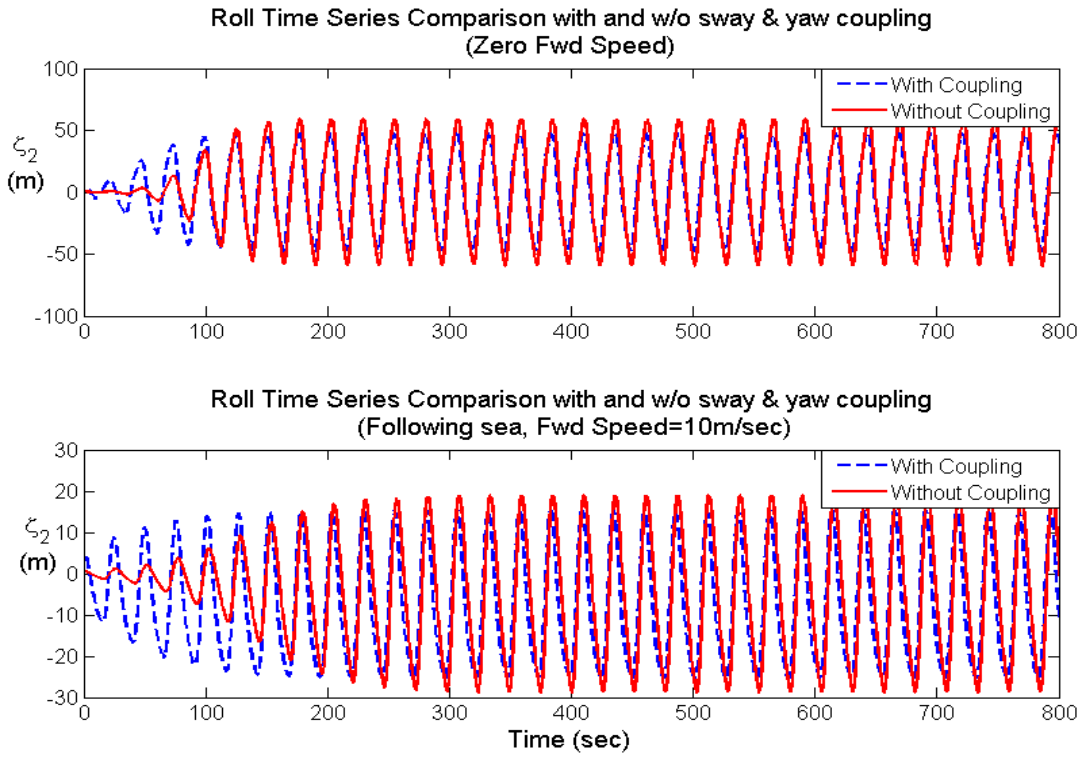

Figure 79. Comparison of roll motion with and without horizontal motion coupling (Top-zero Fwd speed, Bottom- Following sea, Fwd speed =10m/s)

From the results of numerical simulation we see that the bounded roll motion amplitude is lower by about 20% in both the cases. The reduction in amplitude is a clear indication of the sway and roll cross coupling damping terms. The natural frequency of roll has not changed significantly indicating that the added mass/inertia coupling effect is small.

From the above analysis we may conclude that the roll amplitude predicted using a single degree of freedom model is over predicts the roll motion by about 20%.

VITA

Name:	Hisham Moideen
Address:	Ocean Engineering Program, Civil Engineering Department, Texas A&M University, College Station, TX, 77840
Email Address:	hishammoideen@gmail.com
Education:	B.Tech Naval Architecture and Ship Building, Cochin University of Science and Technology, Kerala, India, Nov 2006